

Spring 5-2008

The Design, Synthesis, and Controlled Polymerization of Cationic and Zwitterionic Norbornene Derivatives

David Allen Rankin
University of Southern Mississippi

Follow this and additional works at: <https://aquila.usm.edu/dissertations>

 Part of the [Polymer Chemistry Commons](#)

Recommended Citation

Rankin, David Allen, "The Design, Synthesis, and Controlled Polymerization of Cationic and Zwitterionic Norbornene Derivatives" (2008). *Dissertations*. 1190.
<https://aquila.usm.edu/dissertations/1190>

This Dissertation is brought to you for free and open access by The Aquila Digital Community. It has been accepted for inclusion in Dissertations by an authorized administrator of The Aquila Digital Community. For more information, please contact aquilastaff@usm.edu.

The University of Southern Mississippi

THE DESIGN, SYNTHESIS, AND CONTROLLED POLYMERIZATION OF
CATIONIC AND ZWITTERIONIC NORBORNENE DERIVATIVES

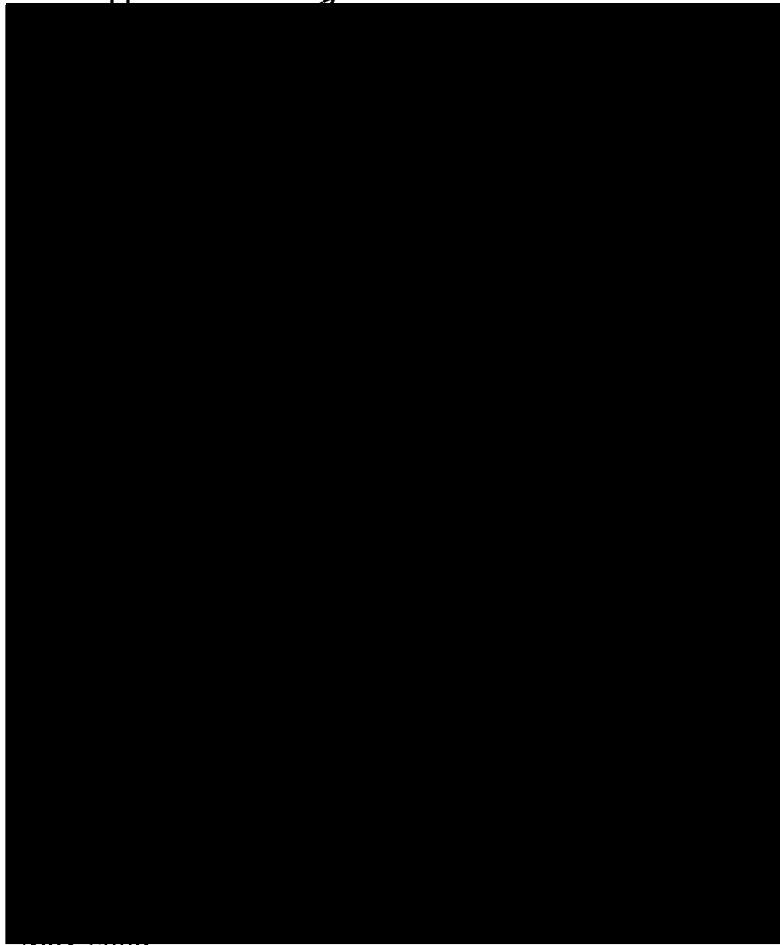
by

David Allen Rankin

A Dissertation

Submitted to the Graduate Studies Office
of The University of Southern Mississippi
in Partial Fulfillment of the Requirements
for the Degree of Doctor of Philosophy

Approved:



May 2008

COPYRIGHT BY
DAVID ALLEN RANKIN

2008

The University of Southern Mississippi

THE DESIGN, SYNTHESIS, AND CONTROLLED POLYMERIZATION OF
CATIONIC AND ZWITTERIONIC NORBORNENE DERIVATIVES

by

David Allen Rankin

Abstract of a Dissertation
Submitted to the Graduate Studies Office
of The University of Southern Mississippi
in Partial Fulfillment of the Requirements
for the Degree of Doctor of Philosophy

May 2008

ABSTRACT

THE DESIGN, SYNTHESIS, AND CONTROLLED POLYMERIZATION OF CATIONIC AND ZWITTERIONIC NORBORNENE DERIVATIVES

by

David Allen Rankin

May 2008

Ring opening metathesis polymerization (ROMP) has been exploited for the controlled polymerization of cationic and zwitterionic norbornene-based monomers and employed in the preparation of homo- and block-copolymer systems in homogeneous *organic media* without the use of post polymerization modification or protecting group chemistries.

Relying on previous knowledge of certain halogenated alcoholic organic solvents capable of solubilizing hydrophilic monomers, the first study, describes the synthesis and controlled polymerization of a series of new permanently cationic ammonium *exo*-7-oxanorbornene derivatives **M31** via ROMP, with the first generation Grubbs catalyst **17**, in a novel solvent mixture comprised of 1:1 vol/vol 2,2,2-trifluoroethanol (TFE)/methylene chloride (CH₂Cl₂). This cosolvent mixture was demonstrated to be a convenient reaction medium facilitating the polymerization of hydrophilic substrates by hydrophobic initiators under homogeneous conditions. Homo- and copolymerizations proceed rapidly yielding materials with controlled molecular masses, and narrow molecular mass distributions. It was demonstrated that this protocol is not limited to the use of TFE as a cosolvent and that additional halogenated alcohols, such as 2,2,2-trichloroethanol (TCE) and 1,1,1,3,3,3-hexafluoroisopropanol (HFIP), are also effective

cosolvents for the controlled polymerization of such substrates. Finally, we demonstrate that the TFE/CH₂Cl₂ mixture has no apparent detrimental effect on 17.

The second study describes results relating to the effect of halide counterion on the ROMP of a permanently cationic *exo*-7-oxanorbornene derivative whose synthesis we described recently in the presence of the 17. Statistical copolymerizations of *exo*-benzyl-[2-(3,5-dioxo-10-oxa-4-aza-tricyclo[5.2.1.0^{2,6}]dec-8-en-4-yl)-ethyl]dimethyl ammonium bromide/chloride were conducted at molar ratios of 25:75, 50:50, and 75:25, and the polymerizations evaluated with respect to their kinetic features as well as their molecular mass profiles as a function of conversion and the ability to produce materials with narrow molecular mass distributions. Direct comparison of the statistical copolymerizations with the corresponding bromide/chloride homopolymerizations indicates that their polymerization characteristics are intermediate of that observed for the homopolymerizations. In all instances the copolymerizations appear controlled. The clearest effect is on the measured polydispersity index which in all instances coincides with that of the bromide homopolymerization and indicates a positive, beneficial effect even with only 25 mol% bromide comonomer. The polymerization characteristics are rationalized in terms of the in situ formation of the mixed Grubbs' derivative RuClBr(PCy₃)₂CHPh and/or the dibromo analog RuBr₂(PCy₃)₂CHPh formed by halide exchange with the bromide counterions in *exo*-benzyl-[2-(3,5-dioxo-10-oxa-4-aza-tricyclo[5.2.1.0^{2,6}]dec-8-en-4-yl)-ethyl]dimethyl ammonium bromide **MON-Bn-Cl**.

The third study describes the synthesis and controlled ROMP of highly functional zwitterionic sulfopropylbetaine- **M32** and carboxyethylbetaine-*exo*-7-oxanorbornene derivatives **M33** with the first generation Grubbs' initiator 17 in a TFE/CH₂Cl₂ solvent

mixture. These are the first examples of such norbornene-based betaine substrates. Both species can be polymerized *directly* in a controlled manner in *organic media* as judged from the kinetic profiles and aqueous size exclusion chromatographic analysis. This represents the first time betaine monomers have been polymerized directly in a controlled fashion by a technique other than a controlled free radical polymerization process, and the first time it has have been achieved in organic, as opposed to aqueous, media. Finally, preliminary results demonstrate that water-soluble, salt-responsive AB diblock copolymers can be prepared and that such materials are able to undergo supramolecular self-assembly in aqueous media to yield nano-sized aggregates simply by controlling the aqueous electrolyte concentration.

In loving memory of
Beatrice and Jordan Ellis, and Clearease Cook.

ACKNOWLEDGEMENTS

First, I would like to thank Dr. Gloria Anderson and Dr. Tawfeq Kamari, my undergraduate mentors at Morris Brown College, for encouraging me to pursue a Ph.D. in chemistry. Dr. Tracy Hamilton of the University of Alabama at Birmingham is also acknowledged for his words of encouragement. I would like to express my sincere gratitude to my graduate research advisor, Dr. Andrew B. Lowe, for granting me the opportunity to work in an environment that fosters learning and scientific discovery. Many thanks to my Ph.D. advisory committee, Dr. Hans-Jörg Schanz, Dr. Douglas Masterson, Dr. John Pojman, Dr. Stephen Boyes and past committee member Dr. David Creed for their time, guidance, and constructive criticism. Dr. Alvin Holder is also acknowledged for being a friend and mentor. Special thanks to Rosie Stuart, Sharon King, and Dr. Robert Bateman for all their assistance over the years. Also, I would like to acknowledge Dr. Gordon Cannon for inviting me to pursue graduate studies in the Department of Chemistry and Biochemistry.

I am grateful to my fellow graduate colleagues and the members of the Lowe Research Group, both past and present, for their friendship and support. Past and present members of AGEM are acknowledged for their camaraderie and support as well. Special thanks to Andre Heath, Dr. Joe Whitehead, and Dr. Rex Gandy for all their support over the years.

Past and present financial support throughout my graduate career, which includes AGEM of the National Science Foundation, MRSEC program of the National Science

Foundation (DMR-0213883) and the Department of Education-funded GAAN program (P200A060323), is gratefully acknowledged.

Finally, I would like to express sincere gratitude to my wife, children, family and friends for unwavering love, words of encouragement, and support throughout my graduate career. Thanks for keeping me grounded. I wouldn't have made it without you. I love you all.

TABLE OF CONTENTS

ABSTRACT	ii
DEDICATION.....	v
ACKNOWLEDGMENTS.....	vi
LIST OF FIGURES.....	x
LIST OF SCHEMES.....	xiv
LIST OF TABLES.....	xvi
CHAPTER	
I. INTRODUCTION.....	1
Water-soluble Polymers.....	1
General Considerations for Water-soluble Polymers.....	2
Ion-containing (co)polymers.....	5
Polyelectrolytes.....	5
Polyzwitterions.....	10
Controlled/‘Living’ Polymerization.....	19
Ring-Opening Metathesis Polymerization (ROMP).....	22
Accepted Mechanism and Other Aspects of ROMP.....	23
Living Ring-Opening Metathesis Polymerization (LROMP).....	32
III-defined ROMP Initiators.....	34
Well-defined ROMP Initiators.....	34
Synthesis of Ion-containing (co)polymers via Classical ROMP, LROMP, and Homogeneous Aqueous LROMP.....	51
II. OBJECTIVES OF RESEARCH.....	63
III. THE CONTROLLED HOMOGENEOUS ORGANIC SOLUTION POLYMERIZATION OF NEW HYDROPHILIC CATIONIC <i>exo</i> -7- OXANORBORNENE WITH $\text{RuCl}_2(\text{Cy}_3)_2\text{CHPh}$ IN A NOVEL 2,2,2 TRIFLUOROETHANOL/METHYLENE CHLORIDE SOLVENT MIXTURE.....	68
Introduction.....	68

	Experimental.....	68
	Results and Discussion.....	77
	Summary/Conclusions.....	102
IV.	OBSERVATION ON THE EFFECT OF HALIDE COUNTERION IN THE ROMP OF THE <i>exo</i> -7-OXANORBORNENE DERIVATIVES <i>exo</i> -BENZYL-[2-(3,5-DIOXO-10-OXA-4-AZA- TRICYCLO[5.2.1.0 ^{2,6}]DEC-8-EN-4-YL)-ETHYL]DIMETHYL AMMONIUM BROMIDE/CHLORIDE IN 2,2,2- TRIFLUOROETHANOL/METHYLENE CHLORIDE.....	104
	Introduction.....	105
	Experimental.....	105
	Results and Discussion.....	106
	Summary/Conclusions.....	117
V.	NEW WELL-DEFINED POLYMERIC BETAINES: FIRST REPORT DETAILING THE SYNTHESIS AND ROMP OF SALT-RESPONSIVE SULFOPROPYLBETAINE- AND CARBOXYETHYLBETAINE- <i>exo</i> -7-OXANORBORNENE MONOMER.....	119
	Introduction.....	119
	Experimental.....	120
	Results and Discussion.....	126
	Summary/Conclusions.....	146
VI.	CONCLUSIONS AND FUTURE DIRECTIONS.....	148
	REFERENCES.....	151

LIST OF FIGURES

Figure

I-1.	Functional groups that impart water solubility.....	2
I-2.	Structural representations of polymer architectures accessible by CLP.....	4
I-3.	Examples of A)anionic and B) cationic polymers.....	6
I-4.	A plot of intrinsic viscosity versus salt concentration illustrates the Hydrodynamic volume of the polycation decreasing with increasing ionic strength.....	7
I-5.	Examples of amine-containing and specialty cationic monomers.....	8
I-6.	A plot of intrinsic viscosity versus salt concentration illustrates the hydrodynamic volume of the polybetaine decreasing with increasing ionic strength.....	11
I-7.	Examples of well-known betaine structures.....	13
I-8.	Common synthetic routes for carboxybetaines (a, b), sulfobetaines (c), phosphobetaines (d), and dicyanoetheneolate betaines (e).....	14
I-9.	Variations of olefin metathesis reactions.....	22
I-10	Early proposed olefin metathesis intermediates that were later disapproved.....	23
I-11.	Proposed mechanism for ROMP of a cyclic alkene.....	25
I-12.	Examples of functionalized norbornene-based monomers (M17-M30) used in ROMP.....	29
I-13.	Various possible combinations of triad tacticity and double-bond Stereochemistry in polynorbornene.....	31
I-14.	Diagnostic plots of $\ln[M]_0/[M]_t$ versus time and M_n versus conversion.....	33
I-15.	Ta catalysts used for obtaining norbornene polymers with narrow MMDs.....	36
I-16.	Example of W-based well-defined Schrock complexes.....	37
I-17.	Tungsten-based oxo-alkylidene complex.....	38

I-18.	Examples of well-defined Mo-based Schrock complexes.....	39
I-19.	Examples of commercially available Grubbs-Hoyveda Ru-complexes.....	47
I-20.	Examples of water-soluble Ru-complexes based on Grubbs-types catalysts.....	50
II-1.	Structure of a series of new permanently cationic ammonium <i>exo</i> -7-oxanorbornene derivatives M31	65
II-2.	Structure of <i>exo</i> -benzyl-[2-(3,5-dioxo-10-oxa-4-aza-tricyclo[5.2.1.02,6]dec-8-en-4-yl)ethyl]dimethyl ammonium bromide/chloride MON	66
II-3.	Structures of <i>exo</i> -propylsulfobetaine-[2-(3,5-dioxo-10-oxa-4-aza-tricyclo[5.2.1.02,6]dec-8-en-4-yl)ethyl]dimethyl ammonium M32 , <i>exo</i> -propylcarboxy-[2-(3,5-dioxo-10-oxa-4-aza-tricyclo[5.2.1.02,6]dec-8-en-4-yl)ethyl]dimethyl ammonium M33 and <i>exo</i> -propyl-[2-(3,5-dioxo-10-oxa-aza-tricyclo[5.2.1.02,6]dec-8-en-4-yl)ethyl]dimethyl ammonium bromide M34	67
III-1.	¹ H (A) and ¹³ C (B) NMR spectra of Bn-quat-Br recorded in D ₂ O with peak assignments.....	78
III-2.	¹ H NMR spectra demonstrating the increase in conversion with time using a comparison of the monomer vs polymeric vinylic signals for a Bn-quat-Br homopolymerization.....	82
III-3.	First order kinetic profiles and conversion vs time plots for the homopolymerization of Bn-quat-Br (A), Prop-quat-Br (B), and Pen-quat-Br (C).....	85
III-4.	ASEC traces (RI signal) for Et-quat-Br (A) and Pen-quat-Br (B) homopolymers with a target M _n of 20,000.....	88
III-5.	¹ H NMR spectrum of a Pen-quat-Br homopolymer (M _{n,theory} = 4,000) recorded in d ₆ -DMSO.....	91
III-6.	M _n vs conversion plot for a Prop-quat-Br homopolymer.....	93
III-7.	¹ H NMR spectrum of a poly(Et-quat-Br-stat-Pent-quat-Br) copolymer with the ASEC trace (RI signal) shown as the inset.....	94
III-8.	ASEC traces (RI signals) demonstrating the formation of a poly(Prop-quat-Br-block-Et-quat-Br) copolymer.....	96
III-9.	ASEC traces (RI signal) for Prop-quat-Br homopolymers prepared using	

	TCE (A) and HFIP (B) as halogenated alcoholic cosolvents.....	98
III-10.	³¹ P NMR spectra of <u>17</u> recorded in a 1:1 TFE/CD ₂ Cl ₂ solvent mixture.....	99
III-11.	First order kinetic profiles for the homopolymerization of Bn-quat-Br (A) and Bn-quat-Cl (B) using <u>17</u> in TFE/CH ₂ Cl ₂ 1:1.....	102
IV-1.	Chemical structures of monomer substrates, MON , and Grubbs' first generation catalyst, <u>17</u>	107
IV-2.	Conversion vs. time and pseudo first order kinetic plots for the homopolymerization of MON with X = Cl (filled symbols) or Br (open symbols) with <u>17</u> in TFE/CH ₂ Cl ₂ at RT.....	108
IV-3.	The ASEC traces (RI signal) for homopolymers derived from MON-Bn-Cl and MON-Bn-Br polymerized with <u>17</u> under identical conditions.....	110
IV-4.	Pseudo-first order rate plots and conversion vs. time plots for the statistical copolymerization of MON-Bn-Cl with MON-Bn-Br using <u>17</u> at varying molar ratios.....	112
IV-5.	ASEC traces (RI signal) demonstrating the evolution of M _n as a function of polymerization time for the 25:75 copolymerization.....	114
IV-6.	Evolution of M _n as a function of conversion as determined by ASEC for all three statistical copolymerizations of MON-Bn-Cl with MON-Bn-Br	115
IV-7.	ASEC traces (RI signal) for copolymers of MON-Bn-Cl with MON-Bn-Br at three different molar ratios, 75:25 (solid line), 50:50 (dashed line), and 25:75(dotted line).....	116
V-1.	Chemical structures of the sulfopropylbetaine, M32 , carboxyethylbetaine, M33 , and propyl-quaternized cationic, M34 , exo-7-oxanorbornene monomers, and Grubbs' first generation initiator, <u>17</u>	127
V-2.	¹³ C NMR spectra of M32 recorded in D ₂ O/NaCl and M33 recorded in d ₆ -DMSO.....	128
V-3.	A series of ¹ H NMR spectra from the homopolymerization of M32 with <u>17</u> , recorded in D ₂ O/NaCl, demonstrating conversion of monomer to polymer as well as the resulting stereochemistry in the polymer backbone. The polymerization was conducted in TFE/CH ₂ Cl ₂ at ambient temperature with <u>17</u>	130

V-4.	Conversion vs. time and pseudo first-order rate plot for the homopolymerization of the sulfopropylbetaine M32 with 17 at 7.38 wt % and ambient temperature.....	132
V-5.	The ASEC trace (RI signal) for a poly M32 homopolymer with a theoretical M_n of 9,100. Analysis was conducted in 0.25M NaBr at a flow rate of 1.0 mL/min. The system was calibrated with a series of narrow molecular weight distribution poly(ethylene oxide) standards.....	134
V-6.	^1H NMR spectrum of a poly M32 homopolymer recorded in $\text{D}_2\text{O}/\text{NaCl}$ with a theoretical M_n of 9,100.....	135
V-7.	ASEC traces (RI signal) for the self-blocking experiment with the sulfopropylbetaine M32 . Analysis was conducted in 0.25M NaBr at a flow rate of 1.0 mL/min. The system was calibrated with a series of narrow molecular weight distribution poly(ethylene oxide) standards.....	137
V-8.	Conversion and kinetic profile for the homopolymerization of the protonated carboxyethylbetaine H-M33 with 17 in TFE/ CH_2Cl_2 at ambient temperature.....	139
V-9.	ASEC traces (RI signal) for the block copolymerization of the sulfopropylbetaine M32 with the propylquat M34 . Analysis was conducted in 0.25M NaBr at a flow rate of 1.0 mL/min. The system was calibrated with a series of narrow MMD poly(ethylene oxide) standards.....	143
V-10.	Hydrodynamic diameter size distributions, as determined by dynamic light scattering, for the M32-M34 AB diblock copolymer in the presence and absence of NaCl. Measurements were made on 0.5 wt% polymer solutions.....	145

LIST OF SCHEMES

Scheme	
I-1.	Introduction of chain end functionality via a chain transfer agent.....26
I-2.	Synthesis of titanacyclobutane complex 935
I-3.	Synthesis of well-defined Ru complexes.....42
I-4.	Preparation of triblock copolymers under ‘living’ ROMP.....43
I-5.	Synthesis of Ru NHC carbene catalyst 19 and 2045
I-6.	Diels-Alder reaction of cyclopentadiene and maleic anhydride and thermal isomerization of the kinetically favored <i>endo</i> -isomer to the more thermodynamically stable <i>exo</i> -isomer.....46
I-7.	Synthetic pathways to polyanions under ROMP conditions using transition metal salt as initiators A) hydrolysis of the anhydride polymer B) hydrolysis of the di-ester polymer C) conversion to the di-acid followed by hydrophobic functionalization followed by hydrolysis and D) conversion of the anhydride monomer to the di-ester, ROMP of the di-ester with decyl norbornene followed by hydrolysis of the di-ester repeat unit.....52
I-8.	LROMP of a norbornene-based ester followed by post polymerization modification to yield the corresponding anionic polyelectrolyte.....53
I-9.	A synthetic route to amphiphilic polyelectrolytes A) cationic amphiphilic polyelectrolytes B) anionic amphiphilic polyelectrolytes derived from 6,6'-dimethylfulvene and maleic anhydride and C) cationic amphiphilic polyelectrolytes D) anionic amphiphilic polyelectrolytes derived from 6-isopropylfulvene and maleic anhydride.....55
I-10.	Synthesis of poly(5-norbornene-2,3-dicarboxylic acid-block-norbornene) via LROMP.....56
I-11.	‘Proof-of-concept’ of homogeneous aqueous LROMP.....59
I-12.	Aqueous ROMP of A) M28 and B) M30 using catalyst 25 under acid conditions.....60
I-13.	Aqueous ROMP of M30 using catalyst 26 without acid.....61

I-14.	Aqueous ROMP of M30 using catalyst 27 or 28 without acid.....	62
III-1.	Synthetic outline for the preparation of the permanently cationic <i>exo</i> -7-oxanorbornene derivatives M31	79
V-1.	Outline for the preparation of the sulfopropylbetaine M32 and carboxyethylbetaine M33 . The intermediate tertiary amine, <i>exo</i> -4-(2-dimethylaminoethyl)-10-oxa-4-azatricyclo[5.2.1.0 ^{2,6}]dec-8-ene-3,5-dione (DMAETDD), was prepared from the reaction of N,N-dimethylethylenediamine with <i>exo</i> -3,6-epoxy-1,2,3,6-tetrahydrophthalic anhydride in a mixture of tetrahydrofuran (THF) and methanol. Subsequent reaction of DMAETDD with 1,3-propanesultone or β -propiolactone in THF yields M32 and M33 respectively.....	127
V-2.	Cartoon demonstrating the salt-induced assembly/disassembly of the M32-M34 AB diblock copolymer.....	146

LIST OF TABLES

Table

I-1.	Functional group tolerance of metal carbene complexes.....	41
III-1.	Summary of the Theoretical and Experimentally Determined Molecular Characteristics for the Cationic (Co)polymers Including the Molecular Masses, Polydispersity Indices, Compositions, R_p Values, and % Trans Content.....	84
V-1.	Summary of the theoretical M_n , measured M_n and M_w/M_n , and the experimentally determined k_p values from the homopolymerizations of the sulfopropylbetaine M32 and the protonated carboxyethylbetaine H-M33	140

CHAPTER I

INTRODUCTION

Water-soluble Polymers

Water-soluble (co)polymers (WSPs) may be categorized into four general classes: biopolymers, nonionic, ionic, and associative materials.¹ Such polymers constitute a diverse class of macromolecules with biopolymers playing an important role in the mediation of life processes to synthetic polymers having a wide range of commercial applications.¹ Interestingly, a number of WSPs may exhibit complex aqueous solution behavior as a result of changes in temperature, pH, and salt concentration. These changes in the aqueous environment can bring about supramolecular self-assembly or more simple conformational changes, many of which are often reversible. Polymers possessing this aqueous solution behavior are termed stimulus responsive, or “smart”, polymers in which macromolecular self assembly, phase transitions, or conformational changes may occur in response to one or a combination of applied external stimuli (i.e. temperature, pH, and/or salt concentration).² From an environmental standpoint, WSPs have been the focus of considerable interest due to the demand for water-based polymeric materials instead of the traditional organic solvent-based species. Given this, over the past two decades considerable research emphasis has been placed on the development of controlled/“living” polymerization (CLP) methodologies that yield WSPs with precise molecular masses (MMs), advanced macromolecular architectures, and a high degree of functionality.³

General Considerations for Water-soluble Polymers

The simplest way to obtain WSPs is, of course, to directly polymerize appropriate water-soluble monomers. Clearly, the hydration of the polymer depends on the type of water-soluble functional groups. A large number of functional groups are capable of rendering a polymer water-soluble, examples of which are shown below in Figure I-1.

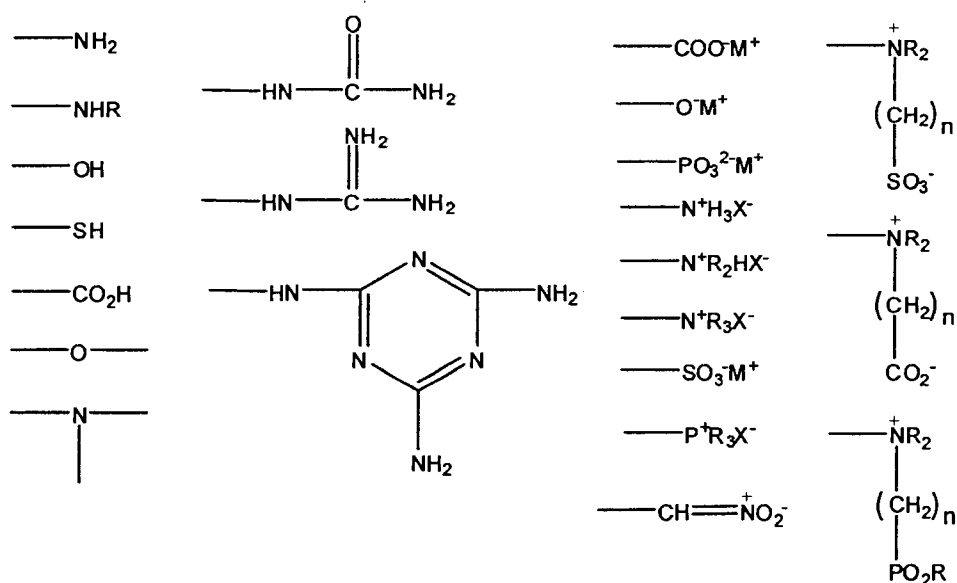


Figure I-1. Functional groups that impart water solubility.

Recognizably, key structural features of WSPs dictate their solution properties and performance in an end application. For instance, primary structure relates to the nature of the repeat unit (i.e., bond lengths and valence bond angles), effective compositions, and location of functional groups along the polymer backbone. The primary structure of WSPs can be derived from the same monomer repeat unit or different monomer repeat units. Depending on the placement of these monomer units, various polymer architectures, including statistical (1), alternating (2), AB diblock (3), ABA triblock (4), ABC triblock (5), AB tapered block (6), graft (7), and star (8) can be

obtained via CLP methodologies (Figure I-2). Another important structural consideration is the secondary structure of WSPs which relates to configuration, conformation, and intramolecular effects such as hydrogen bonding and ionic interactions. In addition to primary and secondary structural considerations, tertiary structure involves intermolecular and water-polymer interactions, while multiple chain aggregation or complexation is required for quaternary structure.

Given the aqueous solution behavior that many WSPs exhibit – at least in terms of conformational changes – their behavior may be described by the hydrodynamic volume (HDV), which is the volume occupied in solution by a solvated chain. The HDV may be greatly influenced by repulsive or attractive ionic interactions. Intrinsic viscosity $[\eta]$ may be obtained from dilute solution measurements, which correlates directly to the HDV of the polymer chain. The Mark-Houwink-Sakurada relationship relates the molecular mass M of a polymer to the intrinsic viscosity $[\eta]$, where K and a are constants that vary with polymer, solvent, and temperature (1).⁴

$$[\eta] = KM^a \quad (1)$$

In addition to intrinsic viscosity $[\eta]$, light scattering techniques can be used to determine HDV, morphology, and may be used along with microstructure to predict rheological behavior.¹

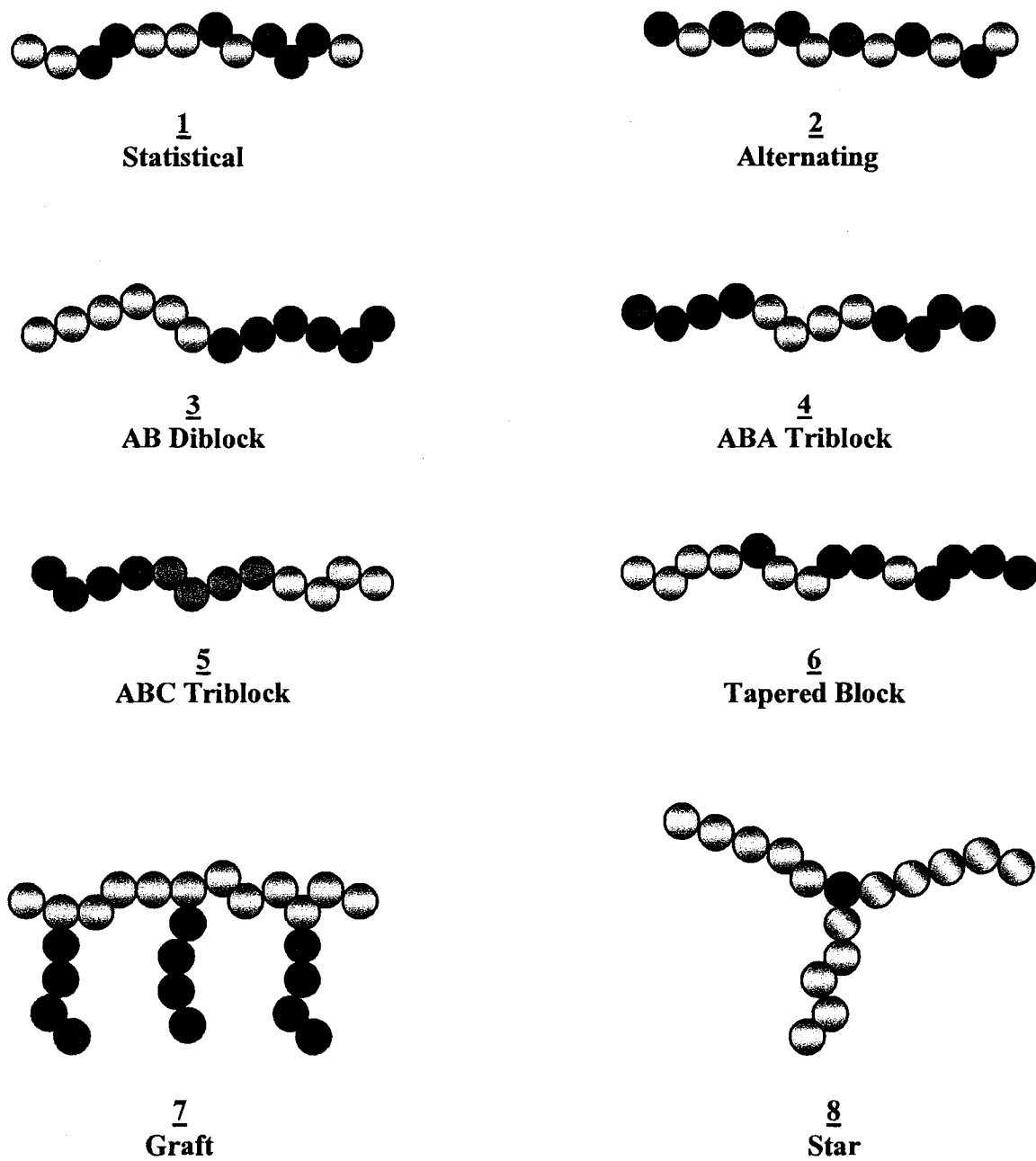


Figure I-2. Structural representations of polymer architectures accessible by CLP.

Ion-containing (co)polymers: Polyelectrolytes and Polyzwitterions

Ion-containing (co)polymers are an important class of WSPs with a variety of commercial applications including water treatment, paper making, mining, pharmaceuticals, personal care products, drag reduction, and enhanced oil recovery.^{1,5} As a result of anionic, cationic, or zwitterionic pendent groups along the polymer backbone, ion-containing (co)polymers possess interesting aqueous solution properties. Ion-containing (co)polymers may be divided into two broad groups: polyelectrolytes and polyzwitterions.⁶ In fact, the aqueous solution properties of polyelectrolytes and polyzwitterions are profoundly different and is dictated primarily by the intra- and intermolecular electrostatic interactions that occur among the charged groups in aqueous media.

Polyelectrolytes

Although the study of the ionization of poly(acrylic acid) and its solution behavior was reported in 1938,⁷ it was not until 1948 that the term “polyelectrolyte” was coined by Fuoss.⁸ Polyelectrolytes contain the same charged functional pendent groups along the polymer chain. As a result, polyelectrolytes may be divided into two subgroups: polyanions (i.e. polymers containing *negatively* charged functional groups) and polycations (i.e. polymers containing *positively* charged functional groups) as shown in Figure I-3. The counterions, or gegenions, that accompany the negative or positive charge results in electroneutrality of the polyion.⁹ By tailoring the molecular structure, solution pH, temperature, and added low molecular weight electrolyte (e.g. NaCl) it is often possible to induce large conformational changes in aqueous media.³

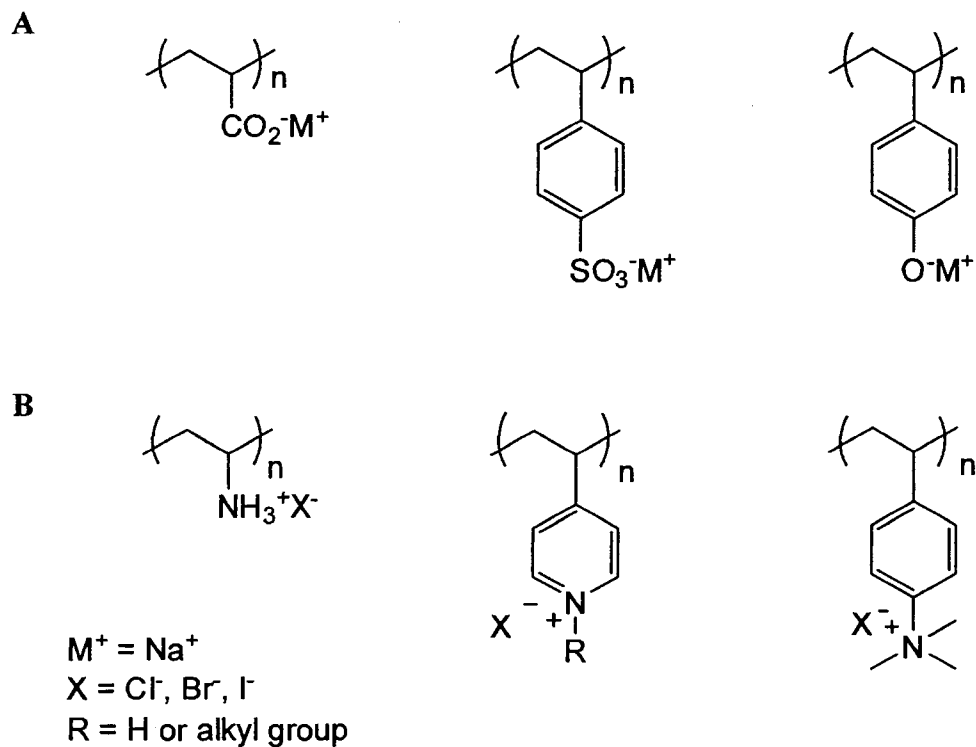
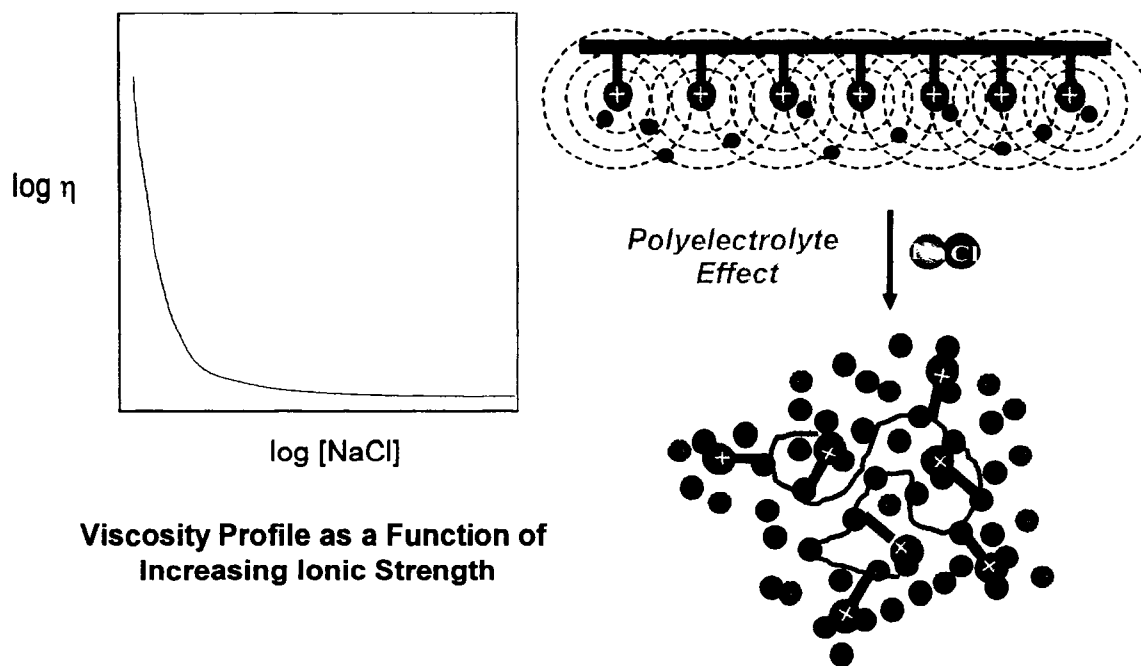


Figure I-3. Examples of A) anionic polymers and B) cationic polymers.

Polyelectrolytes are well known for their salt responsive behavior in aqueous solution.⁸⁻¹⁰ For example, in salt free aqueous media, the repulsive coulombic forces between mutually charged functional groups along the polyelectrolyte chain results in expansion of the polymer chain as evidenced by an increase in the HDV of the polyelectrolyte coil to an essentially rod-like conformation. However, the addition of a low molecular weight electrolyte (e.g. NaCl) results in the shielding of these repulsive forces thereby decreasing the HDV and leading to a lowering of solution viscosity and an adoption of a more compact, entropically favored conformation. Such aqueous solution behavior is termed the *polyelectrolyte effect* (Figure I-4).⁸



Viscosity Profile as a Function of Increasing Ionic Strength

Figure I-4. A plot of intrinsic viscosity versus salt concentration illustrates the hydrodynamic volume of the polycation decreasing with increasing ionic strength.

Cationic Polyelectrolytes. As mentioned above, cationic polymers (polycations) are one of two classes of polyelectrolytes with anionic polymers (polyanions) being the other. The properties of cationic polymers are derived from the density and distribution of positive charges along the macromolecular backbone and polymer molecular mass. In fact, cationic polymers have been evaluated for a wide range of applications such as water purification, antimicrobial coatings, additives for cosmetics, and gene vectoring agents.¹⁰ The conformation and solubility of such polymers depends on the degree of ionization and interaction of positively charged functional groups in water. Cationic polymers may be derived from amino containing 2-, 3-, and 4-vinylpyridines (**M1-M3**), amino styrenics (**M4, M5**), ethyleneimine (**M6**), oxazoline (**M7**), N-vinylamides (**M8**,

M9), acrylamide (**M10**), phosphonium (**M11**), sulfonium (**M12**), pyrylium (**M13**) methacrylate (**M14**), methacrylamide (**M15**), and diallyl ammonium (**M16**) based monomers (Figure I-5).¹

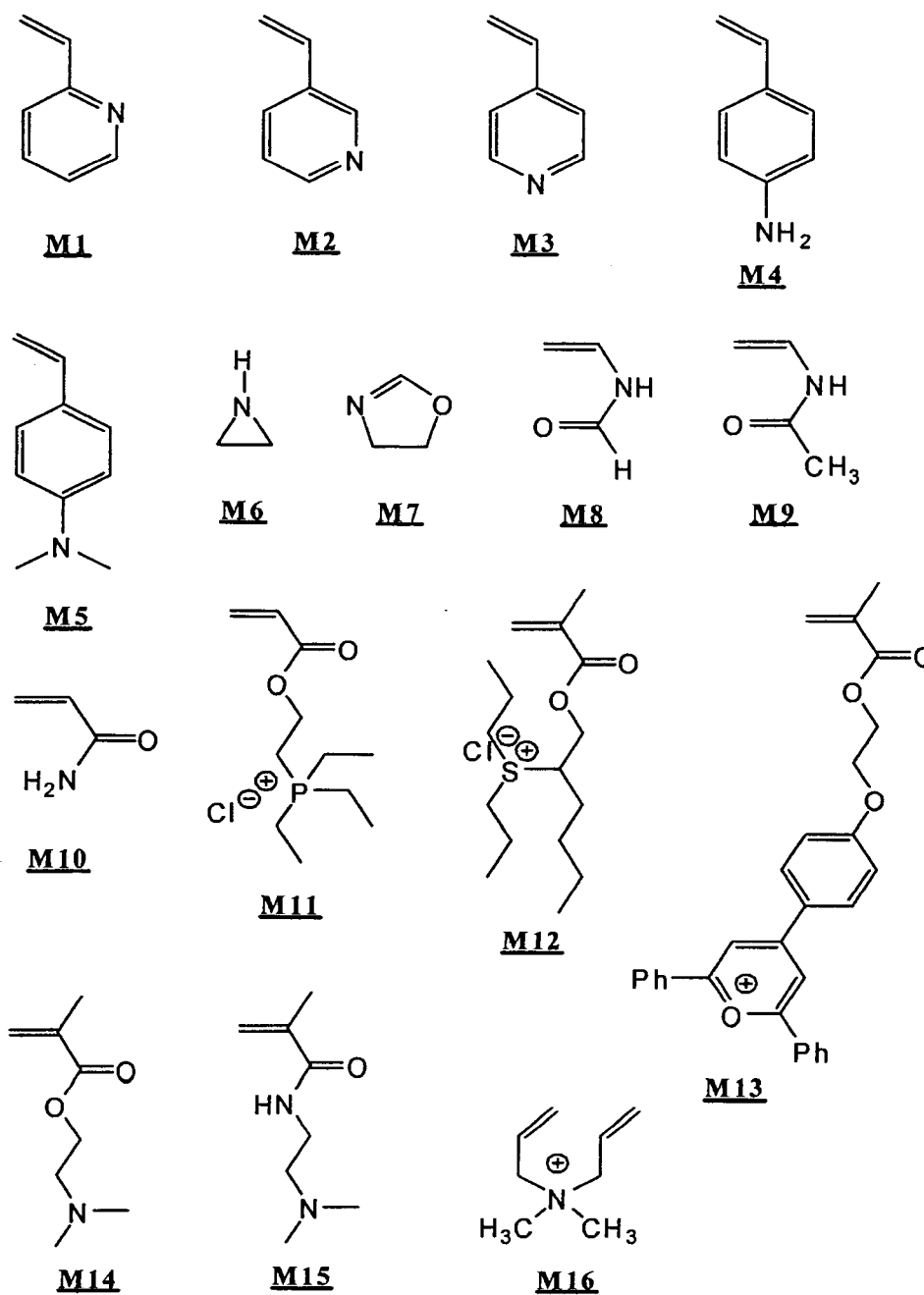


Figure I-5. Examples of amine-containing and specialty cationic monomers.

Amphiphilic Polyelectrolytes. Amphiphilic polyelectrolytes, or hydrophobically modified polyelectrolytes (HMPs), are one of the most important classes of polyelectrolytes, possessing both ionizable groups and hydrophobic groups along or pendent to the polymer backbone.¹¹ Actually, amphiphilic polyelectrolytes is a more general term for this class of ionic polymer with HMPs suggesting a low content of hydrophobes. Amphiphilic polyelectrolytes undergo self-assembly in aqueous media due to secondary forces such as electrostatic, hydrogen bonding, van der Waals, and hydrophobic interactions.

In fact, hydrophobic interactions are most prevalent in water, which leads to a greater increase in entropy, for self-association of hydrophobic domains in amphiphilic polyelectrolytes. Such self-associations are analogous to low molecular weight surfactants. The addition of organic molecules (e.g. alcohols and urea) to the aqueous media breaks up these micellar nanostructures. The first report of amphiphilic polyelectrolytes was by Strauss and co-workers in 1951, in which poly(2-vinylpyridine) was quaternized with *n*-dodecyl bromide yielding a “polysoap”.¹² It was demonstrated that the polymer had a compact conformation in water due to the hydrophobic/self-association of the dodecyl side chain groups. Also, the polymer exhibited analogous behavior to low molecular weight surfactant micelles, since hydrophobic small molecules were able to be solubilized in aqueous media.

The field remained dormant for ca. 30 years when it was realized amphiphilic polyelectrolytes were capable of forming organized structures in aqueous media. In fact, amphiphilic polyelectrolytes are thought to be simple model systems for understanding

biological phenomena such as substrate binding by naturally occurring enzymes, intercalation of carcinogenic substances into DNA strands, and the denaturation of proteins and DNA.¹¹

As a result of their unique aqueous solution behavior, amphiphilic polymers exhibit interesting rheological properties and phase behavior making them useful for a variety of commercial applications such as associative thickeners, rheology modifiers, polymer-based surfactants, emulsifiers, solubilizers, flocculants, and colloids.^{2,13-19} From an industrial and commercial products standpoint, such polymers can be used in the manufacture of paint, coatings, printing, paper, ceramics, drugs, and cosmetics and personal care products.¹¹ Since some amphiphilic polyelectrolytes are sensitive to changes in conditions such as salt concentration, pH, temperature, and shear stress, these stimulus-responsive polymer systems are capable of capturing and delivering materials making them useful in pharmaceutical and environmental applications.^{20,21}

Polyzwitterions

Polyzwitterions (amphoteric polymers) are ionic polymers that can be further divided into two subgroups: polyampholytes and polybetaines.⁶ Polyampholytes contain positive and negative charges on *different* monomer repeat units, whereas polybetaines (polymeric betaines) contain both positive and negative charges on the *same* monomer repeat unit. The salt responsive behavior of polyzwitterions is opposite from polyelectrolytes. Hence, net attractive coulombic interactions between positively and negatively charged repeat units of polyzwitterions *reduce* the HDV resulting in the polymer chain having a collapsed or compact polymer chain conformation in salt free

aqueous media. In some cases, these attractive coulombic electrostatic interactions are so strong that the polyelectrolyte may be insoluble under these conditions with the effective formation of an ionically crosslinked 3D network. However, upon the addition of a low molecular weight electrolyte (e.g. NaCl) the attractive electrostatic coulombic interactions are screened and the polymer subsequently adopts a more expanded conformation. This aqueous solution behavior is termed the *anti-polyelectrolyte effect*, and results in an increase in the polymer chain's HDV and solution viscosity (Figure I-6).⁶

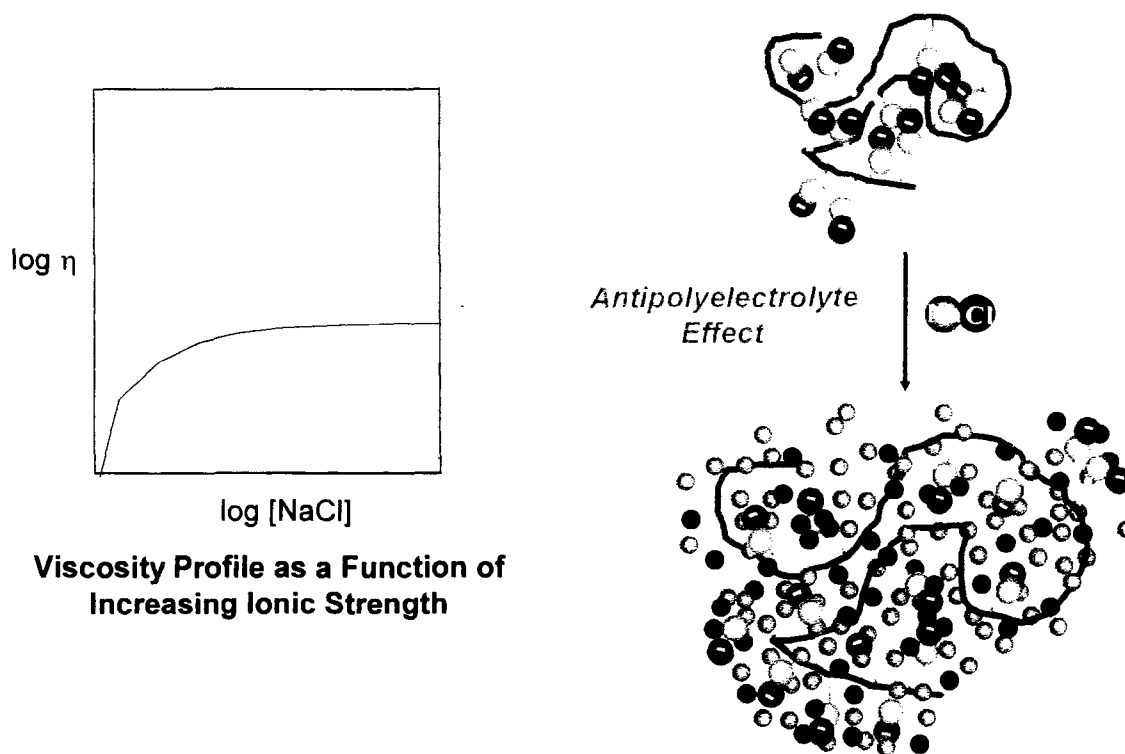
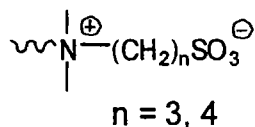
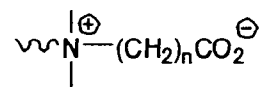
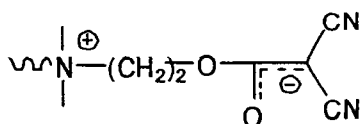
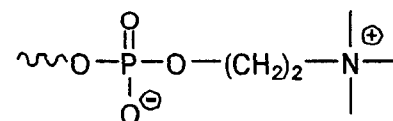


Figure I-6. A plot of intrinsic viscosity versus salt concentration illustrates the hydrodynamic volume of the polybetaine increasing with increasing ionic strength.

Polybetaines. Polymeric betaines are a class of polyzwitterions that contain both cationic and anionic groups on the same monomer repeat unit.⁶ Usually the cationic component is a quaternary ammonium species while the anionic species can be either a sulfonate (sulfobetaines), carboxylate (carboxybetaine), phosphate/phosphonate/phosphinate (phosphobetaines), or a dicyanoethenolate (Figure I-7).⁶ The complex aqueous solution behavior of polybetaines can vary depending on the type of polybetaine, which make them excellent examples of stimulus-responsive materials. For instance, polybetaines are capable of undergoing reversible conformational changes and phase transitions in response to changes in salt concentrations. Although polybetaines are electrically neutral, the attractive forces between the anionic and cationic functional groups form an ionically cross-linked network which typically renders polymeric betaines insoluble in aqueous media (i.e. the electrostatic forces outweigh the osmotic forces that allow solvent into the network which facilitate dissolution).¹⁰

Polybetaines are of great interest because of their structural resemblance to biopolymers and biomembranes. Polybetaines have a number of biomedical applications because of their biomimetic and anti-adherent properties.²² The four well-known classes of betaines are shown in Figure I-7.

**Sulfobetaine****Carboxybetaine****Dicyanoethenolate betaine****Phosphobetaine****Figure I-7.** Examples of well-known betaine structures.

There are a number of ways to synthesize polymeric betaines (Figure I-8). For instance, sulfobetaines are usually prepared by the nucleophilic ring opening of 1,3-propanesultone or 1,4-butanedisultone by a tertiary amine.⁶ Carboxybetaines may be synthesized by a number of routes. For example, tertiary amines can react with α,β -unsaturated acids (e.g. acrylic acid) to yield the carboxybetaine, however this route often gives a mixture of betaine and salt products. The reaction of a tertiary amine with either haloalkylcarboxylates or haloalkylcarboxylic esters is an alternative. Lactones (carbon analogues of sultones) have also been used for the preparation of carboxybetaines, however, their use is limited to the 4 membered ring analogs since higher lactones are prone to nucleophilic attack at the C=O group. Dicyanoethenolate betaines can be synthesized from the reaction of tertiary amine with dicyanoethylene or propylene acetals, e.g. 2,2-dicyanoketene ethylene acetal.⁶ Phosphobetaines are most commonly prepared *via* a two step procedure from the reaction of an alcohol-containing monomer

with 2-chloro-2-oxo-1,3,2-dioxaphospholane followed by ring opening of the intermediate phospholane with trimethylamine.⁶ Several other methods exist, which are covered in comprehensive reviews by Nakaya et al.²³ and, more recently, Kudaibergenov et al.²⁴

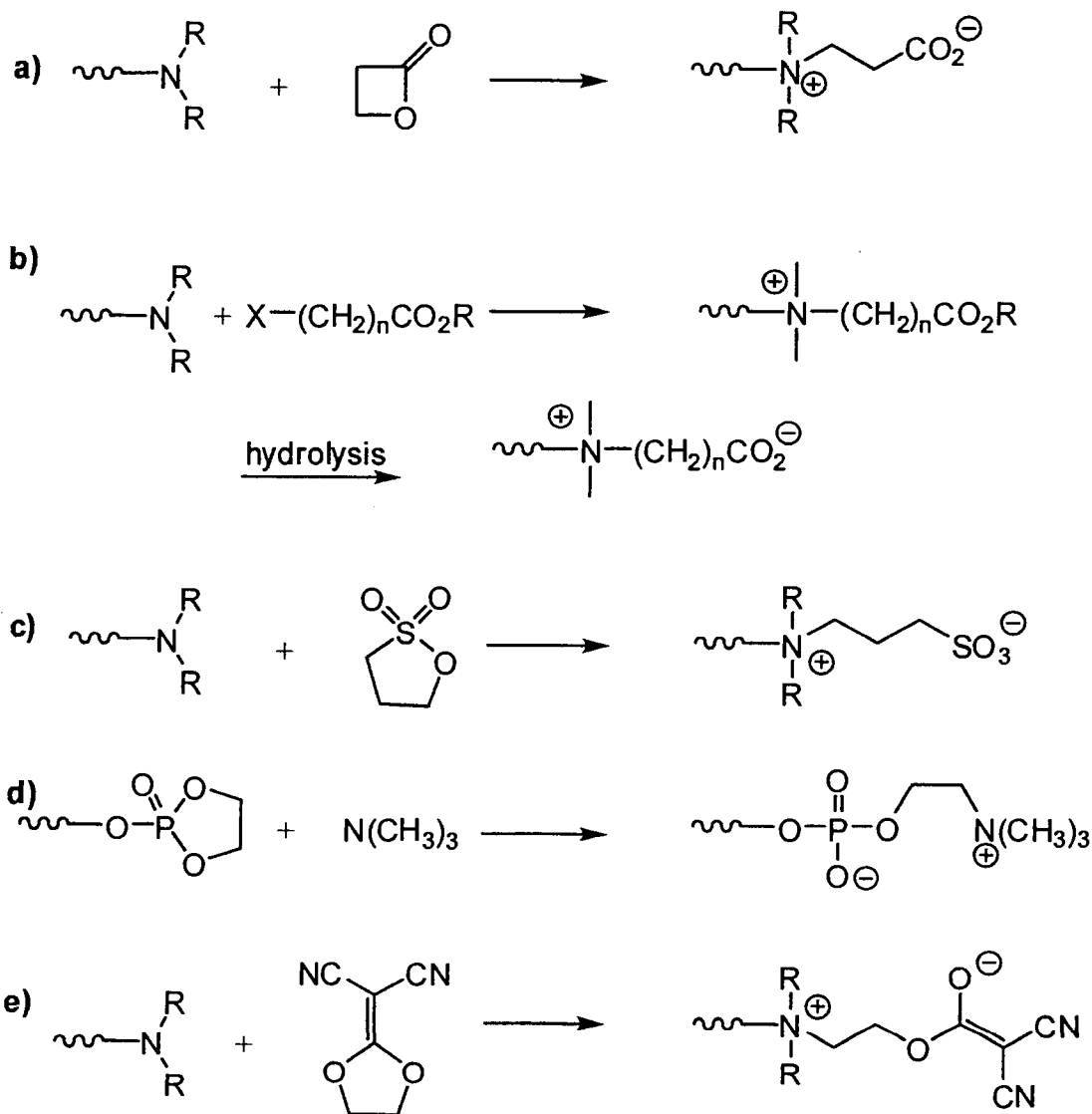


Figure I-8. Common synthetic routes for carboxybetaines (a, b), sulfobetaines (c), phosphobetaines (d), and dicyanoetheneolate betaines (e).

The first example of a synthetic polybetaine was reported by Ladenheim and Morawetz in 1957, and was a polycarboxybetaine derivative of poly(4-vinylpyridine).²⁵ Subsequently, Hart and Timmerman reported the synthesis of the first synthetic polysulfobetaine by quaternizing 2-vinylpyridine and 4-vinylpyridine with 1,4-butanedisulfone.²⁶ The betaine monomer was polymerized directly *via* aqueous free radical polymerization. Since these initial reports, numerous other groups have synthesized and studied the solution properties of polybetaines. For example, Galin et al. studied the solution properties of a series of aromatic and aliphatic poly(sulfopropylbetaines).²⁷ Salamone et al. synthesized poly(vinylimidazolium sulfobetaine) and studied its aqueous solution properties in which several of the polymers were shown to have hydrogel characteristics.²⁸ Itoh et al. investigated the aqueous solution properties of poly(4-vinylpyridinium sulfopropylbetaine) and poly(3-methacryloxyethoxy-carboxylpyridinium sulfopropylbetaine).²⁹ It was found that these polymers were soluble in salt solution and their intrinsic viscosity increased with salt concentration (as a result of the antipolyelectrolyte effect). Similarly, Schulz et al. performed detailed studies on the phase behavior and solution properties of poly[*N*-(3-sulfopropyl)-*N*-methacryloxyethyl-*N,N'*-dimethyl ammonium betaine] using static and dynamic light scattering as well as Raman spectroscopy.³⁰ McCormick et al. reported the synthesis and viscometric studies of poly(2-acrylamido-2-methylpropanesulfonate) and poly(2-acrylamido-2-methylpropanedimethylammonium chloride) in which the reduced viscosity was found to be a function of polymer composition, charge distribution and increasing temperature.³¹ Lee et al. have prepared styrene-[*N,N'*-dimethyl(maleimidopropyl)ammonium propane sulfonate] copolymers and studied their aqueous solution properties.³²

It is clear that the synthesis of polymeric betaines has been primarily accomplished *via* the direct conventional free radical solution polymerization of betaine monomers; however, such a synthetic approach yields materials with broad molecular mass distributions (MMDs) and poorly defined microstructures. The preparation of polymeric betaines under controlled/'living' conditions has been altogether more challenging due to the limited solubility of betaine monomers/polymers^{33,34} as well as finding suitable CLP techniques/conditions that are compatible with the substrates. Therefore, very few examples of well-defined polymeric betaines have been reported in literature.

The first examples of well-defined polymeric betaines, i.e. those with predetermined MMs, narrow MMDs, and advanced architectures, were reported by Lowe et al.³⁵⁻³⁸ in the 1990's. These well-defined materials were prepared indirectly *via* the alkylation of tertiary amine-containing precursor (co)polymers with 1,3-propanesultone. Specifically, (co)polymers containing 2-(dimethylamino)ethyl methacrylate were synthesized *via* group transfer polymerization (GTP) and subsequently modified *via* reaction at the tertiary amine residues with 1,3-propanesultone under facile conditions to yield the corresponding polysulfopropylbetaines. While this approach was effective, it is not ideal since GTP is challenging to execute and such post-polymerization modification reactions are rarely quantitative.

The advent of the controlled/'living' radical polymerization (CLRP) techniques – such as nitroxide mediated polymerization (NMP), atom transfer radical polymerization (ATRP), and reversible-addition fragmentation chain transfer (RAFT) - has allowed for both direct and indirect synthetic pathways toward polybetaines with well-defined

macromolecular architectures to be developed. For example, Jaeger and co-workers have published several reports detailing the synthesis of sulfo- and carboxybetaines *via* NMP utilizing post polymerization modification.³⁹⁻⁴⁴ For reasons mentioned above, such an approach does not lead to quantitative derivatization.

Due to the high temperatures usually required for NMP (>100°C), there are no examples of the direct polymerization of betaine monomers in aqueous media by this technique.⁴⁵ However, in the past decade several groups have reported the direct polymerization of betaine monomers in a controlled manner employing ATRP⁴⁶⁻⁴⁸ and RAFT polymerization,^{45,49-52} with RAFT proving to be the most versatile with respect to monomer choice. For example, in 2001 Lobb and co-workers first reported the controlled homopolymerization of 2-methacryloyloxyethyl phosphorylcholine (MPC) and its copolymerization with 2-(dimethylamino) ethyl methacrylate (DEA) to yield well-defined (co)polymers prepared *via* ATRP in aqueous and alcoholic media.⁴⁷ Although low PDIs (1.18-1.41) were obtained, the living characteristics of this polymerization were not thoroughly examined.

In 2002, Ma and co-workers reported the homopolymerization of MPC *via* ATRP in protic media in which the living characteristics such as first order monomer kinetics, linear M_n vs conversion plots, and low PDIs (1.15-1.35) were obtained in both aqueous and alcoholic media.⁴⁸ In fact, improved living characteristics were obtained in alcoholic media albeit at slower polymerization rates; however, faster polymerization rates were established with the addition of a small amount of water. In the following year, Ma et al. reported the synthesis of well-defined MPC block copolymers *via* ATRP in which the block copolymers were prepared by macroinitiators or sequential monomer addition.⁴⁶

For example, three types of macroinitiators based on poly(ethylene oxide) (PEO), poly(propylene oxide) (PPO), and poly(dimethylsiloxane) (PDMS) were employed for the preparation of block copolymers of PEO-MPC, PPO-MPC, and PDMS-MPC with the PPO-MPC block copolymer exhibiting thermoresponsive behavior.⁴⁶ Also, a variety of methacrylic comonomers were used in the sequential monomer addition route with MPC-[2-(dimethylamino)ethyl methacrylate] (DMAEMA) exhibiting thermo-responsive behavior and the MPC-[2-(diisopropylamino)ethyl methacrylate] (DiPAEMA) demonstrating pH-responsive behavior. In all cases, the PDIs were relatively low ($M_w/M_n = 1.1-1.3$).⁴⁸

Donovan and co-workers first reported the controlled homopolymerizations of 3-[2-(N-methylacrylamido)-ethyl dimethylammonio]propanesulfonate (MAEDAPS), 3-[N-(2-methacroyloxyethyl)-N,N-dimethylammonia]propanesulfonate (DMAPS), and 3-(N,N-dimethylvinylbenzylammonia)-propanesulfonate (DMVBAPS) in aqueous salt media (0.50 M NaBr) by RAFT.⁵¹ These homopolymers were found to be prepared in a controlled fashion as indicated by pseudo-first order kinetics, linear increase in molecular weights with conversion, and low PDIs ($M_w/M_n = 1.06 - 1.08$). Shortly thereafter, Donovan et al. reported the synthesis of AB diblock and BAB triblock copolymers *via* RAFT in aqueous salt media with a water-soluble A block PDMA and salt-responsive B block of [poly{3-[2-N-methylacrylamido)-ethyl dimethylammonio] propane sulfonate} (PMAEDAPS)].⁵² The aqueous solution properties of these block copolymers were examined using ¹H-NMR spectroscopy and dynamic light scattering (DLS) experiments. This was the first example of the synthesis of sulfobetaine-containing triblock copolymers.

Polymeric betaines have been prepared by GTP and free radical polymerization techniques and have been demonstrated to exhibit excellent anti-adherent properties.⁵³ However, it should be noted that free radical polymerizations are limited to 1-substituted or 1,1-disubstituted substrates such as styrenic, (meth)acrylic, and (meth)acrylamido derivatives. What is evident, however, is that *only* CLRP techniques have been employed for the direct polymerization of betaine monomers in a controlled manner.

Controlled/'Living' Polymerization

The synthesis of WSPs has been accomplished by a number of polymerization techniques ranging from conventional chain growth methodologies to controlled/'living' chain growth techniques. Over the past two decades, controlled/'living' chain growth polymerization techniques - such as NMP, ATRP, RAFT, and 'living' ring opening metathesis polymerization (LROMP) - have received tremendous interest as the demand has risen for well-defined polymeric materials.

Conventional free radical polymerization yields polymers with poor control over the MMs, MMDs, the end group functionalities, and an inability to prepare copolymers with advanced architectures. This is due, primarily, to the presence of undesirable side reactions such as chain termination and chain transfer events.

By contrast, the development of CLP methodologies (e.g. NMP, ATRP, RAFT, and LROMP) has allowed for the preparation of well-defined (co)polymers with precise control of MM, narrow MMDs, high end group functionalities, and the ability to prepare complex macromolecular architectures. Over the past two decades, considerable focus has been placed on the preparation of complex macromolecular architectures such as

statistical, alternating, block, graft, and star copolymers due to their potential commercial applications (Figure I-2).

The strictest definition for a 'living' polymerization is a chain growth process that proceeds with no termination or transfer events. However, such a definition only suggests the ability to prepare perfect telechelics and block copolymers by sequential monomer addition. It does NOT imply the ability to control MM or prepare (co)polymers with low polydispersity indices. Webster has outlined more stringent criteria for the classification of a 'living' polymerization:⁵⁴

- (1) Polymerization proceeds to complete conversion with further monomer addition resulting in continued polymerization.
- (2) The number average molecular mass (M_n) increases linearly with conversion.
- (3) Complete and fast initiation, where $k_i \geq k_p$.
- (4) The molecular mass is controlled by monomer/initiator stoichiometric ratios.
- (5) The polydispersity (M_w/M_n) remains low (≤ 1.2).
- (6) Polymers with chain-end functionality can be obtained quantitatively.

While Ziegler⁵⁵ and Flory⁵⁶ described similar concepts, Szwarc introduced the terms 'living polymerization' and 'living polymer' after preparing near-monodisperse polystyrene via 'living' anionic polymerization in 1956.⁵⁷ He proposed that polymers prepared by chain growth methodologies were "born" by initiation, "grow" by propagation, and "die" by termination. In the absence of termination, the polymer

molecules “live” for an indefinite period of time; however, a ‘living’ polymer chain does not grow indefinitely. Szwarc suggested that ‘food’ (monomer) is required for growth to occur in ‘living’ polymerizations. When all monomer is consumed, the polymer chain growth is suspended until the addition of more monomer at which point polymer chain growth resumes.

Following this, the ‘living’ polymerization of vinyl monomers was restricted to anionic polymerization conditions for approximately 30 years. During the 1960’s and 1970’s, however, several cationic ring-opening polymerizations of heterocyclic monomers were discovered to proceed in the absence of undesirable side reactions.⁵⁸⁻⁶⁰ The discovery of a dynamic equilibrium between active and dormant species lead to the development of ‘living’ cationic polymerizations.^{61,62} Over the past three decades, there has been extensive growth in the area of CLP. Currently, the majority of chain growth polymerization techniques such as anionic, cationic, ring-opening metathesis, coordination, and radical polymerization can be conducted in a ‘controlled/living’ manner under appropriate conditions. However, most of these polymerization techniques are not exempt from chain transfer or termination reactions, which has lead to the use of other terms such as controlled, *pseudo-living*, *quasi-living*, and many others in literature.^{63,64} While the usage of various terminology has created debate in the polymer field, the current IUPAC definition states that a ‘living’ polymerization is “a chain-growth polymerization that proceeds in the absence of chain-transfer and chain termination reactions”.⁶⁶

Ring-Opening Metathesis Polymerization (ROMP)

Olefin metathesis is an interchange of alkylidene groups between olefins.⁶⁷

Discovered in the 1950's, olefin metathesis is the brainchild of industry.⁶⁸ There are a number of olefin metathesis reactions such as ring-closing metathesis (RCM), acyclic diene metathesis polymerization (ADMET), and ring-opening metathesis polymerization (ROMP) as shown in Figure I-9.

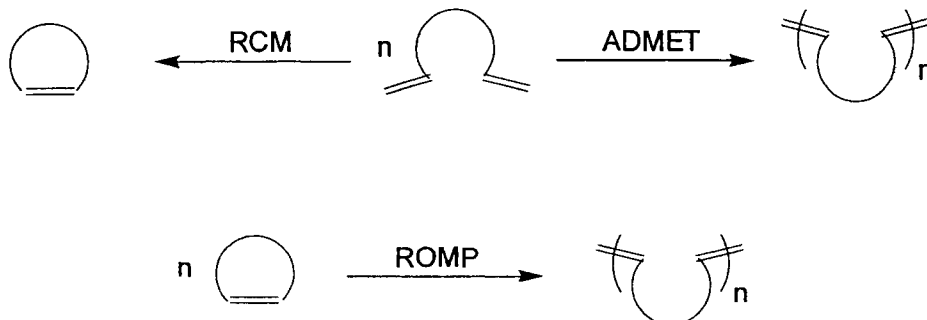


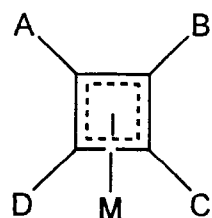
Figure I-9. Variations of the olefin metathesis reaction.

As it relates to olefin metathesis methodologies, ROMP is undoubtedly the most researched in the field of polymer chemistry. In fact, ROMP was discovered serendipitously while investigating the Ziegler-Natta polymerization of norbornene using $\text{TiCl}_4/\text{EtMgBr}$ catalysts during the mid 1950's by Anderson et al.⁶⁸ For a number of years, ROMP and the metathesis of acyclic olefins, originally termed olefin disproportionation,⁶⁹ were thought to be two different reactions. However, Calderon and co-workers found that both ROMP of cyclic olefins and olefin disproportionation of acyclic olefins was the same reaction, but simply the opposite of one another. As a

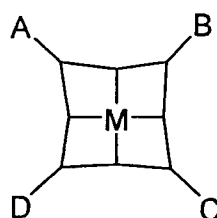
result, in 1967 they coined the term “olefin metathesis”,⁷⁰⁻⁷² which today can be defined as the metal-catalyzed redistribution of carbon-carbon double bonds.⁵⁵

Accepted Mechanism and Other Aspects of ROMP

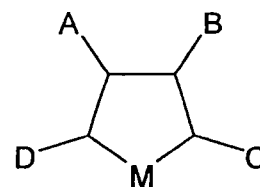
ROMP is a transition metal carbene mediated chain growth polymerization process consisting of initiation, propagation, and termination steps. This polymerization technique converts a cyclic alkene to a ring opened *unsaturated* polymer, which is a distinguishing feature separating ROMP from other olefin addition polymerizations. Early proposed mechanisms for ROMP, and other olefin metathesis reactions, suggested a pairwise exchange of alkylidene groups in which the intermediate transition metal states were described either as being quasi-cyclobutane,⁷⁴⁻⁷⁶ metal tetracarbene,⁷⁷ or metallacyclopentane^{78,79} as shown in Figure I-10.



quasi-cyclobutane



metal tetracarbene



metallacyclopentane

Figure I-10. Early proposed olefin metathesis intermediates that were later disproved.

In 1970, Chauvin and Hérisson performed tungsten-catalyzed cross metathesis experiments and proposed a nonpairwise reaction via metal carbene intermediates.⁸⁰ The metallacyclobutane mechanism has since been supported in mechanistic investigations conducted by other researchers. For example, Katz et al. and Grubbs et al. used elegant

isotope-labeling of olefins to demonstrate the non-existence of a pairwise exchange pathway.⁸¹⁻⁸⁵ Support to the existence of the metallacyclobutane mechanism has come from other discoveries, such as the identification of intermediates (e.g., metallacyclobutanes,⁸⁶⁻⁸⁸ and olefin- π -metal complexes,⁸⁹⁻⁹¹) and is now the accepted mechanism for ROMP. A general mechanism for ROMP, first proposed by Chauvin, is shown in Figure I-11.

Initiation. In the initiation step in ROMP starts with a ligand bound to the metal center dissociating to give a co-ordinatively unsaturated metal species. Such a process is dynamic, and recomplexation of the dissociated ligand competes with π -coordination of the cyclic alkene. Indeed, which of these two processes occurs preferentially is one factor that determines overall catalyst/initiator activity. Following π -coordination of the cyclic alkene a [2+2] cycloaddition leads to the formation of a metallacyclobutane intermediate. A subsequent [2+2] cycloreversion yields a new metal alkylidene with the original alkylidene species now serving as an end-group, Figure I-11, step 1).

are used widely in ROMP due to their high ring strain energy, which is comparable to cyclopropane.

Cyclic olefins possessing low strain energy have very little enthalpic driving force to be polymerized under ROMP conditions. Consequently, the temperature and concentration under ROMP conditions can greatly impact the outcome of such reactions. Using the Gibbs free energy equation, a ceiling temperature can be derived (i.e., the temperature at which the propagation and depropagation rates are equal) for any cyclic olefin.⁹⁴ At this concentration/temperature juncture the entropic penalty is too high to be compensated by the enthalpic contribution associated with the release of ring-strain. These considerations are important when attempting the ROMP of any new cyclic olefin. Generally, the most favorable conditions for a successful ROMP reaction are to use the highest possible monomer concentration at the lowest possible temperature.

Intermolecular chain-transfer and intramolecular chain-transfer (so-called “backbiting”) are other metathetical pathways for establishing equilibria and are generally undesirable in a ROMP reaction.⁹² In an intermolecular chain-transfer reaction, one polymer chain containing an active metal alkylidene on its terminus reacts with any olefin along the backbone of a different polymer chain. While the total number of polymer chains remains the same, the molecular weights of the individual polymers will increase or decrease accordingly. In backbiting reactions, the active terminus of a polymer chain reacts with itself to release a cyclic species and a polymer chain resulting in reduced molecular weight. Both inter- and intramolecular chain-transfer reactions broaden the MMD of a system.

The Jacobson-Stockmayer theory of ring-chain equilibria states that the formation of cyclic oligomers will always accompany the formation of high molecular weight polymer.⁹⁵⁻⁹⁷ The number of cyclic species present depends on factors such as solvent, cis/trans ratio of the polymer backbone, rigidity of the monomer, reaction time, and concentration. At high temperatures and lower concentrations, the formation of cyclic species is favored. Under the criteria of CLP such side reactions are undesirable; however, they can prove advantageous. For instances, the synthesis of cyclic oligomers in high yields can be achieved by conducting ROMP reactions under dilute conditions.

As mentioned above, highly strained cyclic olefins are desired in ROMP. Typical substrates include norbornene, norbornadienes, 7-oxanorbornenes, azanorbornenes, cyclobutenes, cyclooctenes, cyclooctadienes, and cyclooctatetraenes just to name a few.⁹³ Undoubtedly norbornene-based monomers are the most widely used to prepare highly functionalized polymers by incorporating, for example, complex bioactive, electroactive, or liquid-crystalline molecules within the polymer backbone (Figure I-12).⁹³ In most cases, these functional units are prepared by multiple-step synthesis via esterification, etherification, amidation, or imidation reactions. In fact, norbornene carboxylic acid, norbornenol, or norbornene anhydride derivatives are used to connect the functional unit to the polymerizable group. A major consideration regarding the anchor group is its substitution pattern which greatly influences the rate of polymerization. For example, in a mixture of *endo* and *exo*-2-norbornene derivatives, the *exo* isomers polymerizes at a faster rate than the *endo* isomer.⁹³ For less active catalysts, the *endo* isomers do not polymerize, which is attributed to steric and electronic effects. As such, the monomer's stereochemistry must be taken into account before executing ROMP.

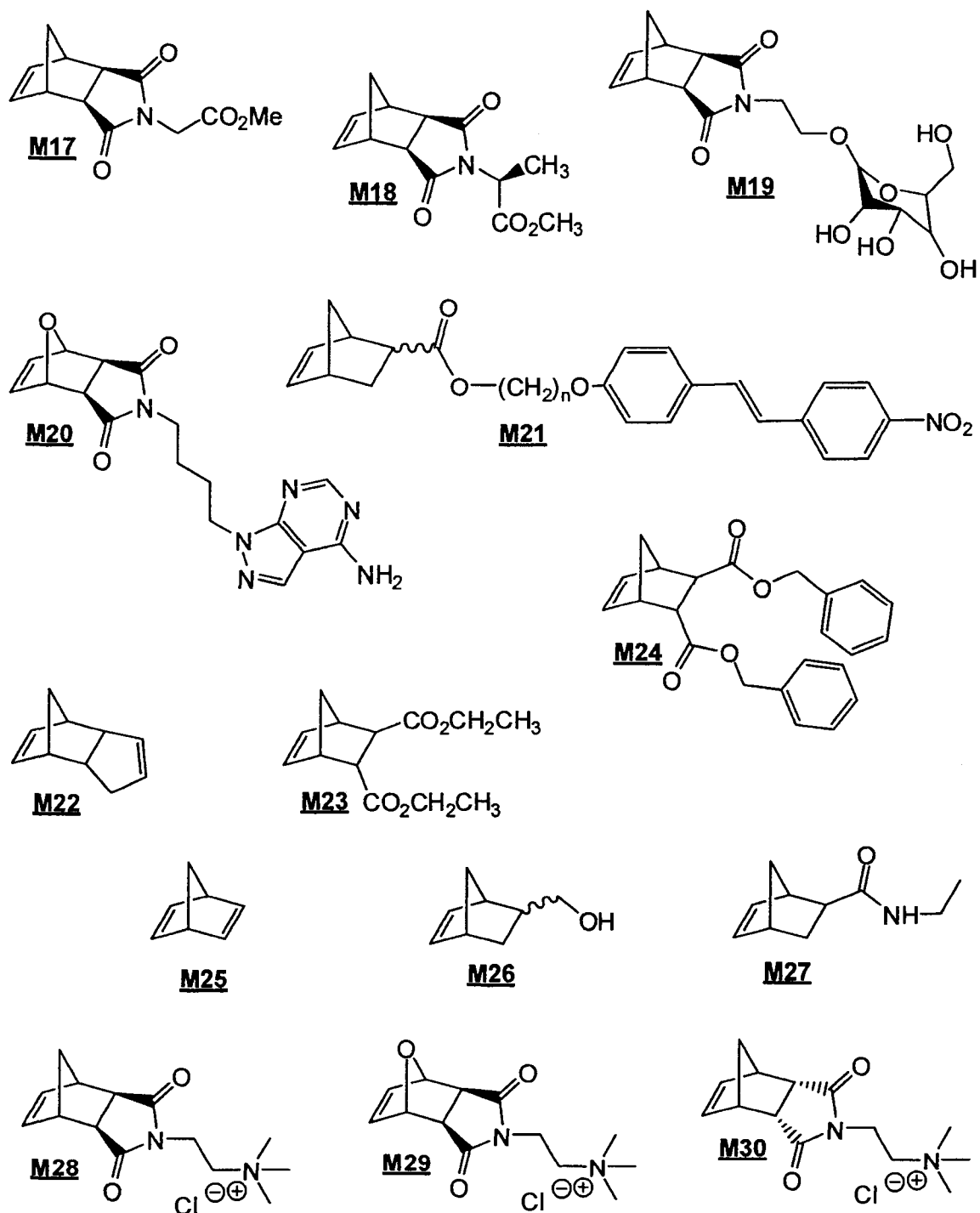


Figure I-12. Examples of functionalized norbornene-based monomers (**M17-M30**) used in ROMP.

Another consideration for successfully executing ROMP is the choice of solvent. Solvents as such benzene, toluene, dichloromethane, acetone, alcohols, water, and many others have been used for different monomers.⁹³ The choice of solvent is dictated by several factors, most important being catalyst, monomer, and polymer solubility. However, pronounced differences in polymerization rates have been observed when using different solvents.⁹³ Given this, solvent mixtures can be used to not only guarantee a homogeneous reaction but may affect polymerization kinetics thereby influencing MM and PDIs.

Of course, the temperature can dramatically affect the rate of polymerization, for example, increasing the temperature increases both propagation (k_p) and initiation (k_i) rate constants. The k_i/k_p ratio is not always affected since both constant increases by approximately the same factor. However, when employing cyclooctenes and unsubstituted norbornene the higher temperatures and prolonged reaction times give rise to secondary metathesis reactions (“backbiting”). Therefore, with highly active catalysts lower temperatures (e.g. -20°C) are desired to suppress chain-transfer reactions.⁹³

Additionally, polymers formed from ROMP reactions are uniquely different from polymers formed from other chain growth processes polymerizations in that the resulting polymer contains unsaturation in the polymer backbone.⁹⁸ As a result, the newly formed double bonds may have cis or trans arrangements. More specifically, norbornene derivatives yield polymers with two chiral allylic carbon atoms making the resulting microstructure of the (co)polymer very complex. Consequently, there exists the possibility of geometric isomerism in the polymer backbone (cis versus trans double

bonds) as well as head-to-tail versus head-to-head (or tail-to-tail) monomer additions resulting from the chiral centers in the monomer substrates (Figure I-13).

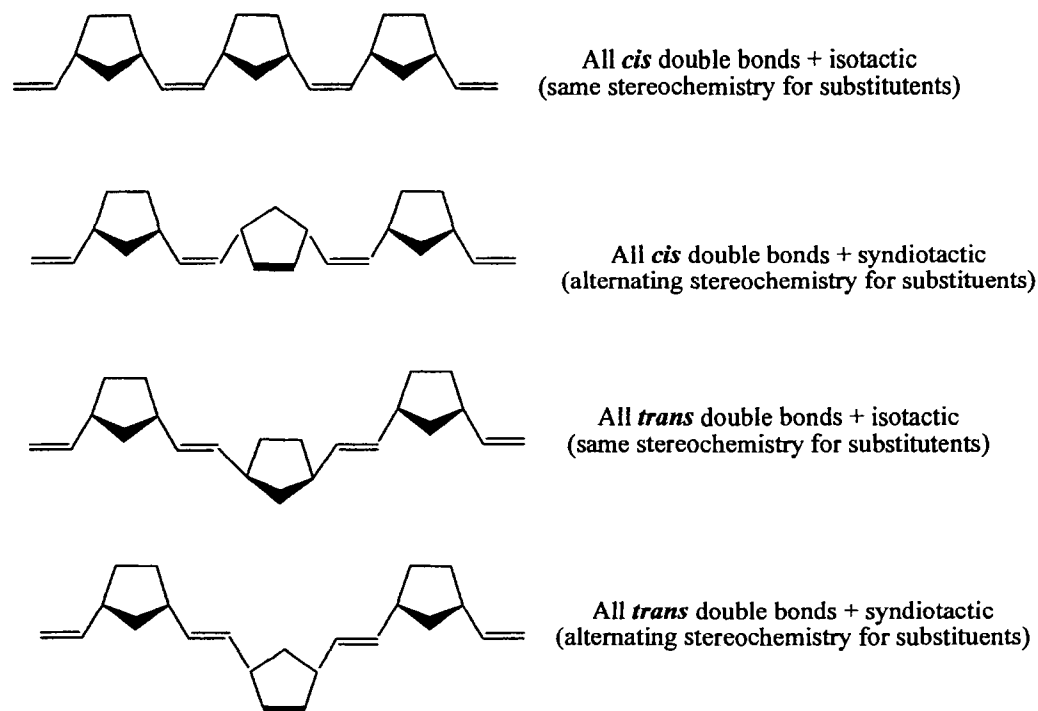


Figure I-13. Various possible combinations of triad tacticity and double-bond stereochemistry in polynorbornene.

Since different ROMP initiators may give various ratios of *cis* and *trans*, this is an important consideration when evaluating the microstructure of the polymer. Both ^{13}C and ^1H NMR spectroscopy can be used to assess the *cis/trans* ratios in ROMP-prepared polymers, which can affect many of the properties of the materials in the solid state and in solution. For example, a high *cis* content in polyalkenamers leads to lower melting temperatures (T_m), glass transition temperatures (T_g), and solution viscosity ($[\eta]/M$).^{98,99} From a MM analysis standpoint, differences in *cis/trans* ratios for polymers of the same MW influence $[\eta]/M$ which may affect retention times. For the aforementioned, it is

important to understand how the use of ROMP initiators influence stereochemistry in the polymer's microstructure (i.e. cis/trans ratios) as this dictates the polymer's properties and performance.

Living Ring-Opening Metathesis Polymerization (LROMP)

As stated above, Swarc defined a 'living' polymerization as one that proceeds without chain transfer or termination events.⁵⁷ In addition to Swarc's original definition, LROMP should exhibit the criteria for a CLP as outlined above and proposed by Webster.⁵⁴ After careful consideration of the metal-mediated and equilibrium nature of ROMP, it is clear that special metathesis catalysts are required for LROMP. Bielawski and Grubbs have outline the following characteristics a catalyst should possess:⁹²

- (1) exhibit fast initiation kinetics (i.e. each polymer chain grows at the same time)
- (2) mediate ROMP *without* inter-/intramolecular chain transfer or termination events
- (3) react with chain transfer agents to facilitate selective end-functionalization
- (4) be soluble in common organic solvents or water
- (5) be stable toward moisture, air, and common organic functional groups.

From a kinetic standpoint, it is advantageous if $k_i \geq k_p$, i.e. initiation is complete prior to any significant propagation to ensure that each polymer chain grows at the same time. Therefore, evaluation of the polymerization kinetics can be used to determine whether or not a polymerization is proceeding in a controlled fashion. It is worth noting that ROMP follows second order kinetics where the rate equation is given by (2).

$$-d[M]_o/dt = R_p = k_p[Ru][M] \quad (2)$$

Under LROMP conditions a plot of $\ln[M]_o/[M]$ or $\ln(1/(1-x))$ versus time, where x is the fractional conversion, should be linear. Therefore, under steady state conditions $[Ru]$ is considered to be constant and the rate of polymerization is first order with respect to monomer in which equation 2 may be forced into the pseudo-first order equation (3).

$$R_p = k_{comp}[M] \quad (3)$$

$$\text{where, } k_{comp} = k_p[Ru]$$

The rate constant of propagation (k_p) can be directly deduced from the slope of the $\ln[M]_o/[M]$ versus time plot where the slope is equal to k_{comp} . Additionally, a linear plot of the experimental number-average molecular mass ($M_{n, exp}$) versus conversion is consistent with the absence of chain-transfer events (Figure I-14).

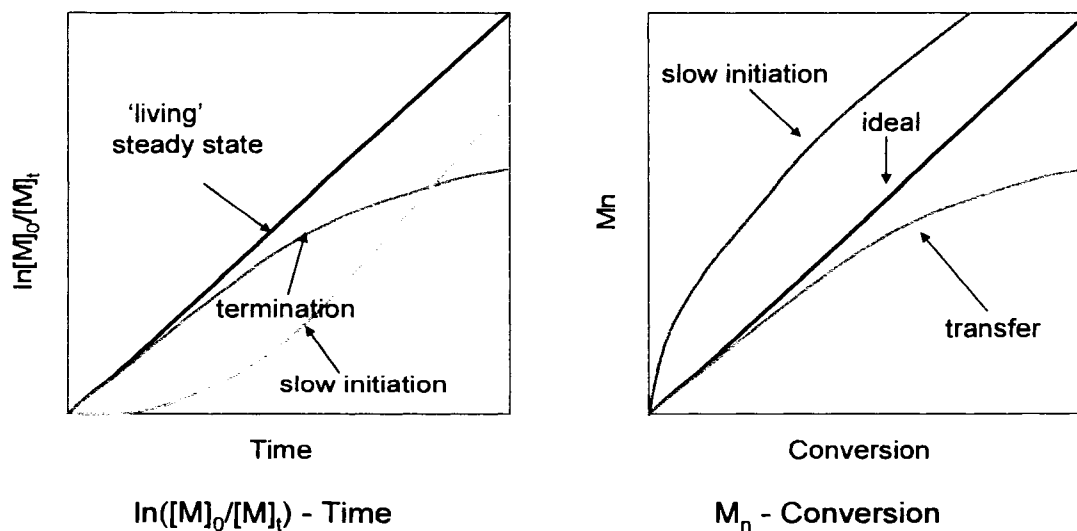


Figure I-14. Diagnostic plots of $\ln[M]_o/[M]_t$ versus time and M_n versus conversion.

Ill-defined ROMP Initiators

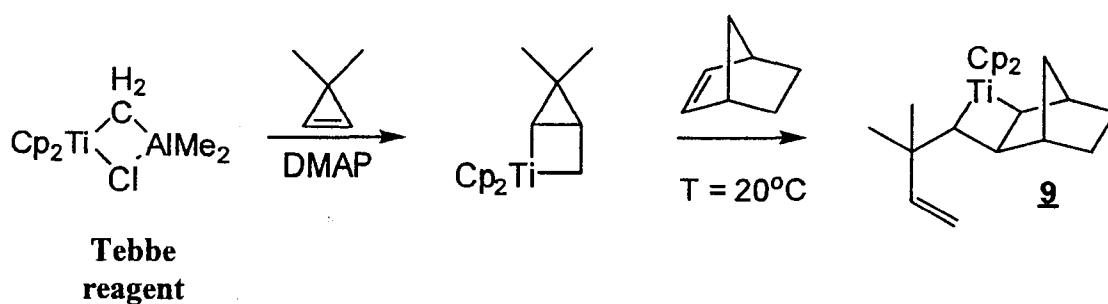
From the early 1960's to the early 1980's, ROMP was conducted using ill-defined catalysts, which included two- or three-component systems and transition metal salts based on Ti, V, Nb, Ta, Cr, Mo, W, Re, Co, Ir, Ru, and Os.^{98,100} Examples of these ill-defined catalysts include $\text{MoO}_3/\gamma\text{-Al}_2\text{O}_3/\text{LiAlH}_4$, $\text{MoCl}_5/\text{Et}_3\text{Al}$, $\text{TiCl}_4/\text{Et}_3\text{Al}$, $\text{TiCl}_4/\text{LiAl}(\text{n-C}_7\text{H}_{15})_4$, $\text{WCl}_6/\text{EtAlCl}_2/\text{EtOH}$, $\text{MoCl}_2(\text{NO}_2)\text{L}_2/\text{EtAlCl}_2$, (L = phosphine or py), $\text{WCl}_6/(\text{n-C}_2\text{H}_5)_4\text{Sn}$, $\text{WOCl}_4/(\text{n-C}_4\text{H}_9)_4\text{Sn}$, $\text{Re}_2\text{O}_7/\text{Al}_2\text{O}_3$, and RuCl_3 in polar solvent media.⁹⁸ These ill-defined catalysts do not facilitate 'living' ROMP and, therefore, do not produce well-defined polymers (i.e. precise MM control, low PDIs, or facilitate the preparation of advanced macromolecular architectures). In fact, these catalyst systems suffer due to the following limitations: (1) the formation of other transition metal species which are not metathesis active, (2) slow generation of the active catalytic species and low initiation efficiency, (3) independent chain growth due to different rates of polymerization for the same system, (4) chain transfer events such as intermolecular and intramolecular (backbiting), and (5) termination events.⁹⁸

Well-defined ROMP Initiators

Given these limitations, mechanistic studies would become extremely important in identifying key intermediates that would allow for the development of single component well-defined catalysts to facilitate LROMP. In 1976 Katz first reported a series of well-defined tungsten catalysts with evident ROMP activity.^{101,102} However, these well-defined catalysts produced polymers with broad MMDs ($\text{PDI} > 1.85$), which suggested the catalyst had poor initiation characteristics and/or promoted secondary

metathesis. Nonetheless, this was a significant contribution, which provided promise to the future development of well-defined catalysts capable of LROMP.

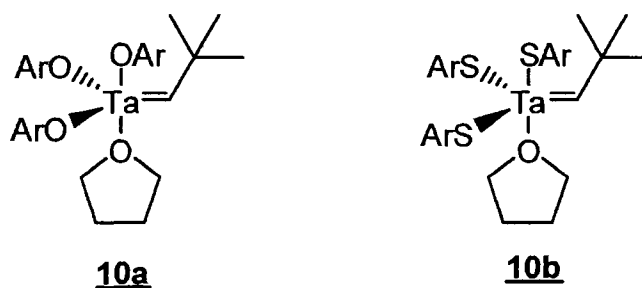
Titanium and Tantalum-based Complexes. The first example of LROMP was reported by Grubbs using single component well-defined catalysts based on the early transition metal Ti such as bis(cyclopentadienyl)titanacyclobutane compounds.¹⁰³ The synthesis of Ti-based well-defined catalysts was carried out by reacting the Tebbe reagent with various olefins, such as norbornene, in the presence of pyridines (to sequester the aluminum) as illustrated in Scheme I-2.¹⁰⁴



Scheme I-2. Synthesis of titanacyclobutane complex **9**.

Catalyst based on **9** were shown to yield norbornene polymers with narrow MMDs (PDI = 1.08), tunable MMs, and advanced macromolecular architectures (i.e. block copolymers). While these results were promising, Ti complexes are not tolerant towards aldehyde, ketone, ester, and hydroxyl functionalities. In fact, these complexes undergo Wittig-type reactions, which was found to be a convenient methodology for quenching the polymerization and introducing end-group functionalities. It was found that these complexes were restricted to pure hydrocarbon-based cyclic olefins with high ring strain.

Shortly after the Ti complexes were reported, Schrock et al. reported a series of Ta complexes which were found to be ROMP-active (Figure I-15).¹⁰⁵ Due to their high activity these complexes were found to promote secondary metathesis reactions leading to (co)polymers with broad MMDs. However, complexes **10a** and **10b** were demonstrated to mediate LROMP producing norbornene polymers with narrow MMDs ($PDI \leq 1.1$).¹⁰⁶

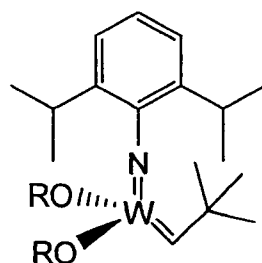


10a, Ar = 2,6-diisopropylbenzene
10b, Ar = 2,4,6-triisopropylbenzene

Figure I-15. Ta catalysts used for obtaining norbornene polymers with narrow MMDs.

Both catalysts were found to react with aldehydes and ketones in a Wittig-type fashion, which allowed termination of the polymerization and incorporation of functional end-groups. Both Ti and Ta are extremely Lewis acidic due to their high oxidation states and, therefore, react rapidly with carbonyls, hydroxyls, and amino functional groups for example. While this has placed limitations on their utility in LROMP, they provided a foundation for catalyst design and tailoring activity. Soon attention was focused towards catalyst design that facilitated LROMP in the presence of a broader range of functional groups.

Tungsten-based Complexes. Schrock et al. prepared single component, well-defined Lewis-acid free, imido-alkoxy W-based catalysts as shown in Figure I-16, that exhibited high ROMP activities.^{107,108}



11a, R = tBu

11b, R = C(CH₃)₂(CF₃)

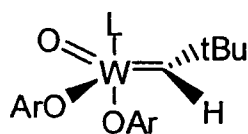
11c, R = C(CH₃)(CF₃)₂

Figure I-16. Example of W-based well-defined Schrock complexes.

The activity of these catalysts was found to be tunable by modifying the alkoxy ligands. For example, the use of **11a** as an initiator afforded norbornene polymers with control of molecular mass and a PDI of 1.03 after being quenched with benzaldehyde.¹⁰⁹ Increasing the electrophilic character of the catalyst (**11b**, **11c**), by replacing the hydrogenated alkoxy ligands with fluorinated analogues, greatly increases their activity in olefin metathesis reactions. However, this increase in activity results in secondary metathesis reactions and fast propagation compared to initiation.

The tungsten-based oxo-alkylidene complexes **12** in Figure I-17 were shown to possess moderate functional group tolerance and catalyze the LROMP of 2,3-dicarbomethoxynorbornadiene and bis(trifluoromethyl)norbornadiene.¹¹⁰ The ROMP of these monomers was found to occur rapidly (< 15 minutes) with the molecular mass of

the polymer increasing linearly with time and yielding materials with PDIs between 1.1 and 1.01.



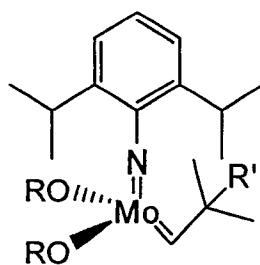
12, L = PMe₃ or PPh₂Me
Ar = 2,6-Ph₂C₆H₃

Figure I-17. Tungsten-based oxo-alkylidene complex.

Additionally, W-based catalysts have been shown to mediate the LROMP of other classes of cyclic olefins including cyclopentene¹¹¹⁻¹¹³ and cyclobutene.¹¹⁴ Cyclopentene has less ring strain than norbornene derivatives and is more difficult to polymerize under ‘living’ conditions since it is capable of undergoing secondary metathesis reactions. However, conducting the polymerization at low temperatures (-40°C) afforded polymers with a PDI of 1.08. By contrast, cyclobutene has a greater ring strain and readily undergoes ROMP. However, since the rates of propagation are greater than the rates of initiation, ROMP of this cyclic alkene leads to polymers with broad MMDs. The addition of a donor ligand such as trimethylphosphine (PMe₃) enables LROMP of this monomer. Notably, ROMP of cyclobutene yields polybutadiene with a perfect 1,4-microstructure.

Molybdenum-based Complexes. While tungsten alkylidene **12** demonstrated that structurally well-defined transition metal-alkylidene complexes are capable of facilitating LROMP, a significant advance came with Schrock’s introduction of well-defined Mo-based alkylidenes (Figure I-18).¹¹⁵ The Mo-complexes are structurally

similar to the W-complexes and show similar activities; however, Mo-complexes display a broader functional group tolerance toward monomers containing ester, amide, imide, ketal, ether, cyano, trifluoromethyl, and primary halogen functionalities. Additionally, these complexes were found to possess greater tolerance toward oxygen, water, and other impurities and exhibit a greater stability towards decomposition and other undesirable side reactions.



13a, R = tBu

13b, R = C(CH₃)₂(CF₃)

13c, R = C(CH₃)(CF₃)₂
(R' = CH₃ or Ph)

Figure I-18. Examples of well-defined Mo-based Schrock complexes.

Like the W-alkylidenes, the activity of the Mo-complexes was found to be tunable by modification of the alkoxy ligand. For example, complex **13a** does not readily facilitate metathesis reactions of acyclic olefins, which lowers the chance of secondary metathesis reactions occurring. By contrast, the fluorinated Mo-complexes, **13b** and **13c**, show increased activities and were found to rapidly isomerize 2-pentene and other acyclic olefins. Comparative ROMP studies of *n*-alkyl *exo*- and *endo*-norbornene dicarboximides revealed that **13a** afforded polymers with lower PDI's than **13b** or

13c.^{116,117} This difference in ROMP activity was attributed to the higher activity of the **13b** and **13c** as well as poor initiation rates associated with the high rate of propagation.

Well-defined Mo-alkylidenes were also found to exert control over polymer stereochemistry.¹¹⁸ Schrock, Feast, and Gibson discovered that polymers obtained from the LROMP of 2,3-bis(trifluoromethyl)norbornene catalyzed by **13a** were highly tactic with a 98% trans content along the polymer backbone. When ROMP of the same monomer was performed using catalyst **13c** the final polymer was highly tactic with 98% cis content. It was found that by vary catalyst ratios of **13a** and **13c**, polymers could be synthesized with pre-determined of cis/trans contents under LROMP conditions.

The success of Mo-based catalysts in mediating LROMP of norbornene based substrates has been extended to a range of cyclic olefins with varying degrees of ring strain and functionality.^{119,120} Polycyclopentene was obtained with controllable molecular mass and low polydispersities (PDI < 1.1) using catalyst **13a**. Unlike the W-mediated ROMP reactions mentioned above, the Mo catalyst mediated LROMP of this monomer at room temperature using a strong donor ligand trimethylphosphine.

Ruthenium-based Complexes. In contrast to early transition metal alkylidene complexes, late transition metal carbene complexes, such as those based on Ru, exhibit low oxophilicity, making them stable toward many polar functional groups. Also, Ru readily forms bonds with carbon which open opportunities for mediating olefin metathesis reactions (Table I-1).

Table I-1. Functional group tolerance of metal carbene complexes.

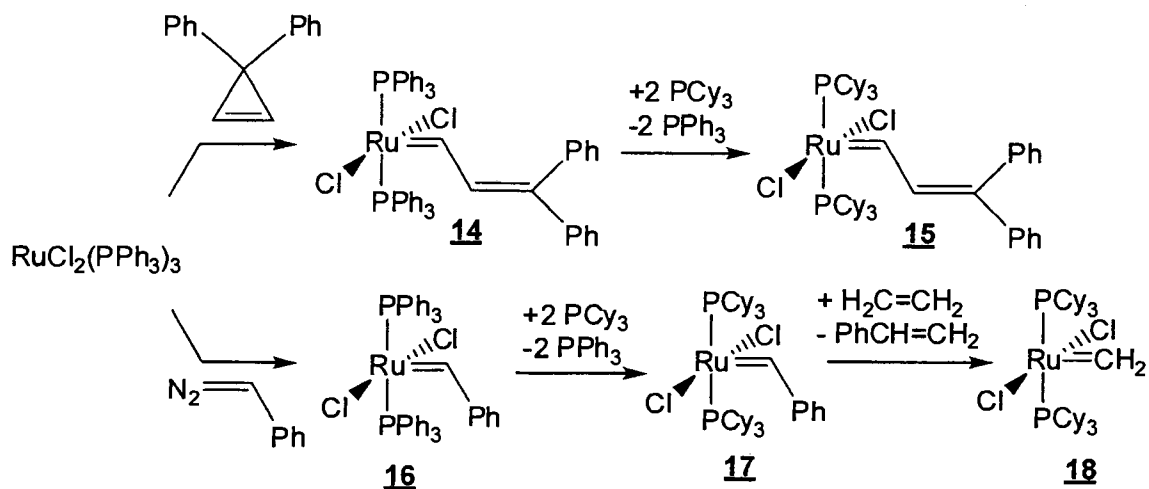
Titanium	Tungsten	Molybdenum	Ruthenium
Acids Alcohols, Waters Aldehydes Ketones Esters, Amides <u>Olefins</u>	Acids Alcohols, Waters Aldehydes Ketones <u>Olefins</u> Esters, Amides	Acids Alcohols, Waters Aldehydes <u>Olefins</u> Ketones Esters, Amides	<u>Olefins</u> Acids Alcohols, Waters Aldehydes Ketones Esters, Amides

↑
**Increasing
Reactivity**

Indeed, these are desirable characteristics and as a result the popularity and use of Ru in olefin metathesis has risen over the last decade.⁷³ During the 1960's, RuCl₃ salts were used to facilitate ROMP of various norbornene derivatives in protic media.¹²¹⁻¹²⁴ After two decades, Ru was reinvestigated for preparing charged polymers via ROMP.¹²⁵ RuCl₃ and Ru(p-toluenesulfonate)₂ were found to mediate non-living ROMP of functionalized norbornenes, 7-oxanorbornenes, and norbornadienes in aqueous or protic solvents thus demonstrating ruthenium's exceptional tolerance toward polar functionalities.^{126,127} Consequently, isolating a well-defined Ru-alkylidene became a priority, since NMR spectroscopy provided evidence for believing Ru based ROMP reactions occurred by the same mechanism as for early transition metal catalysts.¹²⁸⁻¹³⁰

In 1992, the first well-defined, single-component Ru complex that showed activity in ROMP, (PPh₃)₂Cl₂Ru=CH-CH=CPh₂ **14**, was reported.^{131,132} This complex was prepared in a similar fashion to W-based complexes mentioned above by treating (PPh₃)₃RuCl₂ or (PPh₃)₄RuCl₂ with 3,3-diphenylcyclopropene to give **14** in nearly

quantitative yields (Scheme I-3). **14** was found to be stable in degassed and dry organic solvents (benzene, dichloromethane, etc.) for weeks, exhibited indefinite stability in the solid state, and does not show appreciable decomposition after exposure to water, various alcohols, or ethers, and does not react with aldehydes and ketones in a Wittig-type fashion.

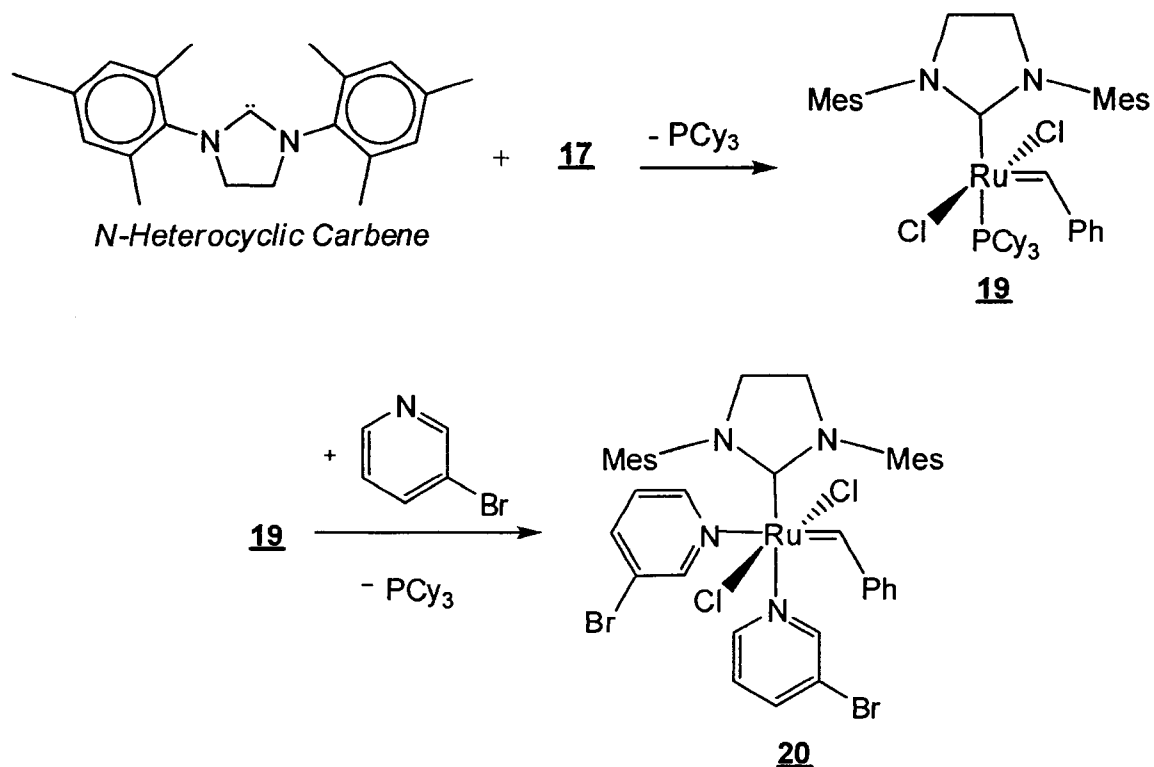


Scheme I-3. Synthesis of well-defined Ru complexes.

Grubb's and co-workers demonstrated the LROMP of norbornene mediated by **14** via elegant deuterium labeling studies.¹³² The propagating alkylidene proton was observed by ¹H NMR spectroscopy at 17.79 ppm. However, the addition of 2,3-dideuterionorbornene results in the disappearance of the signal. The addition of norbornene restored the signal producing a triblock copolymer of the two monomers (Scheme I-4). Termination of the polymerization was achieved using ethyl vinyl ether (EVE) which replaced the Ru alkylidene on the polymer chain end with a methylidene to form a metathesis inactive Fischer carbene complex ([Ru]=CHOR). Although the rate of initiation was lower than

used to prepare Ru complex **15** as shown in Scheme I-3 above.¹³⁵ Other alkylidene catalysts can be prepared by addition of the corresponding terminal olefin, which can have important influences on initiation efficiencies in ROMP reactions.^{136,137} For example, the parent benzylidene complex appears to have the most favorable initiation kinetics in ROMP reactions. In fact, complex **16** was found to polymerize norbornene in a controlled fashion (PDIs = 1.04-1.10) and were found to be better ROMP initiators demonstrated than complex **14**.¹³⁷ Complex **17** was found to be highly active toward functionalized norbornenes and cyclobutenes containing alcohol, ester, amido, and keto pendent groups.¹³⁸⁻¹⁴² Additionally, **17** showed greater thermal stability with a half-life lasting over a week at 55°C.¹⁴³

Extensive investigations have been conducted to understand the mechanism of Ru complexes in ROMP.¹⁴⁴⁻¹⁴⁸ It is believed Ru complexes are activated by a dissociative mechanism in which a phosphine ligand separates from the catalyst prior to the catalyst coordinating with the olefin. This coordination with the olefin was found to be necessary to prevent premature catalyst decompositions. N-Heterocyclic carbenes (NHCs) are known to be strong σ -donating ligands yet less labile than phosphines.¹⁴⁹ In addition to NHC ligands being less favorable for dissociating, they also provide greater stability for intermediates due their increased electron density. This led to the synthesis of complex **19** which was accomplished by a phosphine exchange reaction as shown in Scheme I-5.¹⁵⁰



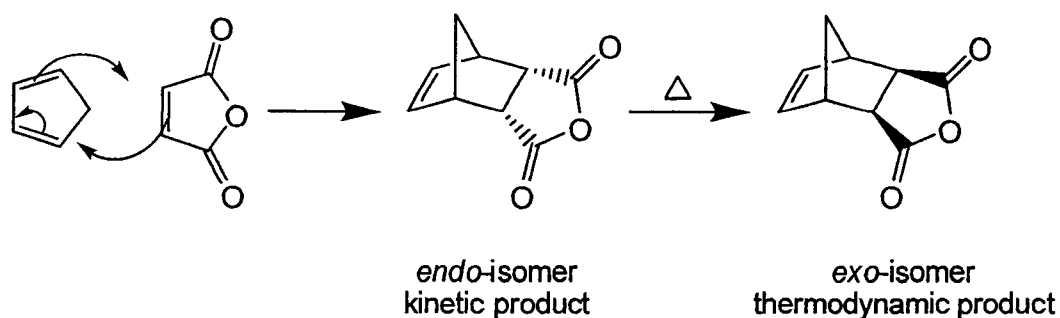
Scheme I-5. Synthesis of Ru NHC carbene catalyst **19** and **20**.

Complex **19** has exceptional activity in numerous ROMP reactions.¹⁵¹ For instance, **19** polymerized cis-cyclooctadiene at higher rates than Schrock's Mo-based catalysts and was ROMP active toward 1,5-dimethylcyclooctadiene and 1,3,5,7-cyclooctatetraene.¹⁵² At the expense of increased activity, **19** yields polymers with uncontrollable molecular mass and broad PDIs due to relatively slow rates of initiation and competing secondary chain transfer reactions.

By fine tuning the ligand environment, a new class of Ru-complexes such as **20** containing weakly coordinating pyridines with the more strongly ligated NHC ligand was developed as shown in Scheme I-5.¹⁵³ Not only do these catalysts show increased ROMP activity but also exhibit fast rates of initiation due to the more labile pyridine ligands.^{154,155} Consequently, LROMP of *endo*-methyl-5-cis-norbornene-2,3-

dicarboxyimide and *endo*-3,2-Bis(tert-butyl-dimethylsilyl)-oxy)methyl)-5-cis-norbornene derivatives were achieved with **20**. In fact, a wide range of monomers have been polymerized using **20** to yield (co)polymers with extremely low PDIs. For example, the ROMP of norbornene was carried out using **20** in which a PDI of 1.06 was obtained. However, it should be noted that ROMP was conducted at -20°C to suppress chain-transfer reactions. In addition to low PDIs, LROMP was further demonstrated in which a variety of diblock copolymers were prepared using **20**.¹⁵⁵

As previously mentioned, certain substituted norbornenes (e.g. 5-cis-norbornene-2,3-dicarboxylic anhydride) can exist in two stereoisomeric forms, more specifically *exo* and *endo* isomers.¹⁵⁶ The monomer synthesis via Diels-Alder reaction yields the *endo* species as the kinetically favored product although the *exo* isomer is the more thermodynamically stable product (Scheme I-6).



Scheme I-6. Diels-Alder reaction of cyclopentadiene and maleic anhydride and thermal isomerization of the kinetically favored *endo*-isomer to the more thermodynamically stable *exo*-isomer.

This can be an extremely important structural consideration since many ROMP catalysts show selectivity for the *exo* isomer to the extent that the *exo* isomer will polymerize

whereas the *endo* isomer will not. As stated previously, the reason for this observation, at least for *exo* vs *endo* dicyclopentadiene, has been attributed to, primarily, steric factors with unfavorable steric interactions between the *endo* substituents on incoming monomer and the penultimate unit in the growing polymer chain. For example, **17** will polymerize *exo*-2,3-bis-[(*tert*-butyldimethylsilyl)-oxy)methyl]-5-cis-norbornene and *exo*-methyl-5-cis-norbornene-2,3-dicarboxyimide monomers; however, it is not as reactive toward the *endo* isomer of these monomers. A solution to this selectivity, or rather lack of activity, for some Ru-alkylidenes is to employ more active catalysts which are non-selective, i.e. readily polymerize both *exo* and *endo* isomers. For example, **20** and its derivatives have been reported to polymerize both the *exo* and *endo* isomer of methyl-5-cis-norbornene-2,3-dicarboxyimide.¹⁵⁵

In addition to the development of Ru-complexes **14-20**, Grubbs-Hoyveda Ru-complexes **21** and **22** have been prepared and demonstrated to be ROMP active (Figure I-19).^{157,158}

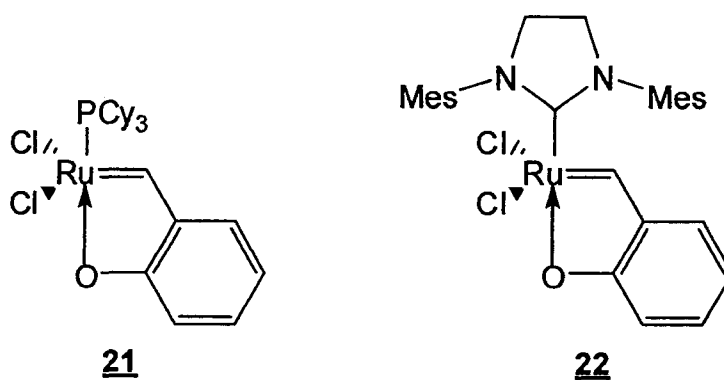


Figure I-19. Examples of commercially available Grubbs-Hoyveda Ru-complexes.

These O-chelating well defined Ru-complexes are highly stable toward oxygen and moisture in organic media for long periods of time. Additionally, **21** and **22** are the first

recyclable metal-based complexes that catalyze homogeneous olefin metathesis reaction with no detectable loss of activity when reused. Using *endo,exo*-5-cis-norbornene-2,3-dicarboxylic acid ethyl ester and (+/-)-*endo,exo*-bis-[5-(4'-cyanobiphenyl-4-yloxy)pentyl]-5-cis-norbornene-2,3-dicarboxylic acid ester, Slugvoc illustrated that **22** is highly ROMP active.^{159,160} In fact, the PDIs at 1.5 were lower than those obtained with **19** ($M_w/M_n = 1.7$). However, these catalysts yield polymers with PDIs of 1.5 compared with **16** which produced polymers with PDIs 1.1.

Water-soluble Ruthenium-based Complexes. In the 21st century, the high demand for environmentally friendly materials has become the driving force for the development of greener polymerization methodologies. For example, conducting polymerizations in water allows for more facile polymerization conditions as a result of higher heat capacity, lower viscosity, and easier processibility.¹⁶¹ Given the ability to fine tune the ligand environment by replacement of phosphines on the metal center with more hydrophilic ligands, metathesis active water-soluble Ru-complexes have been developed. Using quaternary ammonium charged functionalities attached to the phosphine ligand, water-soluble Ru-complexes **23** and **24** have been reported (Figure I-19).¹⁶² These water-soluble catalysts were found to be ROMP active toward certain water-soluble, cationic norbornene-based monomers **M28-M29** in aqueous and alcoholic media, but did not mediate LROMP because of the instability of the propagating species and their rapid decomposition. The instability and decomposition of these catalysts was later attributed to the presence of small amounts of hydroxide ion in solution and unfavorable energetics of phosphine dissociation in water. Later, it was found that the addition of a Brønsted acid (e.g. HCl) during ROMP sequesters any hydroxide present in solution and

encourages faster rates of initiations by protonating dissociated phosphine ligands.^{163,164} The ROMP activities of water-soluble Ru-complexes 23 and 24 are discussed in greater detail in the section below.

Recently, water-soluble Ru-complexes of 25-28 have been prepared and their metathesis activity evaluated in aqueous media (Figure I-20).^{165,166} While ROMP active, like the water-soluble Ru-complexes of 23 and 24, 25 is unstable in aqueous media due to the presence of phosphine ligand. While phosphine-free complex 26 demonstrates greater stability and higher activity than 23-25, it is a macromolecular, polydisperse catalyst susceptible to forming aggregates in water. However, Grubbs and co-workers have recently reported the synthesis of complexes 27 and 28 and their activity in aqueous ROMP which is discussed in greater detail in the section below.¹⁶⁷

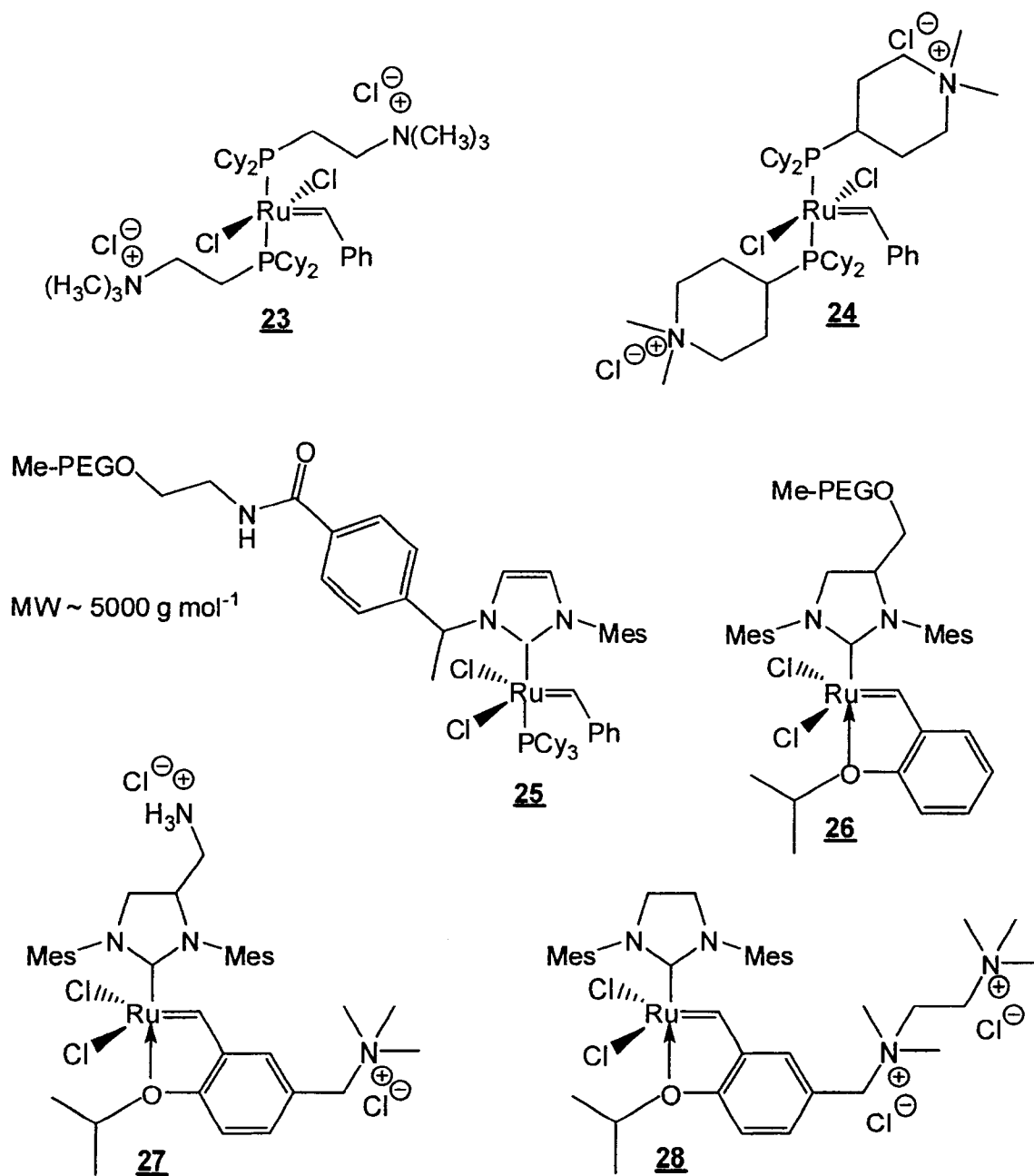
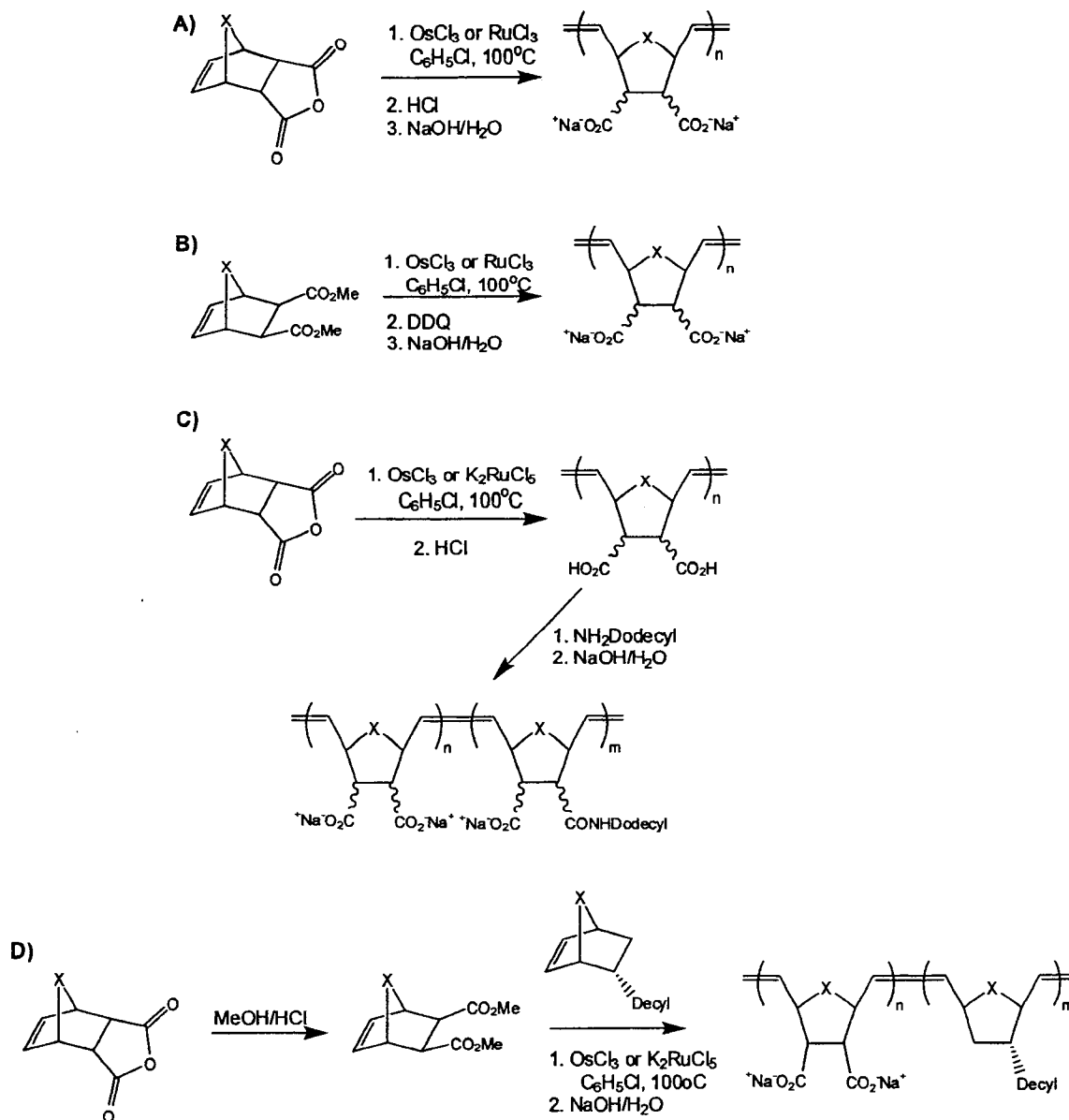


Figure I-20. Examples of water-soluble Ru-complexes based on Grubbs-type catalysts.

Synthesis of Ion-containing Polymers via Classical ROMP, LROMP, and Homogeneous Aqueous LROMP

As mentioned above, a number of polymerization techniques have been used for the synthesis of polyelectrolytes and polybetaines ranging from conventional free radical polymerization to CLP methodologies. However, despite the synthesis of highly functionalized polymers derived from complex biological molecules such as carbohydrates,¹⁶⁸⁻¹⁷¹ nucleic acid bases,^{172,173} peptides,^{174,175} and anti-tumor compounds,¹⁷⁶ there are limited reports detailing the synthesis of polyelectrolytes under classical and LROMP conditions and, to our knowledge, no reports of polybetaines prepared under ROMP conditions. In the sections below we discuss synthetic strategies that have been utilized for the preparation of polyelectrolytes via ROMP.

Synthesis of Polyelectrolytes under Classical ROMP Conditions. Ill-defined initiator systems based on transition metal salts such as RuCl₃, OsCl₃, and MoCl₅ were initially used to prepare polyelectrolytes via ROMP.¹⁷⁷⁻¹⁸⁰ Hamilton and co-workers have synthesized three different types of polyelectrolytes which include conjugated,¹⁸⁰ amphiphilic,¹⁷⁹ and hydrogels¹⁷⁷ under such conditions. This was accomplished by two synthetic approaches: 1) polymerization of an appropriate anhydride monomer followed by hydrolysis to yield the sodium salt or 2) conversion of the anhydride monomer to the di-ester followed by hydrolysis to yield the corresponding sodium salt (Scheme I-7).¹⁷⁸



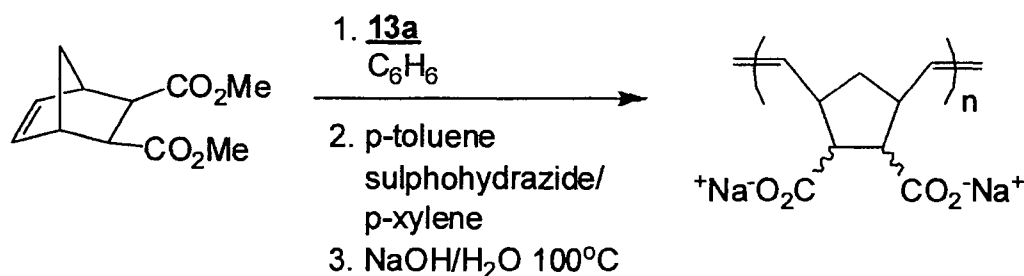
X = CH₂, O

DDQ = 2,3-dichloro-5,6-dicyano-1,4-benzoquinone

Scheme I-7. Synthetic pathways to polyanions under ROMP conditions using transition metal salt as initiators A) hydrolysis of the anhydride polymer B) hydrolysis of the di-ester polymer C) conversion to the di-acid followed by hydrophobic functionalization followed by hydrolysis and D) conversion of the anhydride monomer to the di-ester, ROMP of the di-ester with decyl norbornene followed by hydrolysis of the di-ester repeat unit.

As shown in Scheme I-7, these synthetic strategies provide a convenient route to polyelectrolytes including HMPs. However, the use of ill-defined (multi-component) catalysts does not induce a 'living' polymerization due to an inability to suppress undesirable chain-transfer side reactions which results in ill-defined polymers. Also, low initiator efficiency implies no molecular weight control.

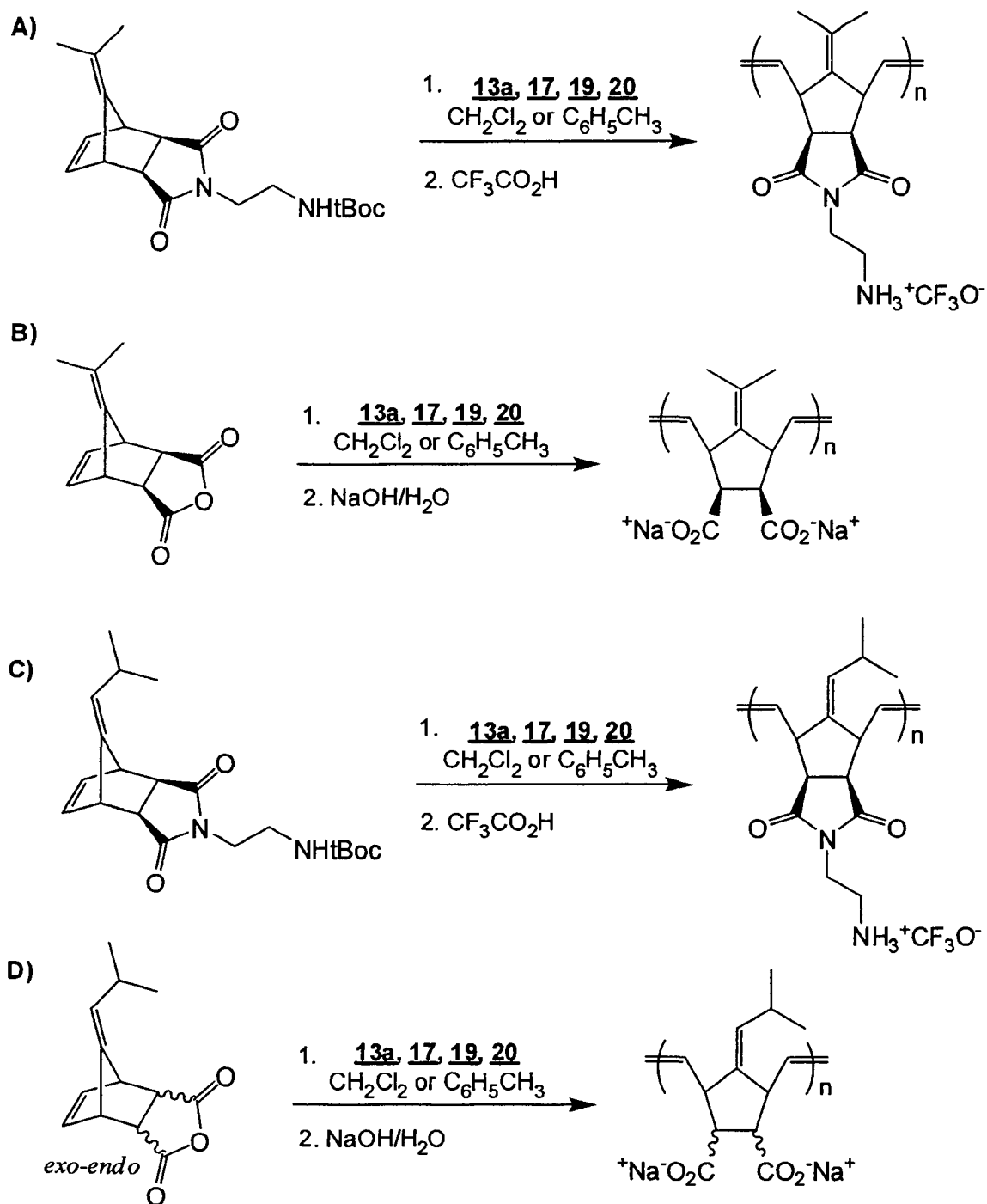
Synthesis of Polyelectrolytes via LROMP. The ROMP of norbornene derivatives using well-defined metal carbenes based catalysts such as **13a-c** and **17** may proceed without termination, thus producing a 'living polymer'. This allows for the preparation of homo and block (co)polymers with control over the MW by adjustment of the monomer to catalyst ratios. Several research groups have exploited this feature for the synthesis of polyelectrolytes as well as polyelectrolyte block copolymers. For example, Feast and co-workers reported the synthesis of poly(1,4-cyclopentenylene-5,6-ethylidene-2,3-disodium dicarboxylate)s derived from the diester using **13a** (Scheme I-8).¹⁸¹



Scheme I-8. LROMP of a norbornene-based ester followed by post polymerization modification to yield the corresponding anionic polyelectrolyte.

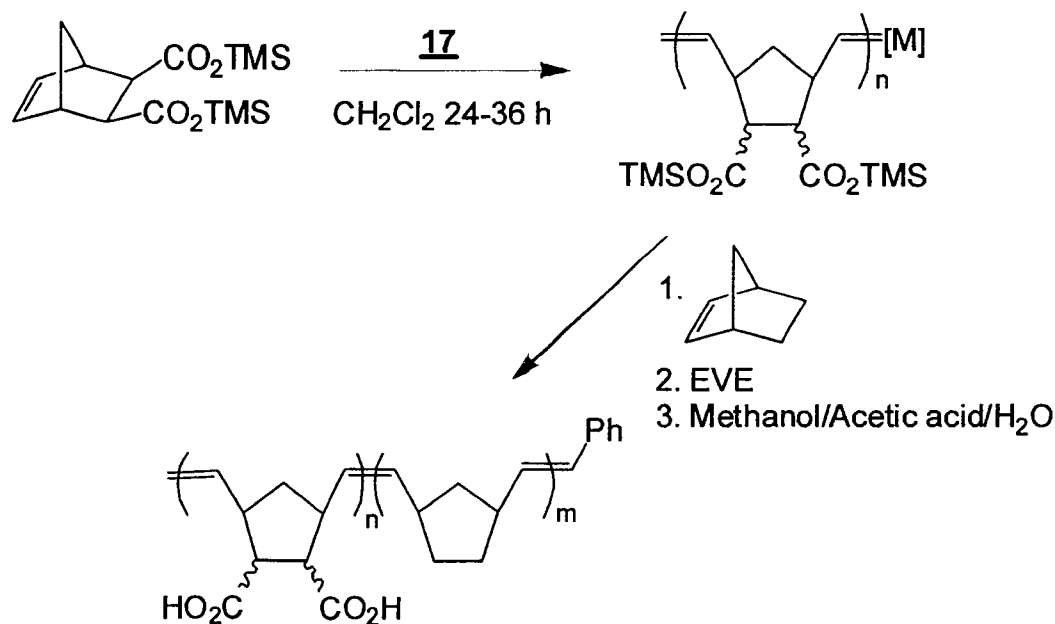
The polydispersity indices (PDIs) ranged from 1.01 to 1.24 prior to hydrogenation and hydrolysis; however, such post polymerization modifications led to an increase in the PDI's to as high as 1.7.

Ilker and co-workers reported the synthesis of amphiphilic polymers, in which the hydrophilic and hydrophobic portions were located on the same monomer.¹⁸² Both cationic and anionic amphiphilic polymers were prepared via LROMP by an indirect method. The t-BOC protected pendant primary amine groups and the anhydride functionality provided nonionic and hydrophobic character to allow for LROMP using **13a**, **17**, **19**, and **20** as illustrated in Scheme I-9. The use of catalysts **13a**, **17**, and **19** for the polymerization of the monomer shown in Scheme I-9 C) required elevated temperatures between 40 and 55°C, whereas catalyst **20** allowed for the polymerization to proceed at room temperature. For catalysts **13a**, **17**, **19**, and **20** the PDIs of the monomer shown in Scheme I-9 C) were 1.23, 1.27, 1.96, and 1.10, respectively. Given these results, catalyst **20** was used for the remaining monomers used in their study in which PDIs of 1.08-1.20 were obtained. Additionally, catalysts **19** and **20** polymerized the *endo*, *exo* monomer mixture shown in Scheme I-9 D). These well-defined amphiphilic polymers were then studied for their phospholipids membrane disruption activities.



Scheme I-9. A synthetic route to amphiphilic polyelectrolytes A) cationic amphiphilic polyelectrolytes B) anionic amphiphilic polyelectrolytes derived from 6,6'-dimethylfulvene and maleic anhydride and C) cationic amphiphilic polyelectrolytes D) anionic amphiphilic polyelectrolytes derived from 6-isopropylfulvene and maleic anhydride.

Admed and co-workers reported the synthesis of diblock copolymers of norbornene and norbornenedicarboxylic acid using catalyst **17**.¹⁸³ While norbornene is susceptible to ROMP using catalyst **19**, it had previously been reported that norbornene was not susceptible to LROMP using catalyst **17**.¹³⁹ However, Admed et al. were able to polymerize the norbornene block in a living fashion by first polymerizing the more functionalized norbornenedicarboxylic acid bis trimethyl silyl ester block followed by the sequential addition of the norbornene monomer. The diblock copolymer was easily converted to the norbornenedicarboxylic acid/norbornene diblock copolymer by removal of the trimethylsilyl groups by treatment with acetic acid/water in methanol as shown in Scheme I-10.



Scheme I-10. Synthesis of poly(5-norbornene-2,3-dicarboxylic acid-block-norbornene) via LROMP.

The use of such protecting group chemistry allowed LROMP to be carried using 17 in organic media. Additionally, it was found that an increase in the norbornenedicarboxylic acid bis trimethyl silyl ester block length led to low PDIs in the range of 1.51 to 1.05.

Liaw and co-workers prepared naphthalene-labeled poly(hydrochloride-quaternized 2-norbornene-5-methylamine) under LROMP conditions using 17 as an initiator.¹⁸⁴ The PDI of the polymer was 1.18, which is one criterion for a 'living' polymerization. Naphthalene labeling allowed for easy evaluation of the aqueous solution properties of the cationic polyelectrolyte obtained by post polymerization modification. Additionally, Liaw and co-workers have also prepared random and block amphiphilic copolymers comprised of a hydrophobic alkyl ester and hydrophilic ammonium groups to evaluate their self-assembly behavior.¹⁸⁵ As with earlier reports of aqueous LROMP, this required post polymerization modification to yield the amphiphilic polyelectrolyte.

More recently, Zheng and co-workers prepared novel imidazolium cationic polyelectrolytes using 17 and a mixed solvent system of chlorobenzene and ionic liquid, namely 1-butyl-3-methylimidazoliumhexafluorophosphate ([BMIM][PF₆]).¹⁸⁶ The novel cationic polyelectrolyte was obtained in excellent yields (>94%) with narrow MMDs (PDI<1.09). Based on these low PDIs, it may be predicted that ROMP occurred under living conditions; however, a detailed study of the homopolymerization kinetics and preparation of block (co)polymers is needed to determine livingness.

Breitnekamp et al. have reported using a 9:1 solvent mixture of 2,2,2-trifluoroethanol and dichloromethane (TFE/CH₂Cl₂) for the preparation of polyolefin-graft-oligopeptide polyelectrolytes using complex 20.¹⁸⁸ Additionally, the aqueous

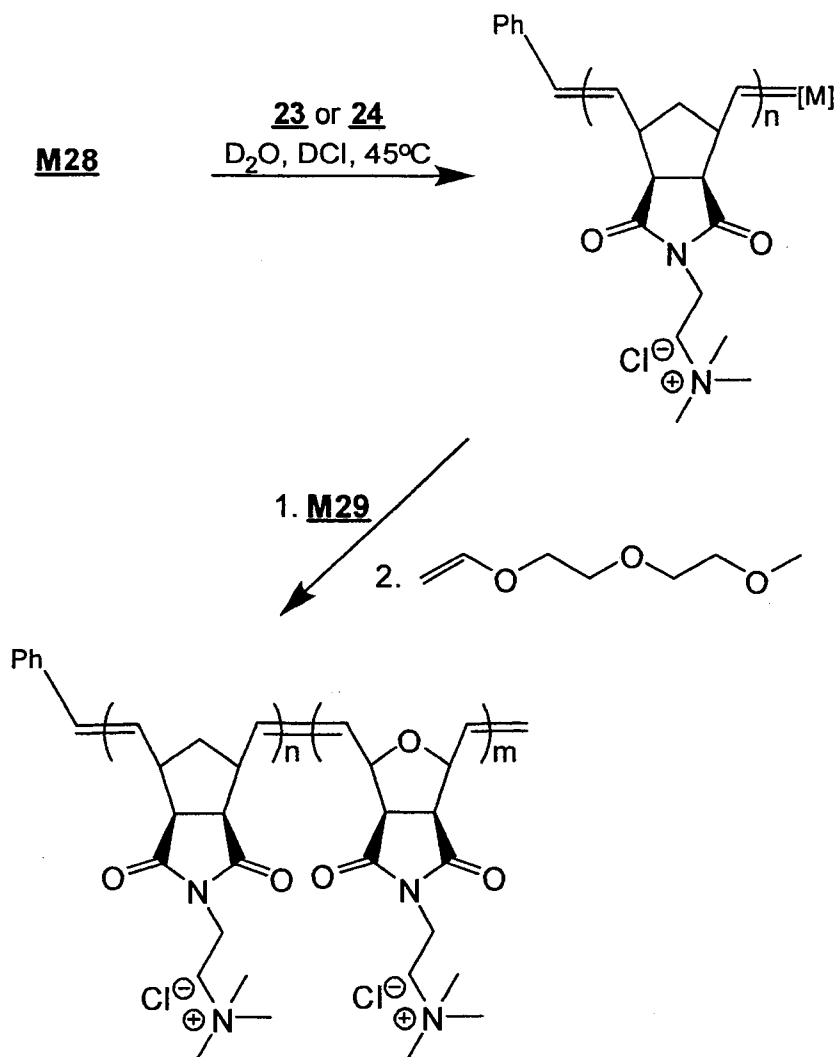
solution behavior was tailored by changing the peptide graft length and density which was evaluated in various salt concentrations.

While the above methodologies have provided a synthetic route to polyelectrolytes using commercially available ROMP initiators, many of them require post polymerization modifications, which can be time consuming and cumbersome. Additionally, such reactions may lead to broadening of the MWD resulting in ill-defined polymeric materials. Additionally, in the all reports mentioned above, no detailed studies have been conducted with regard to kinetic, conversions, MM, and/or MMD features of these polymerizations.

Synthesis of Polyelectrolytes via Homogeneous Aqueous LROMP. Aqueous ROMP of strained cyclic alkenes using group VIII transition metal salts and coordination complexes is well-established.^{125-128,162} Such ill-defined initiators are completely water soluble; however, the lack of a preformed metal-carbene does not allow for aqueous LROMP.

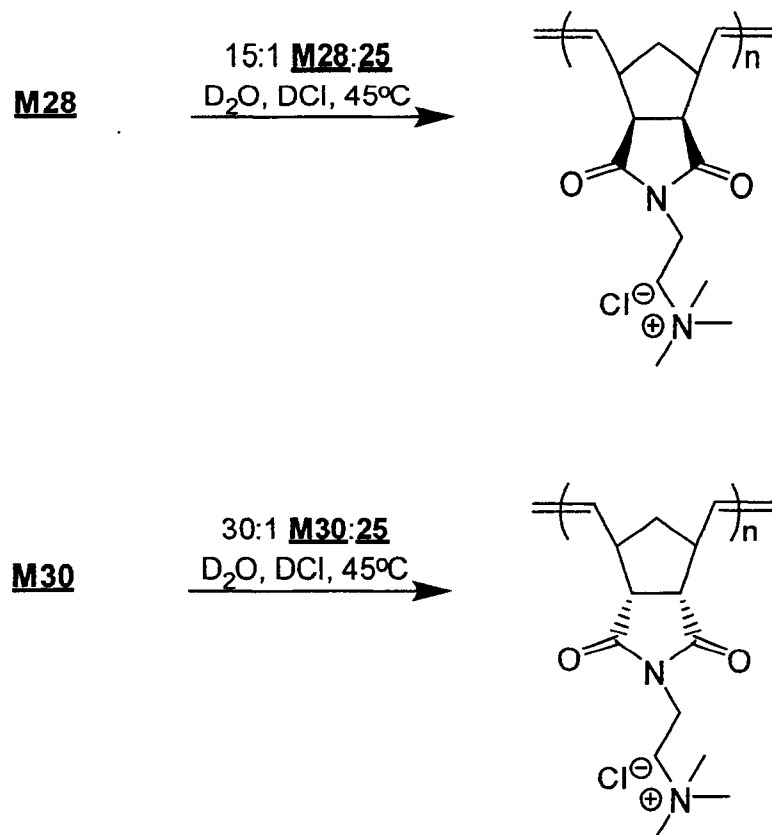
The first example of aqueous LROMP was reported by Grubbs and co-workers, which was a 'proof-of-concept' demonstration.¹⁶³ This was accomplished using previously reported well-defined water-soluble Ru-complexes **23** and **24** in the presence of acid to initiate aqueous LROMP of the water-soluble quarternary ammonium norbornene derivatives **M28** as outlined in Scheme I-11.^{163,164} To evaluate the livingness of the polymerization, NMR-scale polymerizations were conducted in D₂O employing DCI (1.0 eq. relatively to catalyst **23** or **24**). At 95% conversion, the propagating alkylidene proton at 19.2 ppm was observed with no decrease in the signal intensity over the lifetime of the polymerization (15 min). The block copolymerization of monomers

M28 and **M29** was executed via sequential monomer addition to demonstrate the livingness of the polymerization. After the complete polymerization of **M28**, **M29** was added and was completely consumed. The homopolymer had a measured PDI = 1.24 with no observed broadening in the PDI for the block copolymer.^{163,164}



Scheme I-11. ‘Proof-of-concept’ of homogeneous aqueous LROMP.

Gallivan and co-workers developed polyethylene glycol (PEG) conjugated NHC carbene-containing ruthenium benzylidene catalyst **25** which under acidic conditions was shown to be highly active toward *exo* and *endo* cationic norbornene derivatives **M28** and **M30** as shown in Scheme I-12.¹⁶⁵

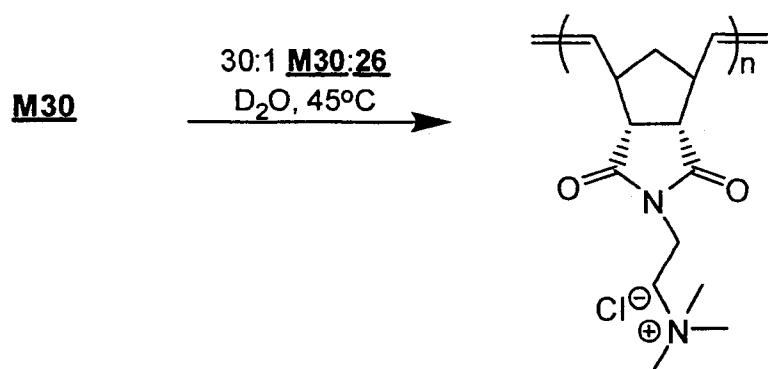


Scheme I-12. Aqueous ROMP of A) **M28** and B) **M30** using catalyst **25** under acid conditions.

For instance, the ROMP of **M28** using **25** in the presence of acid reached 95% conversion in 15 min as determined by 1H NMR spectroscopy; however, in the absence of acid the ROMP of **M28** using **25** reached only 73% conversion after 24 h. These observations are consistent with earlier studies described above by Grubbs.¹⁶⁴ The aqueous ROMP of **M30** under acidic conditions was evaluated to compare the catalytic activity of **23** and **25**. It

was found that **25** polymerized the sterically hindered **M30** to 95% conversion within 24 h as determined by ^1H NMR spectroscopy. By contrast, **23** showed limited activity toward **M30** as evident by the 13% conversion after 24 h. These findings suggest that NHC carbene-containing catalyst **25** is more active in aqueous ROMP. Nevertheless, catalyst **25** had limited stability in pure water and no detailed studies were done relating to kinetics, MM, and MMD profiles.

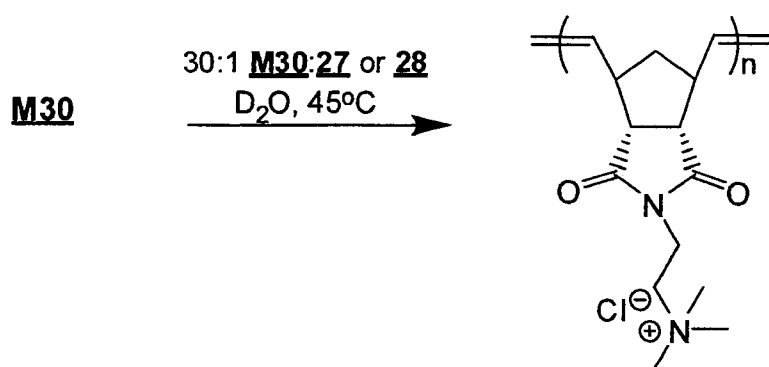
Given the limited stability and solubility of catalyst **25**, Hong and Grubbs reported the more stable water-soluble NHC catalyst **26** based on the Grubbs-Hoyveda structural motif.¹⁶⁶ In addition to the increased stability in water, the aqueous ROMP of cationic norbornene monomer **M30** revealed that the activity of catalyst **26** was higher than catalysts **23-25** (Scheme I-13). However, this study focussed more on aqueous RCM since no details regarding the kinetics, MMs, MMDs, and synthesis of advanced macromolecular architectures were discussed.



Scheme I-13. Aqueous ROMP of **M30** using catalyst **26** without acid.

Recently, Jordan and Grubbs reported the synthesis of small-molecule NHC-containing catalyst **27** and **28** and their subsequent activity in aqueous ROMP.¹⁶⁷ These

catalysts were targeted since catalysts **25** and **26** contain a polydisperse PEG group, which is capable of forming aggregates in water. The activity of catalysts **27** and **28** was found to be comparable to **26** in which the *endo* cationic norbornene derivative **M30** was polymerized to 95% conversion in 45 minutes (Scheme I-14). Again, this study seemed to focus more on RCM catalyst activities and with no reports of kinetics, MM, MMD, and the synthesis of advanced macromolecular architectures.



Scheme I-14. Aqueous ROMP of **M30** using catalyst **27** or **28** without acid.

While these results are somewhat promising, the emphasis of research in aqueous LROMP has been primarily focused on the development of new water-soluble catalysts and not strictly toward the synthesis of novel, well-defined WSPs. Presently, none of these water-soluble catalysts **23-28** are commercially available and, therefore, must be synthesized in the laboratory which can be time-consuming and often not straightforward. Given these shortcomings, what is needed is a synthetic protocol that will allow for the synthesis of novel, well-defined, WSPs without the need for post polymerization modifications or complex catalyst synthesis.

CHAPTER II

OBJECTIVES OF RESEARCH

The overall goal of this research is to prepare well-defined, salt-responsive (co)polymers via LROMP without the use of post polymerization modification methodologies and evaluate the aqueous solution properties of these stimulus-responsive materials. The introduction of a tunable hydrophilic/hydrophobic block into a block copolymer structure can lead to interesting aqueous solution behavior. To the best of our knowledge, the preparation of well-defined, controlled-architecture block copolymers under LROMP demonstrating stimulus-responsive behavior in aqueous media has never been reported in literature.

The Lowe Research Group (LRG) has a long standing interest in the synthesis of novel, well-defined WSPs utilizing CLP techniques. The LRG has a particular interest in the design, synthesis, and characterization of novel, well-defined, salt-responsive materials, and their potential application in the biomedical field and industry. Given this, our research efforts have focused on adapting LROMP for the preparation of well-defined, novel salt-responsive norbornene-based (co)polymers without the need for post-polymerization modification or the synthesis of well-defined water-soluble catalysts.

With these concepts in mind, the work contained in this dissertation is focused on three main topics of interest: (1) optimization of LROMP conditions to obtain well-defined, salt-responsive norbornene-based (co)polymers using commercially available Ru-complexes, (2) synthesis of novel salt-responsive, norbornene-based cationic/betaine AB diblock copolymers systems, and (3) preliminary evaluation of the aqueous solution

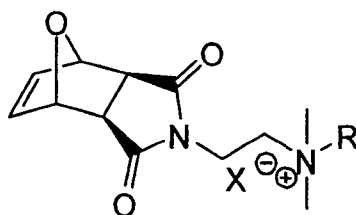
behavior of novel salt-responsive norbornene-based cationic/betaine AB diblock copolymers.

In the latter, a salt-responsive norbornene-based cationic/betaine AB diblock copolymer in which the cationic block is permanently hydrophilic and the betaine block is tunably hydrophilic/hydrophobic should result in a phase transition in which the betaine ('smart') block is insoluble in the absence of a low molecular weight electrolyte, resulting in self-assembly to form polymeric micelles. Subsequent addition of a low molecular weight salt (e.g. NaCl) should allow for complete molecular dissolution in aqueous media in which both blocks are hydrophilic. To the best of our knowledge, such stimulus-responsive block copolymers have never been prepared via LROMP or aqueous-LROMP. The specific objectives of this research are as follows:

- (1) Synthesis of new cationic/betaine, *exo*-7-oxanorbornene-based monomers that are susceptible to LROMP
- (2) Develop optimal conditions for the LROMP of novel cationic/betaine, norbornene-based monomers using commercially available Ru-initiators
- (3) Prepare well-defined, water-soluble cationic/betaine (co)polymers under LROMP in homogeneous organic media without the need for post-polymerization methodologies to evaluate homopolymerization kinetics
- (4) Prepare and characterize well-defined, cationic/betaine statistical and diblock copolymers to demonstrate the controlled behavior of the polymerization systems
- (5) Prepare well-defined, cationic/betaine norbornene-based diblock copolymer that exhibits salt-responsive behavior in aqueous media

- (6) Evaluate the aqueous solution properties of AB diblock copolymer described in (5) with regards to supramolecular self-assembly in aqueous environments using ^1H NMR spectroscopy and dynamic light scattering (DLS).

The completion of the objectives listed above requires the successful optimization of polymerization conditions (choice of solvent, or cosolvents, and ROMP initiator). The organic solvent used should be capable of completely solubilizing both water-soluble cationic and betaine norbornene-based monomers without having deleterious effects on the hydrophobic initiator. Additionally, the ROMP initiator should show high activity and functional group tolerance toward the novel cationic and betaine norbornene-based monomers.



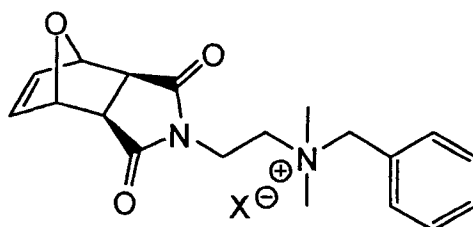
M31

R = ethyl, propyl, butyl, pentyl, octyl, or benzyl
X = Br or Cl

Figure II-1. Structure of a series of new permanently cationic ammonium *exo*-7-oxanorbornene derivatives **M31**.

This work can be divided into three chapters. Chapter III of this dissertation concerns the synthesis and controlled polymerization of a series of new permanently cationic ammonium *exo*-7-oxanorbornene derivatives **M31**. While no aqueous solution studies were carried out with this series of (co)polymers, optimal polymerization

conditions were established to facilitate LROMP of these novel cationic norbornene-based monomers in a homogeneous organic cosolvent system. Additionally, the polymerization conditions developed in the LROMP of these novel cationic norbornene-based monomers were used to evaluate the counterion effect on polymerization kinetics discussed in Chapter IV and the LROMP of betaine norbornene-based monomers discussed in Chapter V.



MON

X = Cl or Br

Figure II-2. Structure of *exo*-benzyl-[2-(3,5-dioxo-10-oxa-4-aza-tricyclo[5.2.1.0^{2,6}]dec-8-en-4-yl)ethyl]dimethyl ammonium bromide/chloride **MON**.

Chapter IV concerns the effect of halide counterion on the LROMP kinetics of permanently cationic *exo*-7-oxanorbornene derivatives. Statistical copolymerizations of *exo*-benzyl-[2-(3,5-dioxo-10-oxa-4-aza-tricyclo[5.2.1.0^{2,6}]dec-8-en-4-yl)ethyl]dimethyl ammonium bromide/chloride **MON** were conducted at varying molar ratios to evaluate the polymerization kinetics and molecular mass profiles.

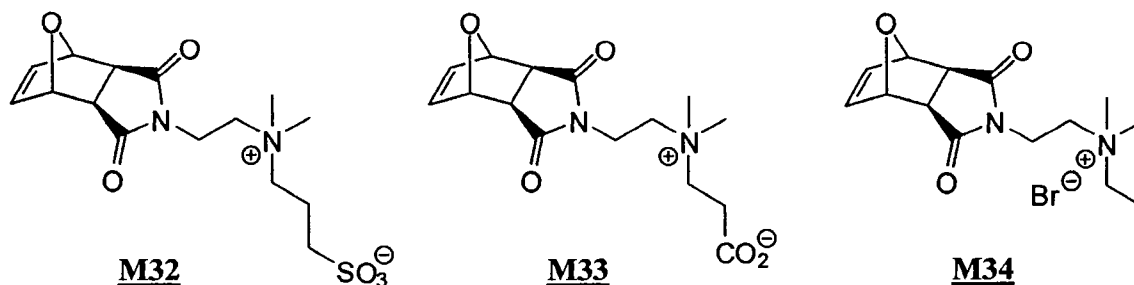


Figure II-3. Structures of *exo*-propylsulfobetaine-[2-(3,5-dioxo-10-oxa-4-aza-tricyclo[5.2.1.0^{2,6}]dec-8-en-4-yl)ethyl]dimethyl ammonium **M32**, *exo*-propylcarboxy-[2-(3,5-dioxo-10-oxa-4-aza-tricyclo[5.2.1.0^{2,6}]dec-8-en-4-yl)ethyl]dimethyl ammonium **M33** and *exo*-propyl-[2-(3,5-dioxo-10-oxa-4-aza-tricyclo[5.2.1.0^{2,6}]dec-8-en-4-yl)ethyl]dimethyl ammonium bromide **M34**.

Chapter V concerns the synthesis and characterization of homo- and diblock copolymers of carboxy and sulfo-betaines. Also, a cationic/betaine AB diblock copolymer was prepared to evaluate its stimulus-responsive behavior in aqueous solution in the presence and absence of NaCl. *exo*-Propylsulfobetaine-[2-(3,5-dioxo-10-oxa-4-aza-tricyclo[5.2.1.0^{2,6}]dec-8-en-4-yl)ethyl]dimethyl ammonium **M32** and *exo*-propylcarboxy-[2-(3,5-dioxo-10-oxa-4-aza-tricyclo[5.2.1.0^{2,6}]dec-8-en-4-yl)ethyl]dimethyl ammonium **M33** betaines were prepared and polymerized under LROMP conditions established in Chapter III. Additionally, **M32** and *exo*-propyl-[2-(3,5-dioxo-10-oxa-4-aza-tricyclo[5.2.1.0^{2,6}]dec-8-en-4-yl)ethyl]dimethyl ammonium bromide **M34** was used to prepare a salt-responsive AB diblock copolymer.

CHAPTER III

THE CONTROLLED HOMOGENEOUS ORGANIC SOLUTION POLYMERIZATION OF
NEW HYDROPHILIC CATIONIC *exo*-7-OXANORBORNENE VIA ROMP WITH
RuCl₂(PCy₃)₂CHPh IN A NOVEL 2,2,2-TRIFLUOROETHANOL/METHYLENE
CHLORIDE SOLVENT MIXTURE**Introduction**

In this chapter we describe the synthesis of a series of new permanently cationic *exo*-7-oxanorbornene derivatives prepared from a common tertiary amine precursor. We have evaluated the homo- and copolymerization behavior of these new monomers under homogeneous organic solution conditions employing Grubbs' first generation catalyst, RuCl₂(PCy₃)₂CHPh, in a novel 2,2,2-trifluoroethanol/methylene chloride (TFE/CH₂Cl₂, 50/50 vol%) solvent mixture. Since we believe this to be the first report in which a fluorinated alcohol has been employed as a (co)solvent in LROMP an emphasis has been placed on the determination of the kinetic features of the polymerizations and a demonstration of their controlled nature. We show that the TFE/CH₂Cl₂ solvent mixtures, as well as two additional halogenated alcoholic cosolvents, are extremely effective media for conducting the polymerization of such cationic substrates under facile, homogeneous conditions, in a controlled fashion. Such findings clearly have significantly wider implications in other, small molecule metathesis chemistries in which solubility matching between catalysts and substrates might be an issue.

Experimental

All reagents were purchased from Aldrich Chemical Company at the highest available purity and used as received unless stated otherwise. 2,2,2-Trifluoroethanol (TFE), 2,2,2-

trichloroethanol (TCE), 1,1,1,3,3,3-hexafluoroisopropanol (HFIP), ethyl vinyl ether (EVE), and dichloromethane (CH_2Cl_2) were distilled, degassed by at least three freeze-pump-thaw cycles, and stored in a nitrogen filled glove box until needed. Grubbs' first generation catalyst, $\text{RuCl}_2(\text{PCy}_3)_2\text{CHPh}$ **17**, was stored in a Plas-Labs N_2 -filled glove box. All polymerizations were conducted under an inert N_2 atmosphere in the glove box.

Synthesis of $\text{exo-4-(2-dimethylaminoethyl)-10-oxa-4-aza-tricyclo[5.2.1.0}^{2,6}\text{]dec-8-ene-3,5-dione}$ (DMAETDD).

The title compound was prepared from the reaction of *exo-3,6-epoxy-1,2,3,6-tetrahydrophthalic anhydride* with *N,N*-dimethylethylene diamine according to a literature procedure.¹⁷⁴ Briefly, to a 250 mL three neck round bottomed flask equipped with a magnetic stir bar was added *exo-3,6-epoxy-1,2,3,6-tetrahydrophthalic anhydride* (5.03g, 30.4 mol) in MeOH/THF (150 mL, 1:1), and was stirred at 60°C. *N,N*-Dimethylethylenediamine (3.35 mL, 30.4 mol) was slowly added to this solution. The reaction mixture was subsequently held at 50°C for 12 h. Following this, the solvent was removed *in vacuo* to yield a gold viscous oil which solidified upon cooling in the freezer. The crude solid was recrystallized from MeOH/hexane (2:1) to yield off-white crystals of DMAETDD. Yield = 76 %, mp = 92.8-95.4°C. ^1H NMR (300 MHz, CDCl_3): δ (ppm) = 6.51 (2H, m), 5.26 (2H, t), 3.59 (2H, t), 2.86 (2H, d), 2.47 (2H, t), 2.26 (6H, s). ^{13}C NMR (75 MHz, CDCl_3): δ (ppm) = 176.44 ($\underline{\text{C}}=\text{O}$), 136.75 ($\underline{\text{C}}\text{H}=\text{CH}$), 81.08 ($\text{HC}-\underline{\text{O}}$), 56.37 ($\text{N}-\underline{\text{C}}\text{H}_2$), 47.67 ($\underline{\text{C}}\text{H}_2-\text{N}(\text{CH}_3)_2$), 45.65 ($\underline{\text{C}}\text{H}-\text{C}=\text{O}$), 37.05 ($(\underline{\text{C}}\text{H}_3)_2-\text{NCH}_2$).

Synthesis of exo-benzyl-[2-(3,5-dioxo-10-oxa-4-aza-tricyclo[5.2.1.0^{2,6}]^{2,6}dec-8-en-4-yl)-ethyl]-dimethyl-ammonium bromide (Bn-quat-Br).

The title compound was prepared via a Menshutkin reaction between DMAETDD and benzyl bromide. To a 100 mL canonical flask equipped with a magnetic stir bar was added DMAETDD (5.11 g, 21.6 mmol) and THF (50 mL). To this was added benzyl bromide (37.2 g, 10 mol eq.). The reaction was heated at 50°C for 48 h, during which time a white precipitate formed. The precipitate was isolated by Buchner filtration and dried *in vacuo* at ambient temperature yielding the title compound as a white powder.

Yield = 95%, mp = 162-165°C. ¹H NMR (300 MHz, D₂O): δ (ppm) = 7.39 (5H, m), 6.42 (2H, t), 5.12 (2H, s), 4.36 (2H, t), 3.87 (2H, t), 3.35 (2H, t), 2.98 (2H, d), 2.87 (6H, s). ¹³C NMR (75 MHz, D₂O): δ (ppm) = 178.46 (N-C=O), 136.56 (HC=CH-CHO), 133.12 (C=CH-CH), 131.18 (C=CH-CH), 129.41 (CH-CH=CH), 126.66 (CH=CH-C), 81.22 (HC-O), 68.55 (CH₂-C₆H₅), 59.60 (N-CH₂), 49.99 (CH₂-N(CH₃)₂), 47.70 (CH-C=O), 32.72 ((CH₃)₂-NCH₂). C₁₉H₂₃BrN₂O₃ (406.09): Anal. Calcd. C, 56.0; H, 5.69; Br, 19.62; N, 6.88; O, 11.78; Found: C, 55.15; H, 5.70; N, 6.79.

Synthesis of exo-benzyl-[2-(3,5-dioxo-10-oxa-4-aza-tricyclo[5.2.1.0^{2,6}]^{2,6}dec-8-en-4-yl)-ethyl]-dimethyl-ammonium chloride (Bn-quat-Cl)

The title compound was prepared in the same manner as Bn-quat-Br except benzyl chloride was used in place of benzyl bromide. Yield = 93%, mp = 150-154°C. ¹H NMR (300 MHz, D₂O): δ (ppm) = 7.41 (5H, m), 6.46 (2H, t), 5.16 (2H, s), 4.39 (2H, t), 3.92 (2H, t), 3.39 (2H, t), 3.02 (2H, d), 2.94 (6H, s). ¹³C NMR (75 MHz, D₂O): δ (ppm) = 178.54 (N-C=O), 136.56 (HC=CH-CHO), 133.19 (C=CH-CH), 131.27 (C=CH-CH),

129.51 (CH-CH=CH), 126.80 (CH=CH-C), 81.31 (HC-O), 68.63 (CH₂-C₆H₅), 59.66 (N-CH₂), 50.10 (CH₂-N(CH₃)₂), 47.80 (CH-C=O), 32.80 ((CH₃)₂-NCH₂). C₁₉H₂₃ClN₂O₃ (406.09): Anal. Calcd. C, 62.89; H, 6.39; Cl, 9.77; N, 7.72; O, 13.23; Found: C, 59.29; H, 6.73; N, 7.47.

Synthesis of exo-[2-(3,5-dioxo-10-oxa-4-aza-tricyclo[5.2.1.0^{2,6}]dec-8-en-4-yl)-ethyl]-ethyl-dimethyl-ammonium bromide (Et-quat-Br).

Et-quat-Br was prepared using the same methodology as detailed above for Bn-quat-Br with ethyl bromide being used in place of benzyl bromide. Yield = 93%, mp = 181-186°C. ¹H NMR (300 MHz, D₂O): δ (ppm) = 6.56 (2H, t), 5.13 (2H, t), 3.76 (2H, t), 3.46 (2H, t), 3.35 (2H, m), 3.08 (6H, s), 2.99 (2H, d), 1.23 (3H, t). ¹³C NMR (75 MHz, D₂O): δ (ppm) = 176.9 (N-C=O), 137.19 (HC=CH-CHO), 81.23 (HC-O), 60.55 (N-CH₂), 58.75 (CH₂-N(CH₃)₂), 50.64 (N(CH₃)₂-CH₂), 47.81 (CH-C=O), 32.58 ((CH₃)₂-NCH₂), 7.82 (N(CH₃)₂-CH₂CH₃). C₁₄H₂₁BrN₂O₃ (344.07): Anal. Calcd. C, 48.71; H, 6.13; Br, 23.15; N, 8.11; O, 13.90; Found: C, 48.41; H, 6.10; N, 8.10.

Synthesis of exo-[2-(3,5-dioxo-10-oxa-4-aza-tricyclo[5.2.1.0^{2,6}]dec-8-en-4-yl)-ethyl]-dimethyl-propyl-ammonium bromide (Pr-quat-Br).

Pr-quat-Br was prepared using the same methodology as detailed above for Bn-quat-Br except propyl bromide was used in place of benzyl bromide. Yield = 87%, mp = 170-174°C. ¹H NMR (300 MHz, D₂O): δ (ppm) = 6.45 (2H, t), 5.20 (2H, t), 3.83 (2H, t), 3.39 (2H, t), 3.20 (2H, m), 3.05 (2H, d), 3.00 (6H, s), 1.64 (2H, m), 0.814 (3H, t). ¹³C NMR (75 MHz, H₂O): δ (ppm) 178.43 (N-C=O), 136.69 (HC=CH-CHO), 81.24 (HC-O), 66.12

(N- $\underline{\text{C}}\text{H}_2$), 59.56 ($\underline{\text{C}}\text{H}_2\text{-N}(\text{CH}_3)_2$), 51.59 ($\text{N}(\text{CH}_3)_2\text{-}\underline{\text{C}}\text{H}_2$), 47.83 ($\underline{\text{C}}\text{H-C=O}$), 32.62 ($(\underline{\text{C}}\text{H}_3)_2\text{-NCH}_2$), 15.92 ($\text{CH}_2\underline{\text{C}}\text{H}_2\text{CH}_3$), 10.08 ($\text{CH}_2\text{CH}_2\underline{\text{C}}\text{H}_3$). $\text{C}_{15}\text{H}_{23}\text{BrN}_2\text{O}_3$ (358.09): Anal. Calcd. C, 50.15; H, 6.45; Br, 22.24; N, 7.80; O, 13.36; Found: C, 50.0; H, 6.40; N, 7.90.

Synthesis of exo-butyl-[2-(3,5-dioxo-10-oxa-4-aza-tricyclo[5.2.1.0^{2,6}]]dec-8-en-4-yl)-ethyl]-dimethyl-ammonium bromide (Bu-quat-Br).

Bu-quat-Br was prepared using the same methodology as detailed above for Bn-quat-Br except butyl bromide was used in place of benzyl bromide. Yield = 88%, mp = 168-171°C. ^1H NMR (300 MHz, D_2O): δ (ppm) = 6.49 (2H, t), 5.20 (2H, t), 3.76 (2H, t), 3.82 (2H, t), 3.23 (2H, m), 3.04 (2H, d), 3.00 (6H, s), 1.65 (2H, m), 1.25 (2H, m), 0.820 (3H, t). ^{13}C NMR (75 MHz, D_2O): δ (ppm) = 178.43 (N- $\underline{\text{C}}=\text{O}$), 136.69 ($\text{HC}=\underline{\text{C}}\text{H-CHO}$), 81.24 (HC-O), 64.56.12 (N- $\underline{\text{C}}\text{H}_2$), 59.48 ($\underline{\text{C}}\text{H}_2\text{-N}(\text{CH}_3)_2$), 51.18 ($\text{N}(\text{CH}_3)_2\text{-}\underline{\text{C}}\text{H}_2$), 47.82 ($\underline{\text{C}}\text{H-C=O}$), 32.63 ($(\underline{\text{C}}\text{H}_3)_2\text{-NCH}_2$), 24.09 ($\text{CH}_2\underline{\text{C}}\text{H}_2\text{CH}_2\text{CH}_3$), 19.23 ($\text{CH}_2\text{CH}_2\underline{\text{C}}\text{H}_2\text{CH}_3$), 13.15 ($\text{CH}_2\text{CH}_2\text{CH}_2\underline{\text{C}}\text{H}_3$). $\text{C}_{15}\text{H}_{25}\text{BrN}_2\text{O}_3$ (372.10): Anal. Calcd. C, 51.48; H, 6.75; Br, 21.41; N, 7.50; O, 12.86; Found: C, 51.9; H, 7.00; N, 7.40.

Synthesis of exo-[2-(3,5-dioxo-10-oxa-4-aza-tricyclo[5.2.1.0^{2,6}]]dec-8-en-4-yl)-ethyl]-dimethyl-pentyl-ammonium bromide (Pen-quat-Br).

Pen-quat-Br was prepared using the same methodology as detailed above for Bn-quat-Br except pentyl bromide was used in place of benzyl bromide. Yield = 80%, mp = 173-176°C. ^1H NMR (300 MHz, D_2O): δ (ppm) = 6.47 (2H, t), 5.17 (2H, t), 3.80 (2H, t), 3.36 (2H, t), 3.22 (2H, m), 3.02 (2H, d), 2.98 (6H, s), 1.62 (2H, m), 1.19 (4H, m), 0.744 (3H, t). ^{13}C NMR (75 MHz, D_2O): δ (ppm) = 178.43 (N- $\underline{\text{C}}=\text{O}$), 136.63 ($\text{HC}=\underline{\text{C}}\text{H-CHO}$),

81.20 (HC-O), 64.67.12 (N-CH_2), 59.38 ($\text{CH}_2\text{-N}(\text{CH}_3)_2$), 51.15 ($\text{N}(\text{CH}_3)_2\text{-CH}_2$), 47.77 (CH-C=O), 32.57 ($(\text{CH}_3)_2\text{-NCH}_2$), 27.70 ($\text{CH}_2\text{CH}_2\text{CH}_2\text{CH}_3$), 21.71 ($\text{CH}_2\text{CH}_2(\text{CH}_2)_2\text{CH}_3$), 13.31 ($\text{CH}_2(\text{CH}_2)_3\text{CH}_3$). $\text{C}_{117}\text{H}_{27}\text{BrN}_2\text{O}_3$ (386.12): Anal. Calcd. C, 52.72; H, 7.03; Br, 20.63; N, 7.23; O, 12.39; Found: C, 52.81; H, 7.00; N, 7.21.

Synthesis of exo-[2-(3,5-dioxo-10-oxa-4-aza-tricyclo[5.2.1.0^{2,6}]dec-8-en-4-yl)-ethyl]-dimethyl-octyl-ammonium bromide (Oct-quat-Br).

Oct-quat-Br was prepared using the same methodology as detailed above for Bn-quat-Br except octyl bromide was used in place of benzyl bromide. Yield = 76%, mp = 158-161 °C. ^1H NMR (300 MHz, D_2O): δ (ppm) = 6.46 (2H, t), 5.14 (2H, t), 3.78 (2H, t), 3.33 (2H, t), 3.16 (2H, m), 3.00 (2H, d), 2.99 (6H, s), 1.60 (2H, m), 1.15 (10H, m), 0.700 (3H, t). ^{13}C NMR (75 MHz, D_2O): δ (ppm) = 178.37 (N-C=O), 136.61 (HC=CH-CHO), 81.20 (HC-O), 64.46.12 (N-CH_2), 59.35 ($\text{CH}_2\text{-N}(\text{CH}_3)_2$), 51.26 ($\text{N}(\text{CH}_3)_2\text{-CH}_2$), 47.77 (CH-C=O), 32.59 ($(\text{CH}_3)_2\text{-NCH}_2$), 31.26 ($\text{CH}_2\text{CH}_2(\text{CH}_2)_5\text{CH}_3$) 28.42 ($(\text{CH}_2)_2\text{CH}_2(\text{CH}_2)_4\text{CH}_3$), 25.60 ($(\text{CH}_2)_3\text{CH}_2(\text{CH}_2)_3\text{CH}_3$), 22.04 ($(\text{CH}_2)_3\text{CH}_2(\text{CH}_2)_3\text{CH}_3$), 13.74 ($\text{CH}_2(\text{CH}_2)_6\text{CH}_3$). $\text{C}_{20}\text{H}_{33}\text{BrN}_2\text{O}_3$ (428.17): Anal. Calcd. C, 55.94; H, 7.75; Br, 18.61; N, 6.52; O, 11.18; Found: C, 55.50; H, 7.69; N, 6.57.

Homopolymerization of quaternary ammonium monomers

Below is a typical procedure for the homopolymerization of the quaternary monomeric substrates: To a single neck Schlenk flask (100 mL capacity) equipped with a magnetic stir bar was added Bn-quat-Br (0.500 g, 1.23 mmol). The flask was subsequently degassed/back-filled with N_2 three times using standard Schlenk line techniques. The

flask was then transferred to a nitrogen filled glove box. To this flask was then added TFE (2.0 mL). The required amount of **17** (based on a targeted molecular mass of 10,000: 0.05 mmol, 20,000: 0.025mmol, and 30,000: 0.0125mmol) was weighed out in the glove box into a scintillation vial. To the catalyst was added CH₂Cl₂ (2.0 mL). The catalyst solution was then added directly to the monomer solution. Polymerizations were left for 15-30 min prior to being terminated with EVE (0.5 mL). This solution was left to stir for 15 min prior to precipitation into a large excess of THF. The polymer was isolated by Buchner filtration, washed with THF, and dried overnight *in vacuo* at ambient temperature.

Statistical copolymerization of Et-quat-Br with Pen-quat-Br

To a single neck, 100 mL capacity, Schlenk flask, equipped with a magnetic stir-bar was added Et-quat-Br (0.5 g, 1.45 mmol) and Pen-quat-Br (0.5 g, 1.30 mmol). The flask was degassed using standard Schlenk line techniques prior to being transferred to a nitrogen-filled glovebox. TFE (2.5 mL) was added to the flask and the mixture allowed to stir until the two monomers were completely dissolved. To a scintillation vial (20.0 mL capacity) was added **17** (40.0 mg, 0.049 mmol). To this vial was then added CH₂Cl₂ (2.5 mL) to dissolve the catalyst. After complete dissolution, the catalyst solution was added directly to the monomer solution. The polymerization was allowed to proceed for 20 min prior to being terminated with EVE. The copolymer was subsequently isolated via precipitation into a large excess of THF, followed by Buchner filtration and drying overnight *in vacuo* at ambient temperature.

Block Copolymerization of Et-quat-Br with Prop-quat-Br

To a single neck Schlenk flask (100 mL capacity), equipped with a magnetic stir-bar was added Et-quat-Br (0.5 g, 1.45 mmol). To a second single neck, Schlenk flask (100 mL capacity), equipped with a magnetic stir bar was added Pro-quat-Br (0.5 g, 1.39 mmol). Both flasks were degassed using standard Schlenk line techniques prior to being transferred to a nitrogen-filled glovebox. TFE (1.5 mL) was added to the flask containing Pro-quat-Br and allowed to stir until the monomer was completely dissolved. To a scintillation vial (20.0 mL capacity) was added Grubbs' catalyst (40.0 mg, 0.049 mmol) followed by CH₂Cl₂ (1.5 mL). After complete dissolution, the catalyst solution was added directly to the Pr-quat-Br monomer solution. The polymerization was allowed to proceed for 5 min prior to taking an aliquot, which was quenched with EVE. The second monomer, Et-quat-Br, was then added as a solid directly to the polymerization mixture. The polymerization was allowed to proceed for an additional 20 min before being terminated with EVE. The block copolymer was subsequently isolated via precipitation into a large excess of THF, followed by Buchner filtration and drying overnight *in vacuo* at ambient temperature.

Stability of 17 in TFE/CH₂Cl₂

The stability of 17 in the TFE/CH₂Cl₂ cosolvent mixture was determined by monitoring the ³¹P NMR spectra of a solution of the initiator over a 30 min period. In a N₂-filled glove box, Grubbs' catalyst (50.0 mg, 0.061 mmol) was added to a standard 5.0 mL NMR tube. To this was added 0.5 mL of 1:1 TFE/CD₂Cl₂. The NMR tube was capped, removed from the Glovebox and ³¹P NMR spectra recorded.

Determination of the dn/dc for poly(Pen-quat-Br)

Six solutions of poly(Pen-quat-Br) (M_n , theory = 20,000) were prepared by adding the homopolymer (25.0-75.0 mg) to individual scintillation vials (20.0 mL capacity). To each vial was added aqueous size exclusion chromatography (ASEC) eluent (10.0 mL) to yield final concentrations of poly(Pen-quat-Br) in the range 2.5-7.5 mg mL. Each solution was subsequently injected into the ASEC instrument. Analysis and dn/dc determination was achieved using the Omnisec Interactive GPC software.

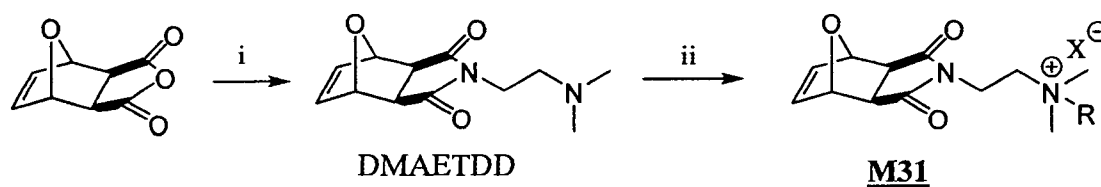
Characterization techniques

^1H (300 MHz), ^{13}C (75 MHz), and ^{31}P (121.5 MHz) NMR spectra were recorded on a Bruker 300 53 mm spectrometer in appropriate deuterated solvents or solvent mixtures. FTIR spectra were recorded on a Thermo Nicolet Nexus 470 FTIR spectrometer equipped with a Smart Orbit. Polymer molecular masses, molecular mass distributions, and polydispersity indices were determined by ASEC in 0.1 M Na_2SO_4 /1 vol % acetic acid flow rate of 0.20 mL min^{-1} at ambient temperature. The system was comprised of a Viscotek VE1122 pump, Viscotek VE3580 RI detector, Viscotek T60 dual viscosity/right angle laser light scattering detector, a CATSEC 1000 7μ (50 x 4.6 mm) guard column followed by a series of two CATSEC columns (CATSEC 1000 7μ 250 x 4.6 mm + 100 5μ 250 x 4.6 mm) with a theoretical linear molecular mass range of 200 – 2,000,000 g/mol. Data were analyzed with the Omnisec Interactive GPC software package. Melting points of the new monomers were determined using an Electrothermal digital melting point apparatus.

Results and Discussion

Monomer Synthesis

Our interest in water-soluble polymers, and especially those with ionic functionality and potential “smart” properties, prompted us to investigate the application of LROMP for the synthesis of new, highly functional materials. In particular, we have a strong interest in cationic monomers as building blocks in novel (co)polymers. Given the relatively sparse literature concerning the *direct* controlled LROMP of permanently cationic monomers under homogeneous conditions we have prepared a series of new cationic *exo*-7-oxanorbornene derivatives **M31**, Scheme III-1, and evaluated their polymerizability under homogeneous conditions in *organic* media with **17** employing a novel cosolvent mixture of TFE and CH₂Cl₂. *exo* Monomer derivatives were targeted exclusively in this study since it is well known that *exo*-norbornene monomers polymerize more readily than the corresponding *endo*-derivatives, especially with first generation Ru-based catalyst derivatives.^{166,188,189}

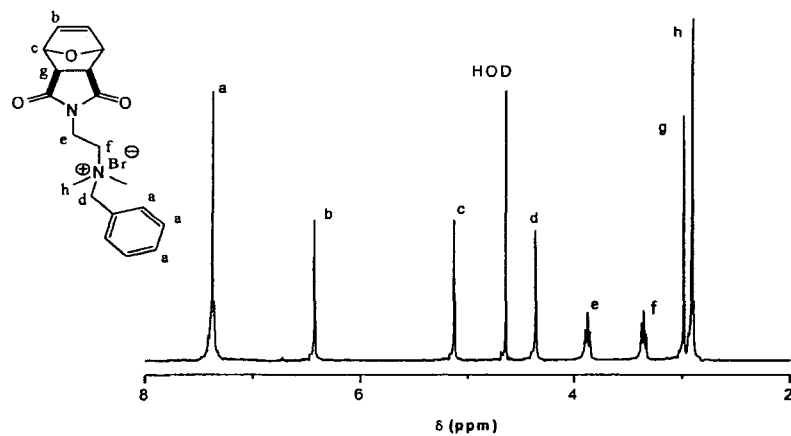


Conditions: (i) N,N-dimethylethylenediamine, MeOH/THF, 50°C
(ii) alkyl halide, THF, 50°C.

Scheme III-1. Synthetic outline for the preparation of the permanently cationic *exo*-7-oxanorbornene derivatives **M31**.

Monomer syntheses were achieved via a multi-step procedure in which commercially available *exo*-3,6-epoxy-1,2,3,6-tetrahydrophthalic anhydride was reacted with *N,N*-dimethylethylene diamine to yield the intermediate tertiary amine-imide derivative, DMAETDD. After purification, this common functional precursor was reacted with various alkyl halides, via a Menshutkin reaction, to yield the desired *exo*-quaternary ammonium monomers. Such facile quaternizations were successfully accomplished using a range of alkyl halides to yield the ethyl, *n*-propyl, *n*-butyl, *n*-pentyl, *n*-octyl and benzyl derivatives in high to near-quantitative yields. The structure of these new permanently cationic monomers was confirmed via a combination of ^1H and ^{13}C NMR spectroscopy. As a representative example, Figure III-1 shows the ^1H and ^{13}C NMR spectra of the benzyl quat derivative Bn-quat-Br, recorded in D_2O , with corresponding peak assignments.

A



B

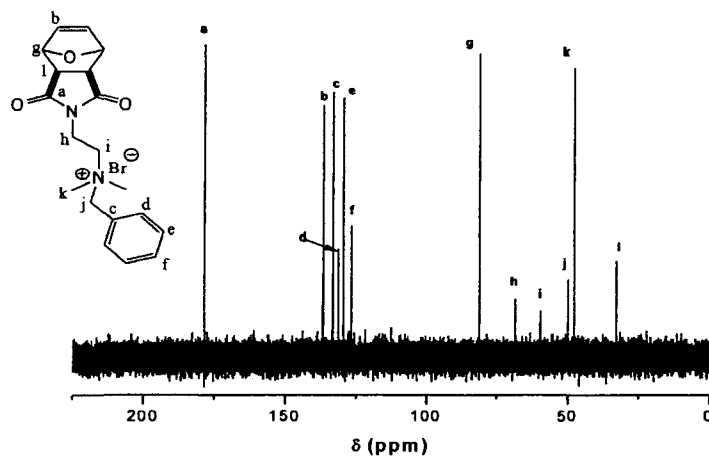


Figure III-1. ^1H (A) and ^{13}C (B) NMR spectra of Bn-quat-Br recorded in D_2O with peak assignments.

Homopolymerization Studies

With a series of new *exo*-quaternary ammonium 7-oxanorbornene derivatives **M31** successfully prepared, we next needed to identify appropriate conditions which would facilitate the direct, controlled, *homogeneous* polymerization of the substrates with the

commercially available Grubbs' initiator **17**. As highlighted above, in previous reports the preparation of such materials, at least under homogeneous conditions, has required either the multi-step synthesis of water-soluble Ru initiators for polymerizations in aqueous media,^{162,164,166} or the application of protection/deprotection protocols,¹⁸² which, unfortunately, also greatly complicates/lengthens the synthesis of the target materials. A significant problem with performing homogeneous polymerizations with the desired monomer/initiator combinations is the inherent incompatibility in solubility between the ionic, hydrophilic monomeric substrates and the hydrophobic initiator. As such, identifying a suitable solvent which was capable of solubilizing these two components, but which did not have any adverse effect(s) on the Ru complex or the polymerization in general, was the first challenge. Initially, we evaluated pure TFE since it has been demonstrated previously to be a thermodynamically excellent solvent for highly polar, zwitterionic monomers and polymers bearing the sulfobetaine functional group.^{6,190} Such materials possess very limited solubility characteristics and are generally soluble only in aqueous salt solutions and certain fluorinated alcohols. Additionally, it is known that TFE is capable of molecularly dissolving amphiphilic methacrylic block copolymers³⁸ thus demonstrating its ability to solubilize species at opposite ends of the polarity scale. As such, we anticipated that TFE might be a suitable solvent for the quaternary ammonium monomers **M31** and **17**. However, while the quaternary ammonium monomers were readily soluble in pure TFE, **17** was not. Fortunately, we subsequently found that both the cationic monomers and **17** readily dissolved in a 1:1 v/v TFE:CH₂Cl₂ solvent mixture. Having identified a suitable solvent mixture capable of yielding a homogeneous solution of monomer and initiator we proceeded to examine the

homopolymerization characteristics of the new quaternary ammonium monomers, **M31**, in this novel cosolvent combination. All homopolymerizations were conducted under an inert N₂ atmosphere in a Plas-Labs glove box at ambient temperature and at a monomer concentration of 0.4 g/mL.

Since both the monomers and the solvent combination represent new ROMP substrates and polymerization conditions respectively we felt it important to investigate whether such substrates could be polymerized in a controlled manner in this solvent system. While the general polymerizability of the quaternary ammonium monomers **M31** was not anticipated to be problematic since structurally similar species have been successfully polymerized previously by Grubbs and co-workers,¹⁶²⁻¹⁶⁶ the presence and possible effect(s) of TFE were unknown. We thus proceeded to evaluate several of the common established criteria for controlled polymerizations, and specifically we investigated the kinetic profiles, the evolution of molecular mass with conversion, the molecular mass distributions, and the ability to prepare materials with advanced architectures.

The kinetic features, i.e. the pseudo first-order kinetic profiles, for three of the new quaternary monomers were evaluated. In each case, aliquots were withdrawn directly from the polymerization vessels, quenched with EVE, and subsequently analyzed via a combination of NMR spectroscopy and ASEC. Conversions were determined from the ¹H NMR spectra of the aliquots by comparing the relative intensities of the monomeric vinyl signal with the backbone vinylic resonances of the polymer. Figure III-2 shows a representative example of a series of ¹H NMR spectra, plotted between $\delta \sim 7.0$ and 5.4 ppm, for the homopolymerization of Bn-quat-Br

highlighting the clear difference in chemical shifts of the monomer vs polymer vinyl protons. The intensity of the monomer proton signals have been normalized to demonstrate the steady increase in relative intensity of the backbone polymeric signals.

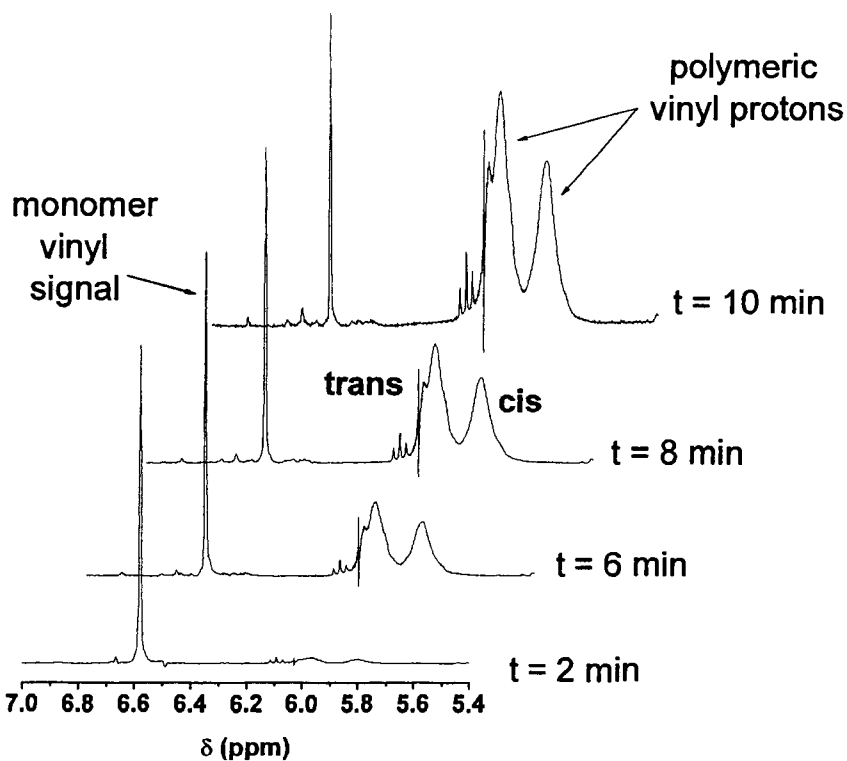


Figure III-2. ¹H NMR spectra demonstrating the increase in conversion with time using a comparison of the monomer vs polymeric vinylic signals for a Bn-quat-Br homopolymerization.

At this point, it should be noted that upon polymerization of such functional norbornene derivatives the resulting microstructure of the (co)polymers can be very complex by virtue of the fact that there exists the possibility of geometric isomerism in the polymer backbone (cis vs trans double bonds) coupled with the presence of chiral centers in the monomeric substrates, and as such the head-to-tail vs head-to-head (or tail-

to-tail) monomer additions become an important consideration when evaluating the microstructure of the resulting materials. While we have not, at this time, conducted a detailed determination of the microstructure, we have as part of the kinetic evaluations examined the cis/trans ratio. The peak splitting associated with the polymeric signals, Figure III-2, is due to the primary stereochemical effect, namely the possibility of geometric isomerism in the backbone. In all instances, the polymerizations yielded homopolymers with a trans-rich content, Table III-1, which is consistent with these types of monomeric substrates polymerized with 17.¹⁹¹ For example, Amir-Ebrahimi and co-workers evaluated the microstructural features resulting from the homopolymerization of 18 different norbornene monomers including examples of dienes, oxa-bridged substrates, and species with various substitution patterns with 17. In all instances homopolymers with trans-rich backbones were formed with molar fractions ranging from 0.9 to 0.5 with typical values around 0.7. These are entirely consistent with our finding in which polymers with approximately 60% trans content are formed.

With the conversion data readily available, the pseudo first-order kinetic profiles for the three cationic monomers were determined. Figure III-3 shows the conversion and pseudo first-order kinetic plots for the homopolymerization of the Bn-, Prop-, and Pen-quat-Br monomers respectively. In the case of Bn-quat-Br, Figure III-3A, we see that the homopolymerization proceeds rapidly with ca. 95% conversion being reached in 12 min at ambient temperature. This is noticeably faster than the analogous methyl-quat-Cl monomer polymerized by Grubbs' in aqueous media employing a water-soluble initiator derivative which required heating at 45°C to achieve high conversion.^{163,164}

Table III-1. Summary of the Theoretical and Experimentally Determined Molecular Characteristics for the Cationic (Co)polymers Including the Molecular Masses, Polydispersity Indices, Compositions, R_p Values, and % Trans Content

Entry	Monomer	Solvent combination (1:1)	Composition	M_n theory	M_n NMR	M_n ASEC	M_w ASEC	M_w/M_n^a	k_p $L/mol\cdot s$	% trans content ^b	% yield (NMR)
1	Bz	CH ₂ Cl ₂ /TFE	-	20,000	-	21,000	24,800	1.12	0.2254	57	95
2	Et	CH ₂ Cl ₂ /TFE	-	20,000	23,300	25,000	29,900	1.19	-	-	95
3	Pr	CH ₂ Cl ₂ /TFE	-	5,000 10,000 20,000	6,300 10,800 21,300	7,700 11,500 19,300	9,300 13,400 21,000	1.24 1.17 1.09	0.4525	64	98
4	Bu	CH ₂ Cl ₂ /TFE	-	20,000	19,700	22,000	24,000	1.09	-	-	96
5	Pent	CH ₂ Cl ₂ /TFE	-	20,000	22,600	21,100	23,700	1.12	0.4513	60	97
6	Oct	CH ₂ Cl ₂ /TFE	-	20,000	18,500	-	-	-	-	-	98
7	Et- <i>stat</i> -Pent	CH ₂ Cl ₂ /TFE	50:50	20,000	20,400	18,900	20,200	1.07	-	-	99
8	Pro Pro- <i>block</i> -Et	CH ₂ Cl ₂ /TFE	50:50	10,000 20,000	11,800 18,500	13,500 21,500	13,800 24,400	1.02 1.13	-	-	86 97
9	Pr	CH ₂ Cl ₂ /TCE	-	20,000	21,400	19,000	21,000	1.10	-	-	97
10	Pr	CH ₂ Cl ₂ /HFIP	-	20,000	20,500	18,200	20,100	1.10	-	-	98

a. As determined by ASEC

b. As determined by ¹H NMR spectroscopy

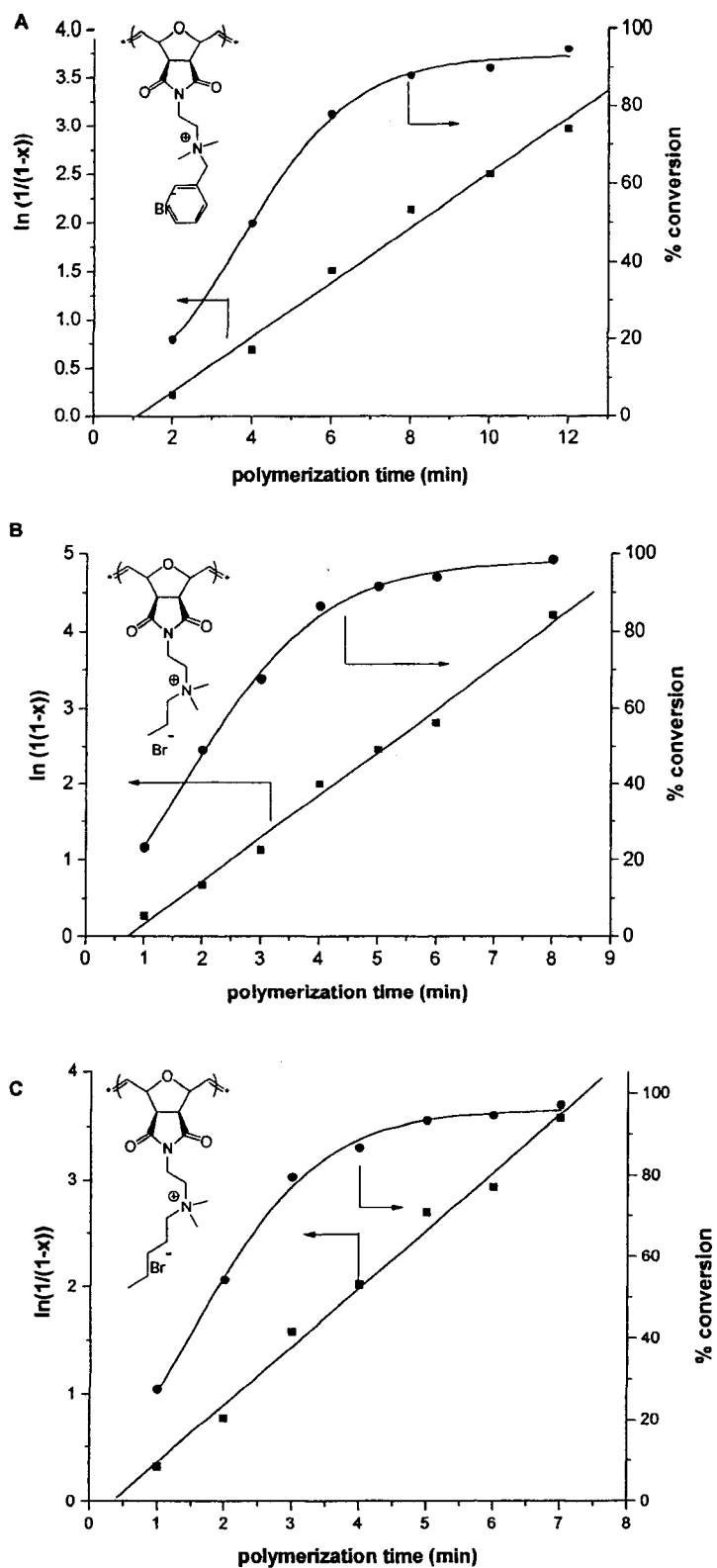


Figure III-3. First order kinetic profiles and conversion vs time plots for the homopolymerization of Bn-quat-Br (A), Prop-quat-Br (B), and Pen-quat-Br (C).

Both the Pr-quat-Br and Pen-quat-Br monomers likewise polymerize rapidly under these conditions. Indeed, both monomers polymerize at even faster rates than Bn-quat-Br. For example, the Pr-quat-Br species reaches essentially quantitative conversion in ca. 8 min under conditions identical to those employed for the Bn-quat-Br species. In all three instances there is an apparent short induction period of ca. 45-60 sec prior to the onset of polymerization. Since we added the catalyst solution, in CH_2Cl_2 , to the monomer solution, in TFE, we attribute this short induction time to a simple mixing phenomenon. Importantly, all three of the first-order plots exhibit linearity over the entire course of the polymerization. Assuming that $[\text{Ru}]$ is constant, which is a reasonable assumption given the good molecular mass control (see below), this indicates the polymerizations are first-order with respect to monomer, i.e. the rate of polymerization, $R_p = k_{\text{comp}}[\text{M}]$, where $k_{\text{comp}} = k_p[\text{Ru}]$ and k_p is the rate constant of propagation. Since the slope of the pseudo first-order kinetic plots is $= k_p[\text{Ru}]$, and $[\text{Ru}]$ is known, k_p is readily obtained (Table III-1). The experimentally determined k_p values for the Bn-, Prop-, and Pen-quat-Br monomers lie in the range 0.23-0.45 L/mol*s (Table III-1). These values are consistent with k_p values reported previously by Holland and co-workers¹⁹² in their kinetic studies of the homo- and copolymerization of the 7-oxanorbornene derivative *exo,exo*-5,6-bis(methoxycarbonyl)-7-oxabicyclo[2.2.1]hept-2-ene in which experimentally determined values for k_p ranged from 0.011-0.59 L/mol*s over the temperature range 273-318 K at a catalyst concentration of 0.0031M and a monomer concentration of 0.19M. We do, however, observe differences in the k_p values between the Pr-, Pen-, and Bn-quat-Br derivatives. While the Pr- and Pen-quat-Br monomers polymerize with a similar k_p there is a significant difference for the Bn-quat-Br monomer. Since all polymerizations

were conducted under identical conditions we attribute these differences to a steric effect, with the larger bulkier Bn-quat-Br monomer polymerizing at a slower rate. These kinetic results suggest that the polymerization of these monomers, in this novel cosolvent mixture, is controlled. In addition to the Bn-, Pr-, and Pen-quat-Br derivatives described above we also prepared homopolymers from the Et-, But-, and Oct-quat-Br monomers. Some specific features of these homopolymerizations will be highlighted below.

In addition to the NMR kinetic analysis, the aliquots withdrawn from the homopolymerizations were analyzed via ASEC to determine the number (M_n), and weight (M_w) average molecular masses, as well as the polydispersity indices (M_w/M_n) for the cationic homopolymers. Figure III-4 shows examples of representative unimodal, symmetric ASEC traces for homopolymers derived from the Et- and Pen-quat-Br monomers.

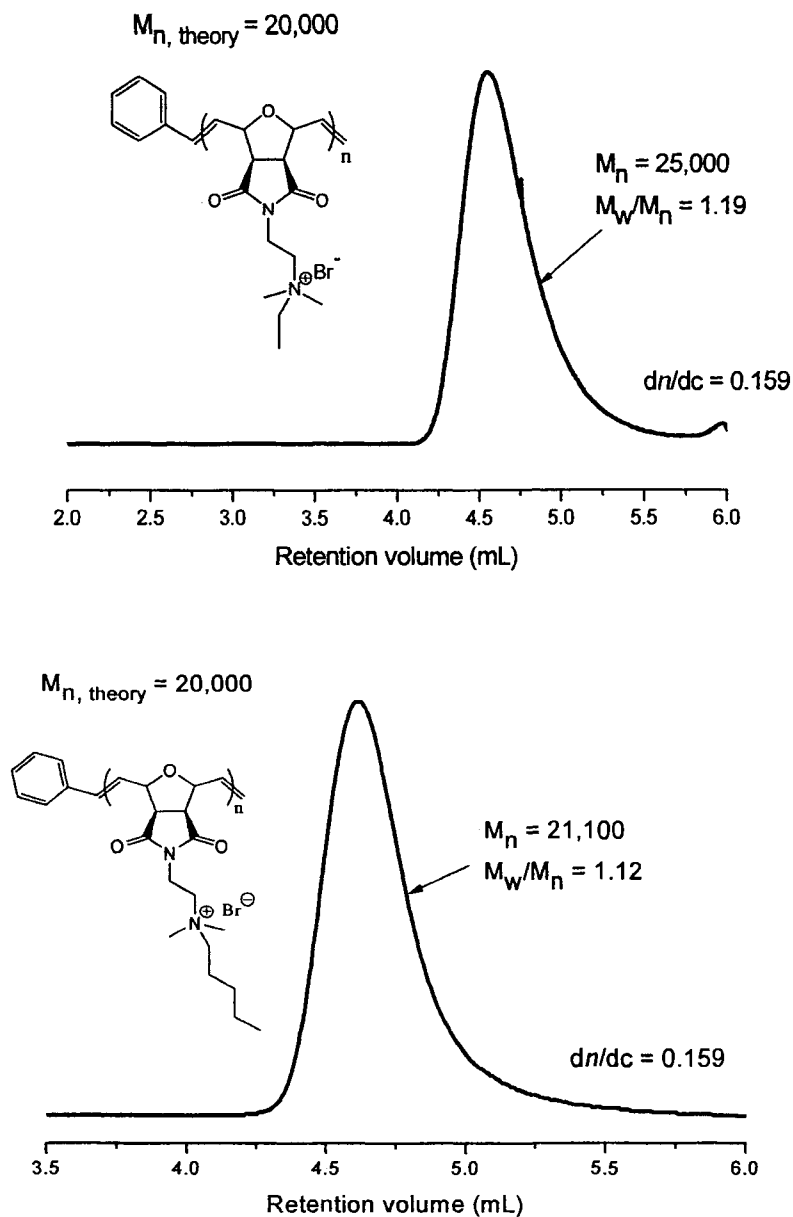


Figure III-4. ASEC traces (RI signal) for Et-quat-Br (A) and Pen-quat-Br (B) homopolymers with a target M_n of 20,000.

Given the application of a light scattering detector in the ASEC analysis we first needed to determine the dn/dc of our polymers in the given ASEC eluent. We elected to determine the dn/dc for the Pen-quat-Br homopolymer, as a representative member of

these cationic materials. Experimentally, we found the dn/dc to be 0.159. We subsequently used this value for the determination of the M_n , M_w and M_w/M_n of all the cationic species, having assumed that the dn/dc will not vary significantly for the different alkyl-quaternized (co)polymers. The M_n (theory, as well as the values determined by NMR and by ASEC) M_w , and M_w/M_n values for the different alkyl quaternized homopolymers are summarized in Table III-1. Several features are worth noting. Firstly, when considering M_n we note that the experimentally determined values match almost identically with the theoretical values. For example, the M_n as determined by ASEC for the poly(Pen-quat-Br) homopolymer, entry 5 Table III-1, was 21,100, whereas the $M_{n,theory}$ was 20,000. Similar agreement between the theoretical and experimentally determined M_n values was observed for all homopolymers. Such close agreement between the $M_{n,theory}$ and experimentally determined values is consistent with the anticipated controlled nature of these homopolymerizations and also indicates quantitative initiation by the Ru complex. Also, we see that the molecular mass can be readily tuned by varying the $[M]/[Ru]$. For example, entry 3 Table III-1, summarizes the results for three different poly(Prop-quat-Br) homopolymers at three different target molecular masses. In all instances the agreement between the theoretically target values and those determined experimentally is good.

With regard to the polydispersity indices, we see that for the homopolymers (entries 1-6, Table 1) that the M_w/M_n values lie in the range 1.09-1.19. Such low PDIs are, of course, consistent with the controlled/“living” nature of these polymerizations. Such narrow molecular mass distributions are often a consequence of the balance between the rate of initiation, R_i , and the rate of propagation, R_p . While not a strict

requirement, many controlled/“living” polymerizations are characterized by R_i 's being greater than, or equal to, R_p . As such, initiation is complete before any significant degree of propagation occurs, and therefore all chains grow simultaneously, at the same rate and to approximately the same length. There are, however, various factors that can affect R_i and R_p in LROMP systems. These include the ligand environment around the Ru metal center and also the nature of the polymerization solvent. For example, Sanford et al. reported that the dielectric constant, ϵ , of the solvent can have a significant effect on R_i , with R_i being roughly proportional to ϵ .¹⁴⁷ They reported that R_i increases in the order: pentane ($\epsilon = 1.84$) < toluene ($\epsilon = 2.38$) < diethyl ether ($\epsilon = 4.34$) < CH_2Cl_2 ($\epsilon = 8.9$) < THF ($\epsilon = 7.32$) for **17** upon examination of the initiation kinetics by UV-Vis spectroscopy. Clearly solvents with higher ϵ favor faster initiation. TFE is a highly polar solvent with a dielectric constant significantly higher than any of those listed above ($\epsilon = 27.7$). As such, and considering the nature of the TFE/ CH_2Cl_2 solvent mixture alone, we might anticipate fast R_i for these polymerizations. Indeed, this is not an undesirable feature since, as noted above, fast R_i , relative to R_p , favors the formation of (co)polymers with narrow molecular mass distributions.¹⁹¹ We were unable to determine the M_n ASEC, M_w ASEC, or M_w/M_n values for the Oct-quat-Br homopolymer since the material was highly surface active, an indication of its amphiphilic character, and was sparingly soluble in the ASEC eluent.

NMR spectroscopy is a convenient, and complimentary, method for determining the *absolute* molecular mass of polymers via end group analysis provided the samples are of a sufficiently low molecular mass to facilitate such analysis. In the case of polymerizations mediated by **17** described herein every single polymer chain should

contain a phenyl end-group, incorporated into the chain from the consumption of the first monomer. With the exception of the Bn-quat-Br monomers this end-group serves as a convenient “NMR tag” for the determination of the absolute molecular mass of the (co)polymers. For example, Figure III-5 shows the ^1H NMR spectrum of a poly(Pen-quat-Br) homopolymer with a target molecular mass of 4,000 recorded in DMSO. At this low molecular mass the resonances associated with the phenyl end-group are clearly visible at ca. δ 7.4 ppm. A ratio of this signal with the signal at ca. δ 0.7 ppm (the $-\text{CH}_3$ group of the pentyl side chain) indicates an average degree of polymerization of ca. 11 and thus an experimentally determined average molecular mass of 4,150. This is in excellent agreement with the target molar mass of 4,000 based on the $[\text{M}]:[\text{Ru}]$.

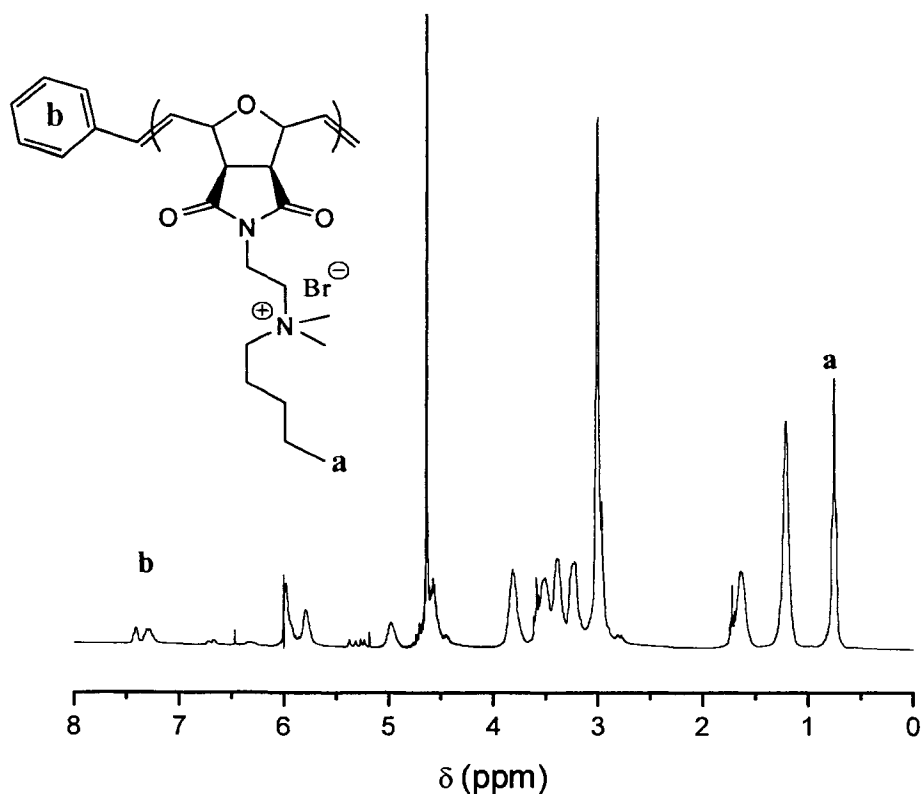


Figure III-5. ^1H NMR spectrum of a Pen-quat-Br homopolymer ($M_{n,\text{theory}} = 4,000$) recorded in d_6 -DMSO.

Again, such close agreement between the theoretical and observed molecular masses indicates quantitative initiation by the Ru initiator, and also suggests that the cosolvent mixture, and in particular the TFE, does not have any detrimental effect on the initiator, at least on the time scale of the polymerization (*vide infra*). The ability to determine the absolute molecular mass by NMR spectroscopy also allows for a simple verification of the molecular masses as determined by ASEC, Table III-1. As a general rule, the agreement between M_n NMR and M_n ASEC (or M_w ASEC) is gratifying and validates the results obtained by ASEC – a technique which can be extremely problematic. Finally, the use of end-group analysis also facilitates the determination of the molecular mass of the poly(Oct-quat-Br) homopolymer which we were unable to characterize by ASEC due to its amphiphilic character. In this instance, the molecular mass for the Oct-quat-Br homopolymer was determined to be 18,500 which is in excellent agreement with the theoretical value of 19,600 for the determined degree of conversion.

Evolution of M_n as a function of conversion

While linear pseudo-order kinetics are an indicator of the controlled nature of these polymerizations, an observation also supported by the excellent molecular mass control and low polydispersity indices, an evaluation of the evolution of M_n with conversion is, arguably, a more crucial verification of their controlled nature. For a controlled, chain-growth process such a plot should be linear and pass through the origin. Again, with the molecular masses readily determined via both ^1H NMR spectroscopy and ASEC, the M_n vs conversion plots are easily generated. As a representative example, Figure III-6 shows

the plot of MM vs conversion, as determined by NMR spectroscopy, along with the theoretically expected values for a Prop-quat-Br homopolymer. The linearity, coupled with the near perfect agreement with the theoretically expected values again is a crucial indicator that the polymerizations of these new cationic monomers in this novel cosolvent mixture proceed in a controlled manner.

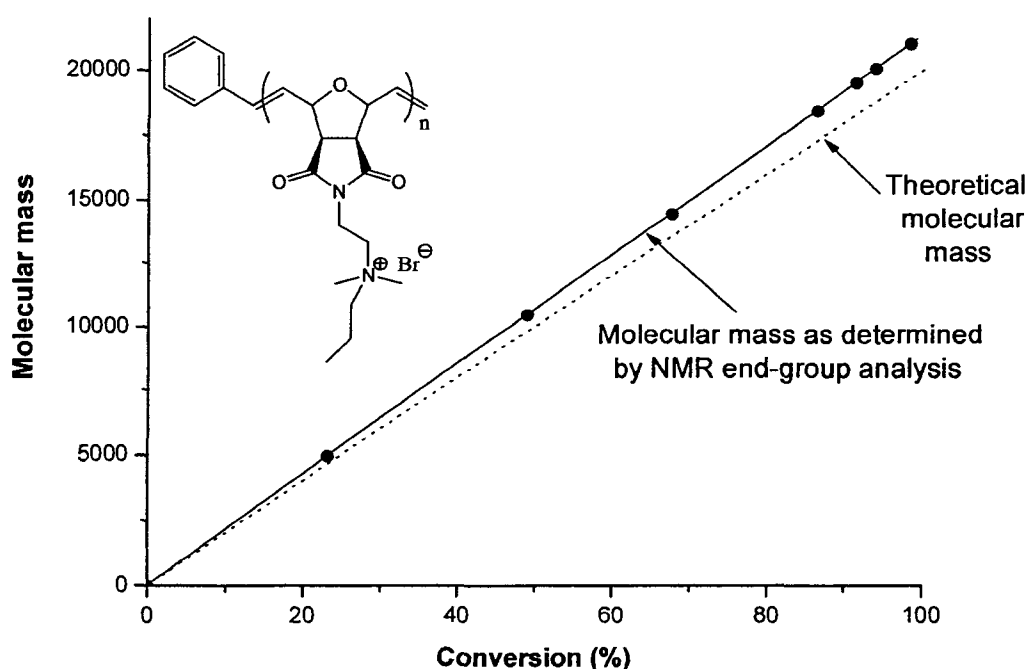


Figure III-6. M_n vs conversion plot for a Prop-quat-Br homopolymer.

Statistical and Block Copolymerizations

Having demonstrated that these new hydrophilic quaternary ammonium monomers polymerize in a controlled fashion under these new solvent conditions, and with the kinetic profiles in hand we proceeded to probe the feasibility of preparing materials with more complex architectures. In particular we have conducted two preliminary

experiments – one to demonstrate the ability to prepare a statistical copolymer and one to verify the ability to synthesize block copolymers. In both instances the copolymers were prepared from monomers derived from this new family of cationic substrates. We first evaluated the statistical copolymerization of Et-quat-Br with Pent-quat-Br, see Table III-1 entry 7, and Figure III-7. It is evident from Figure III-7 that the copolymerization proceeds smoothly given the agreement between the experimentally determined molecular weight (by NMR and ASEC) with the theoretical value of 20,000 as well as the formation of a copolymer with a narrow, unimodal, symmetrical molecular mass distribution with a polydispersity index of 1.07.

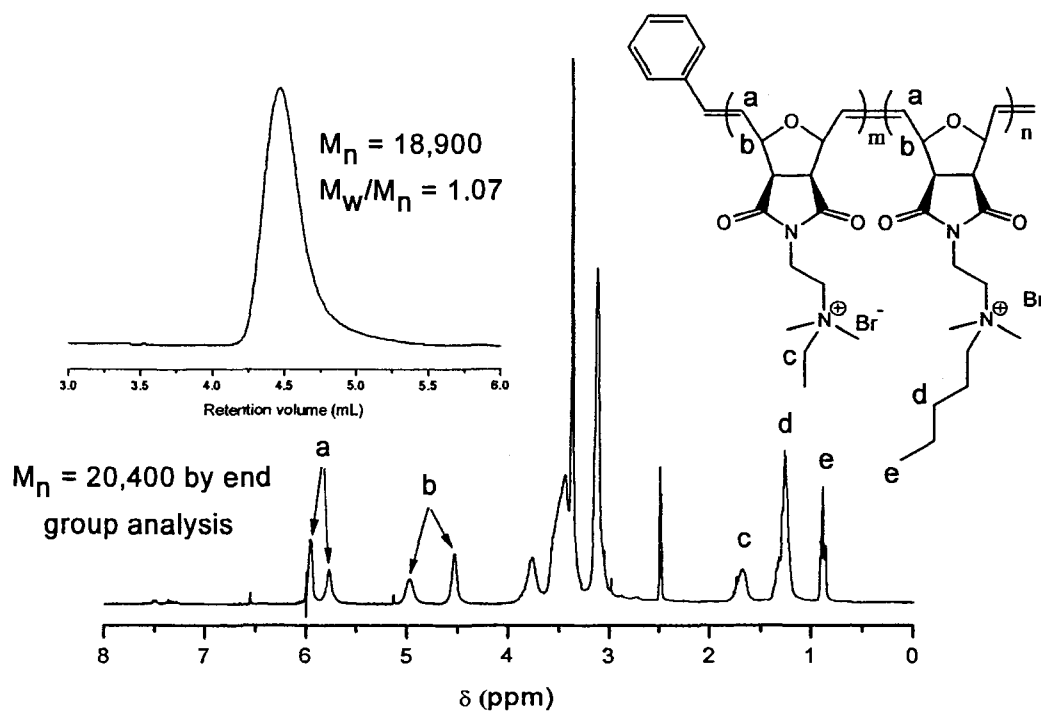


Figure III-7. ^1H NMR spectrum of a poly(Et-quat-Br-stat-Pent-quat-Br) copolymer with the ASEC trace (RI signal) shown as the inset.

Following the statistical copolymerization we next evaluated the ability to prepare block copolymers. Preparing block copolymers via sequential monomer addition is another crucial feature of controlled/“living” polymerizations. Successful block copolymerization indicates both retention of chain end functionality as well as activity, and also suggests the absence, or at least detectable occurrence, of undesirable side reactions such as chain transfer or termination. We first homopolymerized Prop-quat-Br to ca. 86 % conversion, under standard conditions described above, and withdrew an aliquot for ASEC analysis prior to adding Et-quat-Br, as a solid to the polymerization mixture. Et-quat-Br was intentionally added prior to near quantitative conversion of Pr-quat-Br in an effort to minimize undesirable side-reactions which can become prevalent under monomer starved conditions. ASEC analysis of the Pro-quat-Br homopolymer aliquot (target $M_n = 10,000$) yielded an M_n ASEC of 13,500 with a corresponding M_w/M_n of 1.02. After the addition of Et-quat-Br (target $M_{n,\text{total}} = 20,000$), polymerization and subsequent quenching, ASEC analysis indicated the formation of a block copolymer with a measured M_n ASEC = 21,500 and a corresponding M_w/M_n of 1.12. While the ability to prepare block copolymers is clearly demonstrated an inspection of the individual chromatograms for the homo- and block copolymer, Figure III-8, indicates that there is some tailing to low molecular mass for the block copolymer. While such non-symmetry in chromatograms is not an uncommon feature in ASEC (given the problems often associated with ASEC as an analytical technique), the near-symmetric traces that have been observed for the homopolymers suggests that the tailing this is not due to a chromatographic/separation issue. The occurrence of tailing in chromatograms can be due to several problems including adsorption of the (co)polymer to the column packing

material, or for block copolymers, can indicate the presence of homopolymer impurity. The presence of such an impurity is usually due to dead, non-active, chains which are formed via undesirable side reactions of the functional/active chain ends. Note: The impurity might be cyclic species of homopolymer from inter/intramolecular chain transfer.

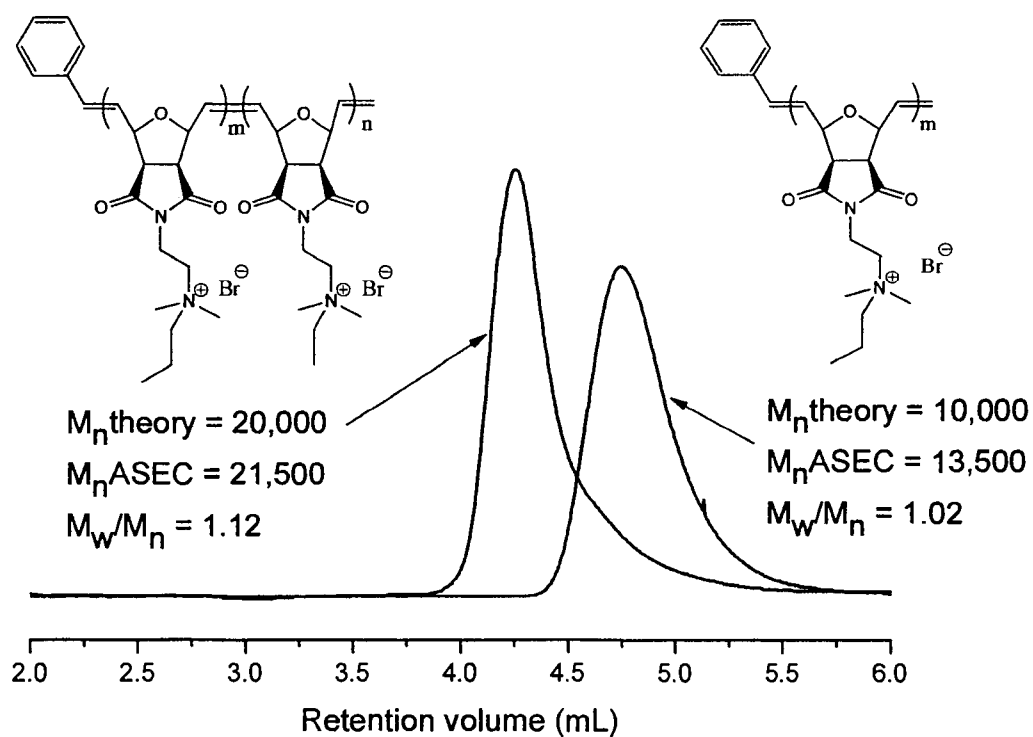


Figure III-8. ASEC traces (RI signals) demonstrating the formation of a poly(Prop-quat-Br-block-Et-quat-Br) copolymer.

The effect of halogenated cosolvent

In light of the effectiveness of the TFE/ CH_2Cl_2 cosolvent mixture as a medium for the preparation of these permanently cationic (co)polymers under facile LROMP conditions

we briefly examined two additional halogenated alcohols as co-solvents with CH_2Cl_2 to determine if there was anything particularly unique about TFE. While TFE is clearly a highly effective and convenient cosolvent, which greatly simplifies the preparation of the target cationic functional materials, it is expensive and toxic. As such, in addition to TFE we also examined TCE and HFIP as potential co-solvents, with CH_2Cl_2 , for the homopolymerization of Pr-quat-Br. While we have not, at this point, conducted a detailed kinetic evaluation of the polymerization characteristics in these additional cosolvent mixtures, Figure III-9 shows the ASEC traces for the two homopolymers obtained after polymerization in the TCE/ CH_2Cl_2 and HFIP/ CH_2Cl_2 solvent mixtures. Both polymerizations were conducted under identical conditions to those in TFE/ CH_2Cl_2 with $M_{n,\text{theory}} = 20,000$. In both instances the solutions remained homogeneous throughout the course of the polymerization and yielded homopolymers with both controllable molecular mass and narrow molecular mass distributions. While these results do not point to a preferred choice of halogenated alcoholic cosolvent for such LROMP reactions it does suggest that a possible broad range of co-solvents could be employed based on particular solubility desires/issues. Also, it seems clear that both TCE and HFIP could also be employed in a broader sense for other, small molecule, metathesis reactions.

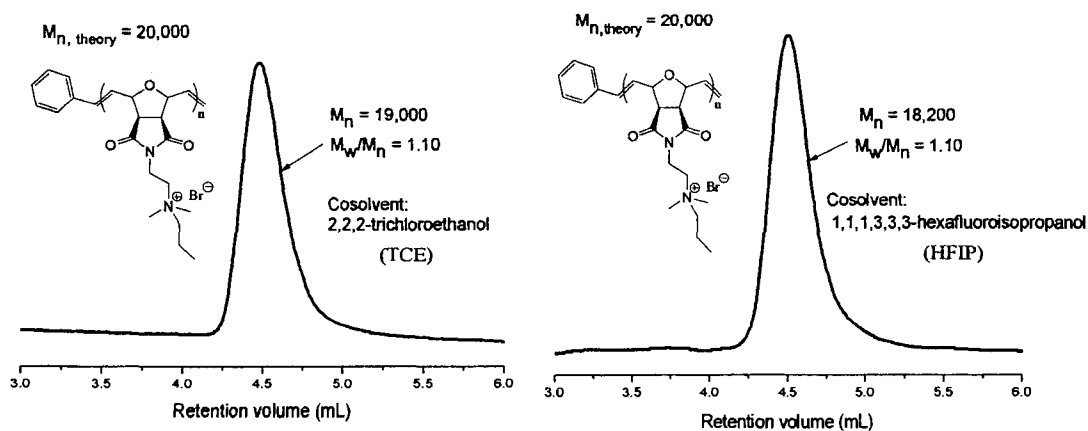


Figure III-9. ASEC traces (RI signal) for Prop-quat-Br homopolymers prepared using TCE (A) and HFIP (B) as halogenated alcoholic cosolvents.

Stability of Grubbs' catalyst in the TFE/ CH_2Cl_2 solvent mixture

The excellent control observed for the homo and copolymerization of these new cationic monomers with respect to their kinetic profiles and the control over the molecular weight, and low polydispersities, as determined by ASEC and NMR spectroscopy indicates that the novel TFE/ CH_2Cl_2 solvent mixture (or the TCE and HFIP cosolvents) does not have any significant detrimental effect on the Ru initiator/catalyst, at least on the time scale of the polymerizations. The presence of TFE as a cosolvent in these systems was a potential concern since Grubbs' catalyst, while exhibiting a high functional group tolerance, is known to be reactive towards alcohols. For example, it has been reported that **17** degrades slowly in methanol.¹⁹² To confirm the stability of **17** under these conditions we conducted a control ^{31}P NMR spectroscopic experiment in which spectra were recorded at 10, 20, and 30 min (well beyond the timescale of the homopolymerization experiments) for a solution of **17** in 1:1 TFE/ CD_2Cl_2 . Figure III-10 shows a waterfall plot of the ^{31}P NMR spectra of **17**. It is evident that the ^{31}P NMR

spectra do not change noticeably over a period of 30 min, the main peak at ca. $\delta \sim 37$ ppm due to 17. We do observe a small, second resonance at ca. $\delta \sim 35$ ppm although its concentration appears to be very low and does not increase over the course of the experiment. While this may be a degradation product, its low concentration coupled with the control described above for the (co)polymerizations indicates that there is no inherent barrier to the use of TFE as a (co)solvent in LROMP reactions.

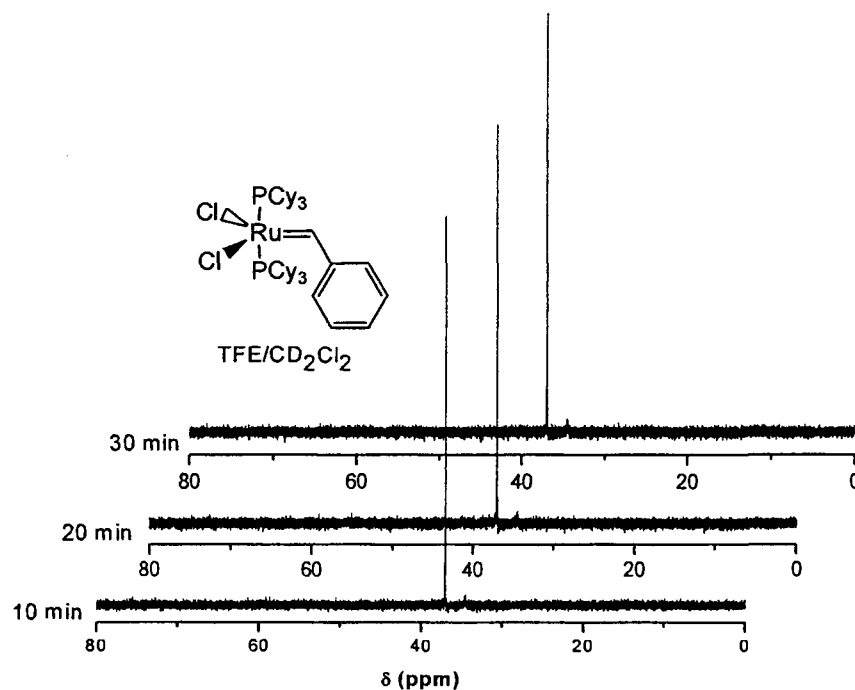
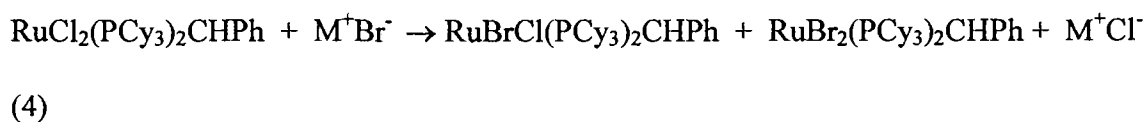


Figure III-10. ^{31}P NMR spectra of 17 recorded in a 1:1 TFE/ CD_2Cl_2 solvent mixture.

Homopolymerization of Bn-quat-Br vs Bn-quat-Cl

The homo- and copolymerization experiments described above employed quaternary ammonium monomer derivatives with a *bromide* counterion. This was not, at the time,

intentionally planned but was merely a result of the quaternizing reagents we had in the early stages of this investigation. Given the large excess of monomer relative to initiator we could not discount the possibility of halide exchange at the Ru metal center resulting in the *in situ* formation of a new Ru-complex(es) according to (4) where M^+ is the cationic monomer.



In principle, the formation of two new Ru complexes could occur – the mixed halide complex with Br and Cl ligands and/or the corresponding dibromo Grubbs' derivative.⁹⁸ Indeed, such halide exchange has been previously reported to be very facile between 17 and the surfactant DTAB (dodecyltrimethylammonium bromide) in emulsion polymerization studies of norbornene, even in CH_2Cl_2 .¹⁶⁴ Such exchange reactions are a very important consideration since it is known that even small changes in the ligand environment at the Ru metal center in 17 can result in complexes/initiators with, in some instances, drastically different metathesis characteristics/activities.¹⁴⁷ Grubbs and co-workers have demonstrated that the nature of the coordinating halide ligands can have a very significant effect on R_i . Complete exchange of the chloride ligands for the less electronegative bromide in 17, for example, results in a 3 fold increase in R_i . While such an effect may be considered minor it is significantly more pronounced when chloride is substituted for iodide which results in an approximately 250 fold increase in R_i ! While halide exchange results in faster R_i it actually leads to a lower R_p , indeed, R_p was reported

to be inversely proportional to R_p . As such, exchanging chloride for bromide is beneficial in the sense that (co)polymers with narrower molecular mass distributions should be accessible, but this additional control is at the expense of slower overall R_p , which while not necessarily pronounced for the dibromide complex, can be especially pronounced for the diiodide complex, $\text{RuI}_2(\text{PCy}_3)_2\text{CHPh}$.¹⁴⁷

Given the possibility of a counterion effect resulting in the in situ formation of different catalytic species for the (co)polymerization of these new quaternary ammonium monomers we first prepared the Bn-quat monomer with the chloride counterion (Bn-quat-Cl) simply by substituting benzyl bromide with benzyl chloride in the Menschutkin reaction during the monomer synthesis, and subsequently examined the homopolymerization kinetics in TFE/ CH_2Cl_2 with **17**, Figure III-11. We did observe very different behavior for this monomer compared to Bn-quat-Br. For the Bn-quat-Br monomer, as highlighted above, we observed a linear pseudo-first order rate plot in which the conversion increased in a linear fashion with time reaching ca. 95% after 12 min. Indeed all the experimental data indicate a well-controlled polymerization for the quaternary ammonium monomers with the Br counterion. In contrast, the Bn-quat-Cl species exhibited a non-linear kinetic profile and reached very high conversion (ca. 90%) within two min indicating a much higher R_p . Since all experimental conditions were identical this observed difference must be due to the nature of the halide counterion. Assuming some halide exchange is occurring in the case of the Br-counterion containing monomers the faster rate observed with the Bn-quat-Cl is consistent with the reported effect of halide ligand around the metal center, with Br-ligand species exhibiting slower R_p . This effect is discussed in more detail in the next chapter.

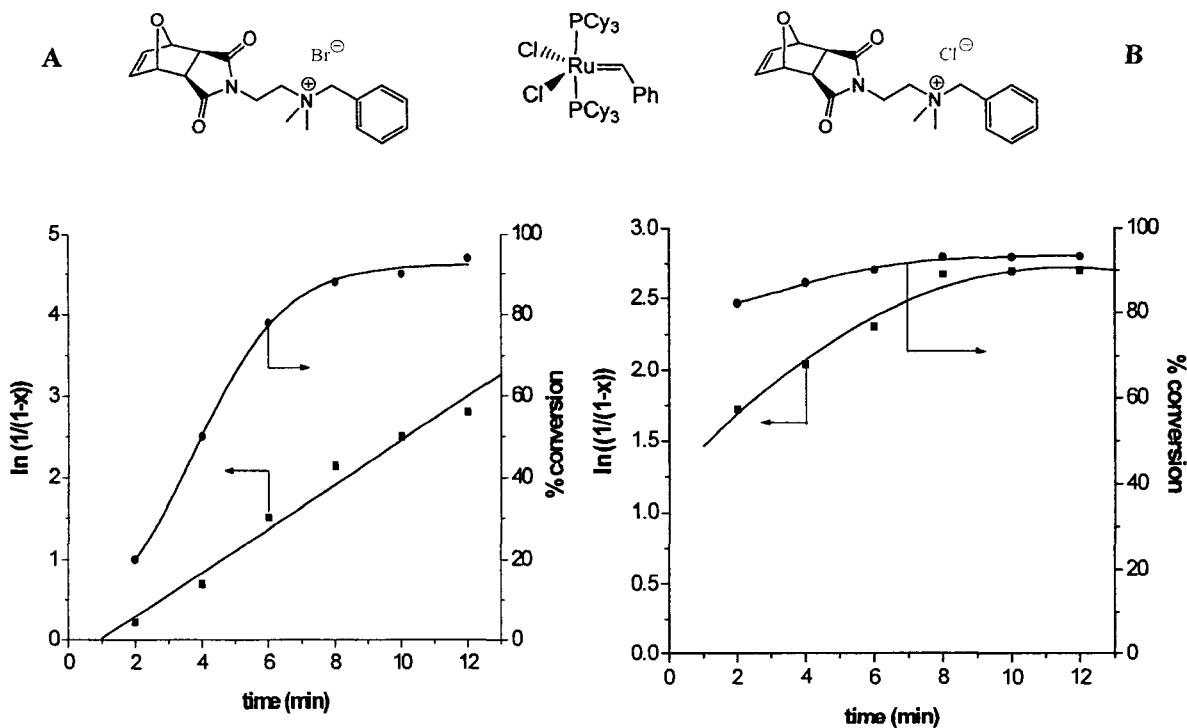


Figure III-11. First order kinetic profiles for the homopolymerization of Bn-quat-Br (A) and Bn-quat-Cl (B) using **17** in TFE/CH₂Cl₂ 1:1.

Summary

In this chapter we have described the synthesis of a series of new permanently cationic *exo*-7-oxanorbornenes and evaluated their (co)polymerization via ring-opening metathesis polymerization in a novel solvent mixture comprised of 1:1 v/v TFE/CH₂Cl₂ using Grubbs' first generation catalyst **17**. We have demonstrated that such a solvent mixture facilitates the homogeneous solution polymerization of these monomers without the need for catalyst synthesis, post polymerization modification, or protection/deprotection protocols and as such is a considerably simpler approach than previously reported methods. We have shown that these polymerizations proceed with all the characteristics of a living system and allows for the control of the molecular

masses, molecular mass distribution and also facilitates the synthesis of (co)polymers with more advanced architectures. Such an approach is not limited to the use of TFE and also works for other halogenated cosolvents such as TCE, and HFIP. Finally we demonstrated, via ^{31}P NMR spectroscopy, that TFE has little/no effect on 17.

CHAPTER IV

OBSERVATIONS ON THE EFFECT OF HALIDE COUNTERION IN THE ROMP OF THE *exo*-7-OXANORBORNENE DERIVATIVES *exo*-BENZYL-[2-(3,5-DIOXO-10-OXA-4-AZA-TRICYCLO[5.2.1.0^{2,6}]DEC-8-EN-4-YL)-ETHYL]DIMETHYL AMMONIUM BROMIDE/CHLORIDE IN 2,2,2-TRIFLUOROETHANOL/METHYLENE CHLORIDE**Introduction**

In Chapter III we described the synthesis and controlled polymerization of a range of new permanently cationic *exo*-7-oxanorbornene substrates using **17** in a TFE/CH₂Cl₂ solvent mixture – other halogenated alcohols such as TCE and HFIP were also shown to be effective as cosolvents with CH₂Cl₂.¹⁹⁴ This study was motivated by the desire to significantly simplify the direct preparation of such permanently cationic polymers via ROMP, i.e. was developed to negate the need for the synthesis of water-soluble catalysts for polymerizations conducted under homogeneous aqueous conditions and/or circumventing the need for post-polymerization modification. The use of the TFE/CH₂Cl₂ solvent mixture readily facilitated the controlled homogeneous polymerization of the *exo*-7-oxanorbornene cationic substrates **M31** in a controlled manner. Cationic monomers were prepared with both bromide and chloride counterions and their polymerizations evaluated with respect to their kinetic profiles, molecular weight control, MWDs, and the ability to prepare materials with advanced architectures, namely statistical and block copolymers. Interestingly, during these studies we observed very different kinetic characteristics for monomeric substrates that differed only in the nature of the halide counterion. Such differences were attributed to the in situ formation of the mixed Grubbs' catalyst RuClBr(PCy₃)₂CHPh and/or the dibromo analog RuBr₂(PCy₃)₂CHPh in the case of polymerizations conducted with monomers bearing a

bromide counterion. In light of these differences we decided to examine this apparent monomer counterion effect in more detail. In this chapter we describe our observations regarding the kinetic and MWD effects of monomer halide counterion on the polymerization characteristics of a permanently cationic *exo*-7-oxanorbornene derivative. We believe this is the first report in which the nature and effect of a monomer counterion has been directly evaluated in a ROMP polymerization.

Experimental

All chemicals were purchased from the Aldrich Chemical Company at the highest available purity and used as received unless stated otherwise. *exo*-Benzyl-[2-(3,5-dioxo-10-oxa-4-aza-tricyclo[5.2.1.0^{2,6}]dec-8-en-4-yl)-ethyl]dimethyl ammonium bromide (MON-Bn-Br), was prepared according to the procedure described in Chapter III. The analogous monomer with the chloride counterion was prepared via the direct alkylation of *exo*-4-(2-dimethylaminoethyl)-10-oxa-4-aza-tricyclo[5.2.1.0^{2,6}]dec-8-ene-3,5-dione with benzyl chloride according to the same general procedure. Polymerizations were conducted under an inert atmosphere with degassed solvents in a PlasLabs nitrogen-filled glovebox according the procedure recently disclosed.¹⁹³ Polymerization conversions were determined by ¹H NMR spectroscopy via a direct ratio of the vinylic resonances associated with the monomer vs. those of the polymer.

Characterization techniques

¹H (300 MHz) NMR spectra were recorded on a Bruker 300 53 mm spectrometer in appropriate deuterated solvents or solvent mixtures. Polymer molecular weights,

molecular weight distributions, and polydispersity indices were determined by ASEC in 0.1 M Na₂SO₄/1 vol % acetic acid at a flow rate of 0.20 ml/min at ambient temperature. The system was comprised of a Viscotek VE1122 pump, Viscotek VE3580 RI detector, a CATSEC 1000 7 μ (50 x 4.6 mm) guard column followed by a series of two CATSEC columns (CATSEC 1000 7 μ 250 x 4.6 mm + 100 5 μ 250 x 4.6 mm) with a theoretical linear molecular mass range of 200 – 2,000,000 g/mol. The system was calibrated with a series of narrow molecular mass distribution poly(ethylene oxide) standards (620-460,000 g/mol). Data were analyzed with the OmniseC Interactive SEC software package.

Results and Discussion

The synthesis of cationic polymers by ROMP has been achieved both directly^{138,163,164} and indirectly.¹⁸² In the former case, syntheses have, for example, been accomplished in aqueous media under homogeneous conditions; however, this approach required the synthesis of suitably active water-soluble, first generation Grubbs' initiators. The indirect approach, which allows for the use of commercially available initiators and for polymerizations to be conducted in organic media, requires either the application of protecting group chemistry or some specific post-polymerization modification to generate the target cationic materials.¹⁸² We recently described an approach that combines the benefits of both of these processes and was discussed in Chapter III. We demonstrated the ability to directly polymerize permanently cationic *exo*-7-oxanorbornene derivatives in *organic* media with the Grubbs' first generation complex **17**. Key to success was the identification of a suitable solvent mixture capable of solubilizing, and maintaining the solubility, of all components. A 50/50 v/v mixture of TFE/CH₂Cl₂, or other halogenated

alcoholic cosolvent, was found to fit the criteria and facilitated the rapid, controlled homo- and copolymerization of the *exo*-cationic substrates at ambient temperature. During these studies we observed a pronounced effect in a direct comparison of the kinetic features for the homopolymerization of **MON**, Figure III-1, depending on whether the counterion, X^- , was chloride or bromide.

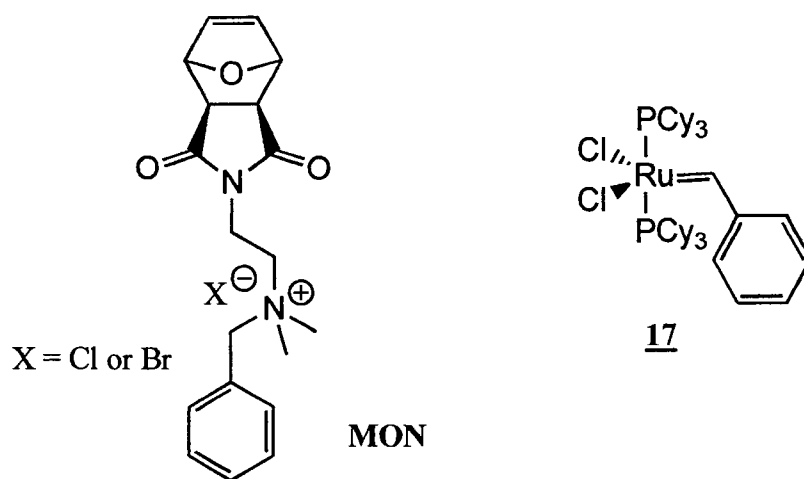


Figure IV-1. Chemical structures of monomer substrates, **MON**, and Grubbs' first generation catalyst, **17**.

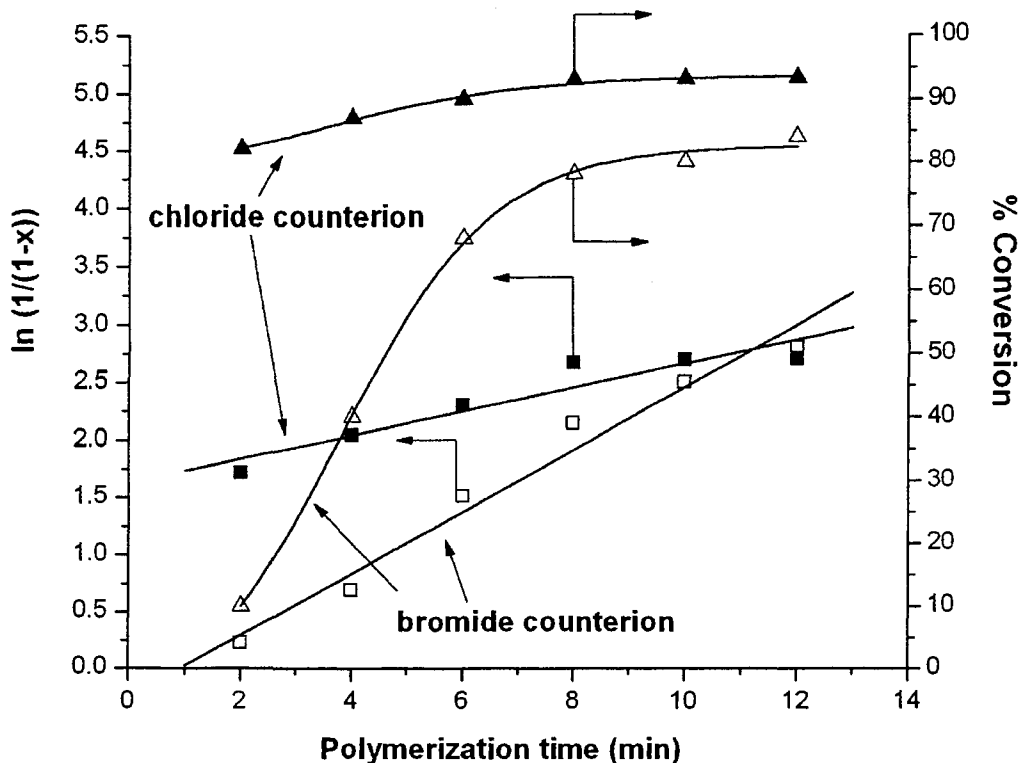


Figure IV-2. Conversion vs. time and pseudo first order kinetic plots for the homopolymerization of **MON** with $X = \text{Cl}$ (filled symbols) or Br (open symbols) with **17** in $\text{TFE}/\text{CH}_2\text{Cl}_2$ at RT.

Such differences are evident in Figure IV-2 that shows the kinetic and conversion profiles for the homopolymerization of **MON** with both halide counterions and **17** in 50/50 v/v $\text{TFE}/\text{CH}_2\text{Cl}_2$. The most noticeable difference between the two monomers can be seen in the conversion profiles. In the case of the **MON-Bn-Cl** substrate, conversion very rapidly reaches ca. 85% in approximately 2 min after which it changes little, steadily increasing to ca. 95% after 12 min. In contrast, the conversion profile for **MON-Bn-Br** is very different. Conversions of ca. 10% are observed after 2 min, which increases steadily reaching ca. 80% after 8 min. Beyond this, the conversion increases more slowly to a

value of ca. 85% after 12 min - **MON-Bn-Br** clearly polymerizes at a slower rate than the analogous chloride monomer. The pseudo first-order kinetic profiles are also different. In the case of the **MON-Bn-Br** monomer we observe linear kinetics, indicating that the polymerization is first order in monomer, with the plot passing close to the origin. The non-zero intercept is attributed to a mixing phenomenon as described previously.¹⁹⁵ In the case of the chloride monomer, the plot is also linear but would appear to have a non-zero intercept. However, it should be noted that the first point in the plot corresponds to ca. 85% conversion and as such the bulk of the polymerization is complete. Consequences of these differences in polymerization kinetics also manifest themselves in the resulting MWDs and the level of achievable control over the MWD. For example, Figure IV-3 shows the ASEC traces (RI signal) for homopolymers of **MON-Bn-Cl** and **MON-Bn-Br** prepared under identical conditions. While the experimentally determined M_n values do not agree well with the theoretical values (due to system calibration with linear, nonionic poly(ethylene oxide) standards which are clearly poor equivalents for the cationic, unsaturated polymers), a clear difference in the measured polydispersity indices is evident. In the case of the homopolymer derived from **MON-Bn-Cl** the experimentally determined M_w/M_n value is 1.34, which is significantly larger than that for the **MON-Bn-Br** homopolymer, which was found to be 1.20.

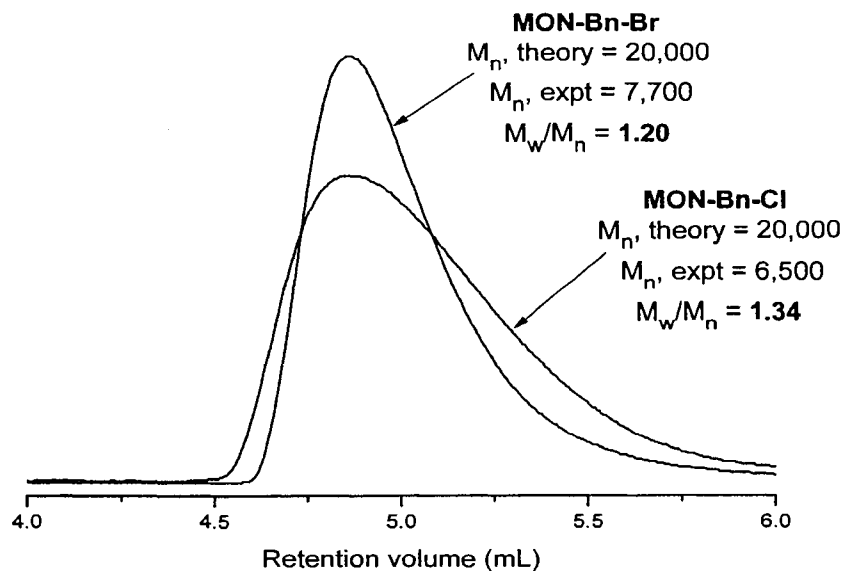


Figure IV-3. The ASEC traces (RI signal) for homopolymers derived from **MON-Bn-Cl** and **MON-Bn-Br** polymerized with **17** under identical conditions.

Such differences in the polymerization behavior of these two, essentially structurally identical monomers, are rationalized in terms of the in situ generation of either the dibromo Grubbs' initiator, $\text{RuBr}_2(\text{PCy}_3)_2\text{CHPh}$, and/or the mixed halide species $\text{RuClBr}(\text{PCy}_3)_2\text{CHPh}$ in the case of monomer(s) with a bromide counterion. As reported previously by Sanford et al.¹⁴⁷ the nature of the halide ligands around the Ru metal center has an effect on both k_i and k_p . Specifically, exchanging the chloride ligands for the less electronegative bromide results in the formation of species in which k_i is enhanced but at the expense of slower propagation. The effect, however, is not drastic in the case of the bromide ligands but is significantly more pronounced in the case of the diiodo derivative. Such an effect can clearly be invoked in a rationalization of the above kinetic and ASEC data. A monomer with a bromide counterion would polymerize more slowly overall, due

to the in situ formation of the mixed/dibromo catalyst analog, but should have a narrower MMD by virtue of the established effect on k_i and k_p .

Given that the monomers with bromide counterions exhibit all the features one associates with a controlled polymerization¹⁹³ we decided to examine the effect of halide counterion in more detail in an effort to determine if there existed a critical molar concentration of **MON-Bn-Br** that would induce a (co)polymerization with apparently enhanced “living” characteristics. Following these homopolymerizations we conducted a series of statistical copolymerizations of the two **MON** derivatives. **MON-Bn-Br** was copolymerized with **MON-Bn-Cl** at various molar ratios ranging from 25 to 75 mol % **MON-Bn-Br**, and the kinetic, conversion, and MWDs evaluated. Figure IV-4 shows the first order kinetic plots and conversion vs. time profiles for the copolymerization of **MON-Bn-Cl** with **MON-Bn-Br** at molar ratios of 75:25 (A), 50:50 (B), and 25:75 (C). In the case of the copolymerization rich in **MON-Bn-Cl** (Figure IV-4A) the conversion profile is little different from that of the homopolymerization of **MON-Bn-Cl**. For example, we observe ca. 80% conversion within two minutes rising gradually to near quantitative conversion after ca. 10 min. In contrast, the 50:50 and 25:75 copolymerizations exhibit conversion profiles more consistent with the **MON-Bn-Br** homopolymerization. For example, in the case of the 50:50 copolymerization approximately 35% is reached after two minutes, after which it increases steadily to essentially quantitative conversion after 12 min.

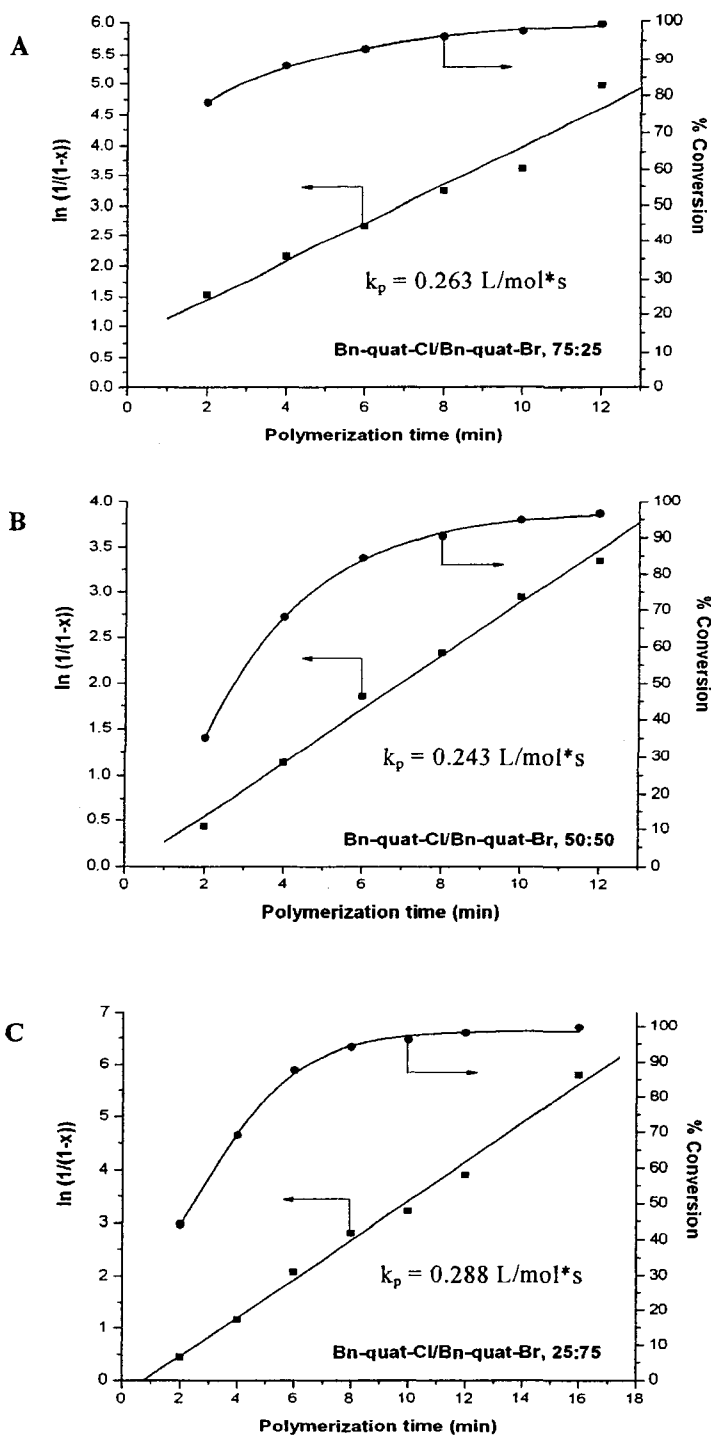


Figure IV-4. Pseudo-first order rate plots and conversion vs. time plots for the statistical copolymerization of MON-Bn-Cl with MON-Bn-Br using **17** at varying molar ratios.

In all instances the first-order kinetic plots are linear which indicates a first order dependence in monomer. In the case of the 75:25 copolymerization extrapolation would indicate a non-zero intercept, which again is consistent with the profile observed for the **MON-Bn-Cl** homopolymerization. Both the 50:50 and 25:75 copolymerization exhibit kinetic profiles more similar in nature to the **MON-Bn-Br** homopolymerizations, i.e. they have zero or near-zero intercepts. Given the first order dependence in monomer, it follows that the rate of polymerization, $R_p = k_p[\text{Ru}][\text{MON}]$, where k_p is the rate constant of propagation. The slope of the pseudo first order plot is $= k_p[\text{Ru}]$, and thus k_p is readily calculated. The calculated k_p values lie in the range 0.243 – 0.288 L/mol*s which are consistent with the values we,¹⁹³ and others,¹⁹² have reported for *exo*-7-oxanorbornene derivatives. All these data are consistent with controlled polymerizations. However, again it should be noted that in the case of the 75:25 copolymerization the kinetic profile is only valid for the last 10% of conversion.

Beyond the kinetic profiles several other criteria can be evaluated to confirm the controlled nature of the polymerizations and evaluate the effect, if any, of the counterion. These include examining the evolution of M_n with conversion, and the ability to form materials with narrow MWDs. SEC is a convenient, and fast, method for evaluating the evolution of M_n and the MWDs. Figure IV-5 shows an example of a series of ASEC traces (RI signals) for the 25:75 copolymerization. The systematic shift of the MWD to lower retention volume with increasing conversion is a qualitative indicator of a

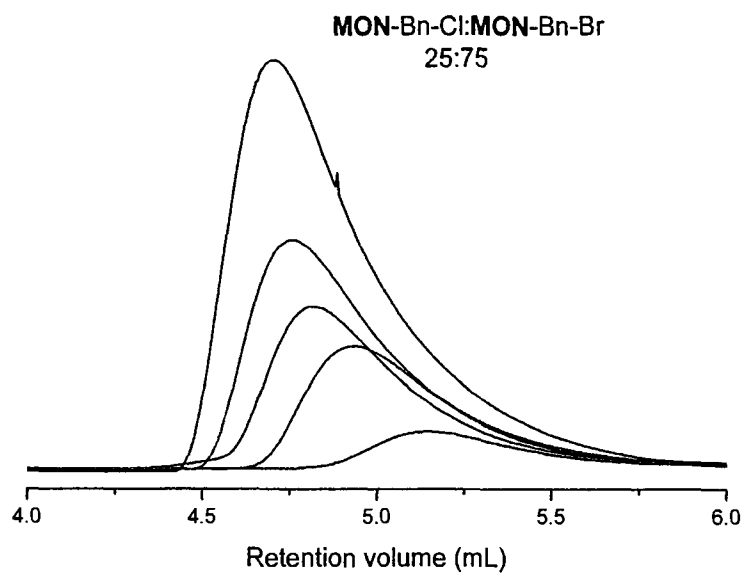


Figure IV-5. ASEC traces (RI signal) demonstrating the evolution of M_n as a function of polymerization time for the 25:75 copolymerization.

A better indicator, however, is the plot of number average molecular weight, M_n , vs conversion. Ideally, such a plot should be linear, pass through the origin and coincide with the predicted M_n , based on the ratio of monomer to initiator, at any given degree of conversion. Figure IV-6 shows the M_n

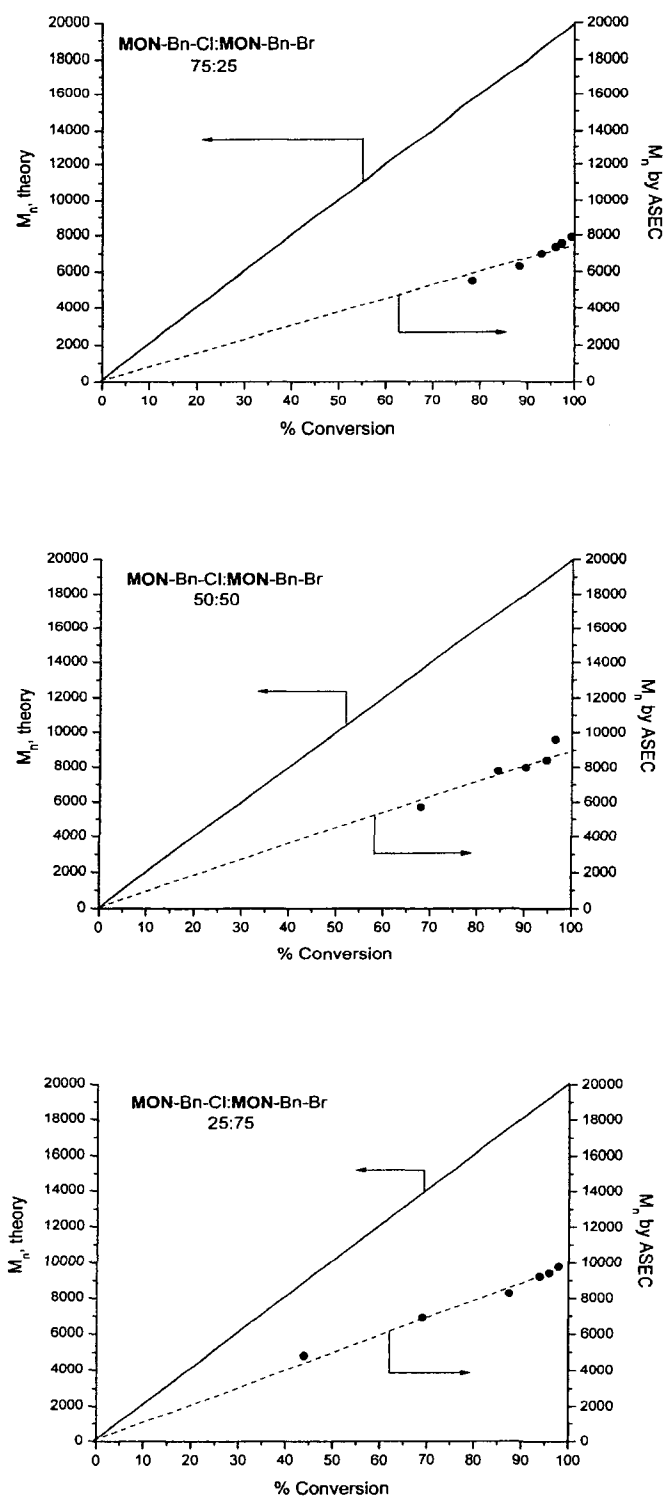


Figure IV-6. Evolution of M_n as a function of conversion as determined by ASEC for all three statistical copolymerizations of MON-Bn-Cl with MON-Bn-Br.

For all three copolymerizations the experimentally determined M_n vs. conversion plots exhibit acceptable linear profiles – this is a key indicator of the controlled nature of such copolymerizations. In all instances the experimentally determined M_n values do not agree with the theoretical values at any given degree of conversion. This discrepancy is most likely due to the nature of the calibration standards. The ASEC system was calibrated with a series of narrow MM poly(ethylene oxide) standards that, as noted earlier, are clearly poor equivalents for the cationic, non-linear polynorbornene derivatives examined here.

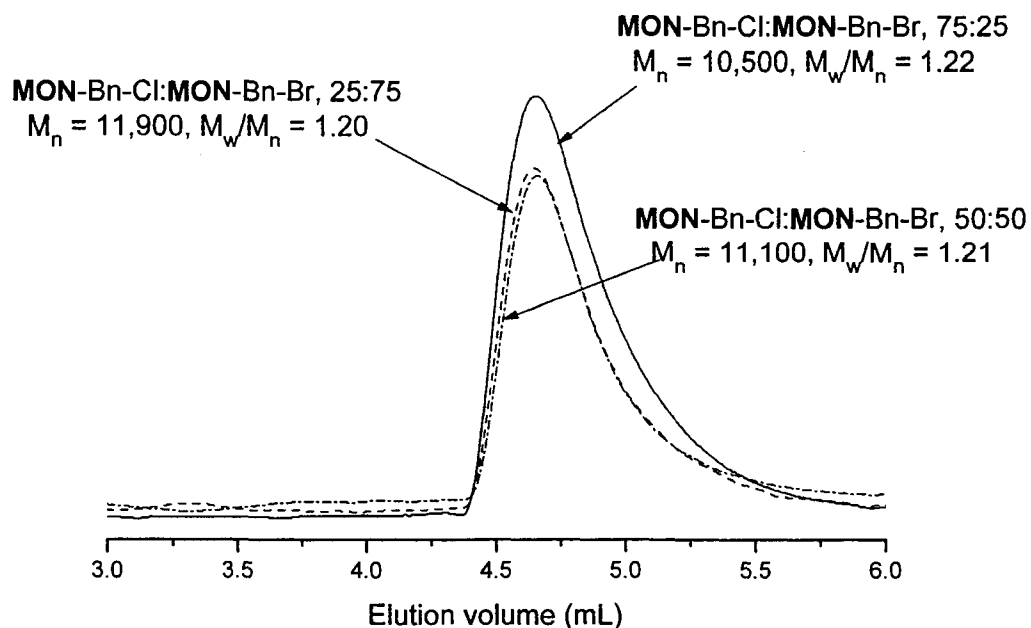


Figure IV-7. ASEC traces (RI signal) for copolymers of **MON-Bn-Cl** with **MON-Bn-Br** at three different molar ratios, 75:25 (solid line), 50:50 (dashed line), and 25:75 (dotted line).

Figure IV-7 shows the ASEC traces for three copolymers, at the three different comonomer ratios, at near-quantitative conversion. All three traces are essentially

identical. All are unimodal with no evidence of either high or low MW impurities. There appears to be some tailing to low MW (longer elution volumes), although this is not uncommon in ASEC. More importantly, all the polydispersity indices, M_w/M_n , are low and range between 1.20-1.22 – these can be considered to be identical. These values are similar to those determined for the **MON-Bn-Br** homopolymerization and are significantly better than those determined for the **MON-Bn-Cl** homopolymerization. These results would seem to suggest that while kinetic differences may be observed for these copolymerizations the ultimate effect on MW control and the breadth of the MWD are not significant, at least at the molar ratios of **MON-Bn-Cl:MON-Bn-Br** examined. Indeed, it would appear that even at 25 mol% **MON-Bn-Br** the effect on the MWD is beneficial compared to the **MON-Bn-Cl** homopolymerization, with final polydispersity indices comparable to those of the **MON-Bn-Br** being observed.

Summary/Conclusions

In this chapter we have described our observations regarding the effect of halide counterion on the kinetics and molecular weight/distribution control for copolymers of a permanently cationic *exo*-7-oxanorbornene monomer differing only in the nature of the halide counterion, polymerized with **17** in a 1:1 TFE:CH₂Cl₂ solvent mixture. Kinetically, the copolymerizations exhibit behavior intermediate of that of the respective homopolymerizations. The 75:25 (**MON-Bn-Cl:MON-Bn-Br**) exhibits a kinetic profile typical of a **MON-Bn-Cl** homopolymerization whereas the 50:50 and 25:75 copolymerizations are more typical of a **MON-Bn-Br** homopolymerization. It must be noted, however, that the effect is not significant under the conditions examined. All

copolymerizations exhibit the features associated with a controlled polymerization including linear M_n vs. conversion profiles and the ability to prepare (co)polymers with narrow molecular mass distributions. In all instances the final polydispersities are essentially identical, and are better than those observed for the homopolymerization of **MON-Bn-Cl**, and are more consistent with those observed for the homopolymerization of **MON-Bn-Br**. From the data gathered it would appear that the presence of 25 mol% **MON-Bn-Br** is sufficient to improve overall control with respect to the molecular weight distribution, relative to the homopolymerizations, while still maintaining a fast rate of polymerization (relative to **MON-Bn-Br**).

CHAPTER V

NEW WELL-DEFINED POLYMERIC BETAINES: FIRST REPORT DETAILING THE SYNTHESIS AND ROMP OF SALT-RESPONSIVE SULFOPROPYLBETAINE- AND CARBOXYETHYLBETAINE-*exo*-7-OXANORBORNENE MONOMERS**Introduction**

In this chapter we describe the synthesis and direct ROMP of new sulfopropylbetaine and carboxyethylbetaine monomers, **M32** and **M33** Figure V-1, based on the *exo*-7-oxanorbornene structural motif. These are, to the best of our knowledge, the first examples of such 7-oxanorbornene-based betaine monomers. Monomers **M32** and **M33** were subsequently polymerized with the commercially available first generation Grubbs' initiator **17** Figure V-1, in a 1:1 v/v solvent mixture of TFE/CH₂Cl₂ – the same solvent mixture that we described in Chapters III and IV to be an extremely effective medium for ROMP reactions with cationic *exo*-7-oxanorbornene substrates. Since such betaine substrates have never before been prepared/polymerized under ROMP conditions, this chapter evaluates the basic polymerization characteristics and demonstrates the ability to prepare materials with advanced architectures, and stimulus-responsive properties. These studies further highlight the functional group tolerance of Grubbs'-type initiators and the applicability of the TFE/CH₂Cl₂ solvent mixture for preparing materials with high degrees of functionality under facile conditions without recourse to either novel catalyst synthesis or post-polymerization modification.

Experimental

All reagents were purchased from the Aldrich Chemical Company at the highest available purity and used as received unless stated otherwise. Initiator **17** was stored and handled in a PlasLabs nitrogen-filled glove box. TFE, CH₂Cl₂, and EVE were degassed by at least three freeze-pump thaw cycles using a high vacuum Schlenk line, then blanketed in nitrogen and stored in the glove box until needed. *exo*-3,6-Epoxy-1,2,3,6-tetrahydrophthalic anhydride was recrystallized from 1:1 v/v ethyl acetate/hexane solvent mixture and then stored in a freezer until needed. *exo*-4-(2-Dimethylaminoethyl)-10-oxa-4-aza-tricyclo[5.2.1.0^{2,6}]dec-8-ene-3,5-dione (DMAETDD) was prepared by the reaction between N,N-dimethylethylenediamine and *exo*-3,6-epoxy-1,2,3,6-tetrahydrophthalic anhydride as described in Chapter III. *exo*-[2-(3,5-Dioxo-10-oxa-4-aza-tricyclo[5.2.1.0^{2,6}]dec-8-en-4-yl)ethyl]dimethylpropyl ammonium bromide (Pr-quat-Br, **M34** Figure 1) was prepared according to the procedure outlined in Chapter III.

*Synthesis of *exo*-[2-(3,5-dioxo-10-oxa-4-aza-tricyclo[5.2.1.0^{2,6}]dec-8-en-4-yl)-ethyl]-dimethylpropylsulfobetaine, **M32**.*

The sulfopropylbetaine derivative **M32** was prepared by a multi-step procedure as follows:

DMAETDD (5.11 g, 21.6 mmol) and THF (50 mL) were added to a 100 mL canonical flask equipped with a magnetic stir bar. 1,3-Propanesultone (3.16 g, 1.2 mol eq.) was then added to the flask in one portion. The reaction was heated at 50°C for 48 h, during which time a white precipitate formed. The precipitate was isolated by Buchner filtration and dried *in vacuo* at ambient temperature yielding the title compound as a white powder.

Yield = 87%, mp = 188-190°C. ^1H NMR (300 MHz, D_2O): δ (ppm) = 6.63 ($\text{CH}=\text{}$, 2H, m), 5.35 (OCH , 2H, m), 3.98 (imideN- CH_2 , 2H, t), 3.56 (imideN- CH_2CH_2 , 2H, t), 3.55 ($\text{N}(\text{CH}_3)_2\text{CH}_2$, 2H, t), 3.20 ($\text{C}=\text{OCH}$, 2H, t), 3.18 ($\text{N}(\text{CH}_3)_2$, 6H, s), 2.99 ($\text{CH}_2\text{-SO}_3$, 2H, t), 2.22 ($\text{CH}_2\text{CH}_2\text{CH}_2$, 2H, m). ^{13}C NMR (75 MHz, H_2O): δ (ppm) 178.69 ($\text{N}-\text{C}=\text{O}$), 136.93 ($\text{HC}=\text{CH}-\text{CHO}$), 81.41 ($\text{HC}-\text{O}$), 63.07 ($\text{N}-\text{CH}_2$), 59.83 ($\text{CH}_2-\text{N}(\text{CH}_3)_2$), 51.46 ($\text{N}(\text{CH}_3)_2-\text{CH}_2$), 48.02 ($(\text{CH}_3)_2-\text{NCH}_2$), 47.54 ($\text{CH}_2\text{CH}_2\text{CH}_2\text{SO}_3^-$), 32.78 ($\text{CH}-\text{C}=\text{O}$), 18.59 ($\text{CH}_2\text{CH}_2\text{CH}_2$). $\text{C}_{15}\text{H}_{24}\text{N}_2\text{O}_6\text{S}$ (360.14): Anal. Calcd. C, 49.99; H, 6.71; N, 7.77; O, 26.63; S, 8.90; Found: C, 48.9; H, 6.70; N, 8.00; S, 8.94.

*Synthesis of exo-[2-(3,5-dioxo-10-oxa-4-aza-tricyclo[5.2.1.0^{2,6}]dec-8-en-4-yl)-ethyl]-dimethylpropylcarboxybetaine, **M33**.*

The title compound was prepared by a reaction between DMAETDD and β -propiolactone under a nitrogen atmosphere as follows:

DMAETDD (5.07 g, 21.5 mmol) and THF (50 mL) were added to a 100 mL canonical flask equipped with a magnetic stir bar. Subsequently, β -propiolactone (1.86 g, 1.2 mol eq.) was added to the flask in one portion. The reaction was left at room temperature for 24 h, during which time a white precipitate formed. The precipitate was isolated by Buchner filtration and dried *in vacuo* at ambient temperature yielding the title compound as a white powder. Yield = 90%, mp = 118-121°C. ^1H NMR (300 MHz, D_2O): δ (ppm) = 6.48 ($\text{CH}=\text{}$, 2H, t), 5.20 ($\text{O}-\text{CH}$, 2H, t), 3.85 (imideN- CH_2 , 2H, t), 3.51 ($\text{N}(\text{CH}_3)_2\text{CH}_2$, 2H, t), 3.40 (imideN- CH_2CH_2 , 2H, m), 3.01 ($\text{N}(\text{CH}_3)_2$, 6H, s), 3.04 ($\text{C}=\text{OCH}$, 2H, m), 2.56 (CH_2-CO_2 , 2H, t). ^{13}C NMR (75 MHz, H_2O): δ (ppm) 178.43 ($\text{N}-\text{C}=\text{O}$), δ (ppm), 176.27

(CH₂-CO₂⁻), 136.69 (HC=CH-CHO), 81.78 (HC-O), 62.12 (N-CH₂), 59.56 (CH₂-N(CH₃)₂), 51.59 (N(CH₃)₂-CH₂), 47.76 ((CH₃)₂-NCH₂), 32.57 (CH-C=O), 30.73 (CH₂CH₂CO₂⁻). C₁₅H₂₂N₂O₅ (310.15): Anal. Calcd. C, 58.05; H, 7.15; N, 9.03; O, 25.78; Found: C, 57.8; H, 6.98; N, 8.6.

Protonation/Deprotonation of carboxybetaine M33

Carboxybetaine M33 was protonated by stirring 1.00g of monomer in 3.0 mL of 5.0 M solution of HCl for 30 min. The protonated monomer (H-M33) was recovered by precipitation into a large volume of THF, followed by Buchner filtration and drying *in vacuo*. Protonation was confirmed by FT-IR spectroscopy.

Homopolymerization of sulfopropylbetaine M32 and carboxyethylbetaine M33

Below is a typical procedure for the homopolymerization of the betaine monomeric substrates:

Protonated carboxybetaine M33 (0.5 g, 1.45 mmol) was added to a single necked Schlenk flask (100 mL) capacity equipped with a magnetic stir bar. The flask was subsequently degassed/back-filled with N₂ three times using standard Schlenk line techniques prior to being transferred to a nitrogen filled glove box. TFE (2.0 mL) was then added to the flask. Initiator 17 (20.6 mg, 0.025 mmol for a target M_n of 20,000) was weighed into a scintillation vial (20 mL) capacity, and then CH₂Cl₂ (2.0 mL) was added. The catalyst solution was then added directly to the monomer solution with stirring. The polymerization was left for 8 min prior to quenching with EVE (0.5 mL). The solution

was left to stir for 15 min prior to precipitation into a large excess of THF. The polymer was isolated by Buchner filtration, washed with THF, and dried *in vacuo*. Yield: 95 %.

Self-block copolymerization

Below is a typical procedure for the self-block copolymerization of the betaine monomeric substrates:

The sulfobetaine **M32** (0.5 g, 1.30 mmol) was added to two separate Schlenk flasks (100 mL, 0.5 g in each) capacity equipped with magnetic stir bars. Both flasks were simultaneously evacuated/back-filled with N₂ at least three times using standard Schlenk line techniques prior to transfer to a PlasLabs N₂ filled glove box. TFE (5.0 mL) was then added to each flask. Initiator **17** (0.041 g, 0.05 mmol, M_n theory = 10,000) was weighed out in a scintillation vial (20 mL capacity) and CH₂Cl₂ (5.0 mL) was then added. The catalyst solution was then added directly to one of the flasks containing monomer solution. The polymerization was allowed to proceed for 2 min prior to extracting an aliquot, which was quenched with EVE, for ASEC analysis. The second monomer solution was then added directly to the homopolymer solution. The solution was left to stir for 5 min prior to quenching with EVE (0.5 mL). Homo- and diblock copolymers were recovered by precipitation in to a large excess of THF, isolated by Buchner filtration, and dried overnight *in vacuo* at ambient temperature.

*Block polymerization of the sulfopropylbetaine **M32** with the propylquat **M33***

The sulfobetaine **M32** (0.5 g, 1.39 mmol) was added to a single neck Schlenk flask (100 mL capacity) equipped with a magnetic stir bar. The cationic monomer **M34** (1.17 g,

3.24 mmol) was added to a second identical flask. Both flasks were degassed/back-filled with N₂ three times using standard Schlenk line techniques after which they were transferred to a PlasLabs N₂ filled glove box. TFE (2.50 mL) was subsequently added to each flask and allowed to stir until each monomer was completely dissolved. Grubbs initiator 17 (41.0 mg, 0.05 mmol) was added to a scintillation vial (20.0 mL capacity). To this vial was then added CH₂Cl₂ (2.50 mL). After complete dissolution of 17, the catalyst solution was added directly to the flask containing the TFE solution of M32. The homopolymerization of M32 was allowed to proceed for 1.5 min prior to the extraction of an aliquot, which was immediately quenched with EVE. The TFE solution of M34 was immediately added to the polyM32 solution. The block copolymerization was allowed to proceed for 20 min prior to quenching with EVE. The M32-M34 AB diblock copolymer was recovered by precipitation into a large excess of THF, followed by isolation via Buchner filtration and drying *in vacuo* overnight at ambient temperature. Target molar composition 30:70 M32:M33, experimentally determined composition via ¹H NMR spectroscopy recorded in D₂O + NaCl: 31:69. M_n determined by ASEC: 14,300 with M_w/M_n = 1.34.

Characterization techniques

¹H (300.1 MHz) and ¹³C (75.9 MHz) NMR spectra were recorded on a Bruker 300 53 mm spectrometer in appropriate deuterated solvents or deuterated solvent mixtures. Melting points of the new monomers were determined using an electrothermal digital melting point apparatus.

Aqueous Size Exclusion Chromatography (ASEC)

Polymer molecular masses, molecular mass distributions, and polydispersity indices were determined by ASEC in 0.25 M NaBr at a flow rate of 1.00 mL min⁻¹ at ambient temperature. The system was comprised of a Viscotek VE1122 pump, Viscotek VE3580 RI detector, and a Viscotek PW_{XL} guard column followed by a series of two Viscotek columns (ViscoGEL G5000PW_{XL} 7.8 mm (ID) x 30.0 cm (L) + G4000PW_{XL} 7.8 mm x 30.0 cm (L)) with a theoretical linear molecular mass range of 200 – 1,000,000 g/mol poly(ethylene oxide) (PEO). The system was calibrated with a series of narrow molecular mass distribution PEO/poly(ethylene glycol)(PEG) standards (MW range: 620 – 460,000). Data were analyzed with the OmniseC Interactive SEC software package.

Mass Spectrometry

Mass spectra were acquired on a Thermo Finnigan LXQ electrospray ionization-mass spectrometry (ESI-MS) ion-trap instrument using Xcalibur 2.0 for data acquisition and processing. The spectrometer was optimized using the Autotune feature of Xcalibur for the ions of interest. The spectrometer was used in ESI full scan mode from 150-2000 amu. Samples were introduced in to the MS using the direct liquid infusion (DLI) method, and at least 50 scans were overlaid for each sample. Samples were prepared by dissolving 1.00 mg of monomer in 1.00 mL of MeOH/H₂O (1:1) 0.5% Acetic acid solution. Pipetted 1.00 μL of this solution and diluted with an additional 1.00 mL of MeOH/H₂O (1:1) 0.5% Acetic acid. Injected 300 μL of sample solution by direct liquid injection (DLI) using a Hamilton syringe.

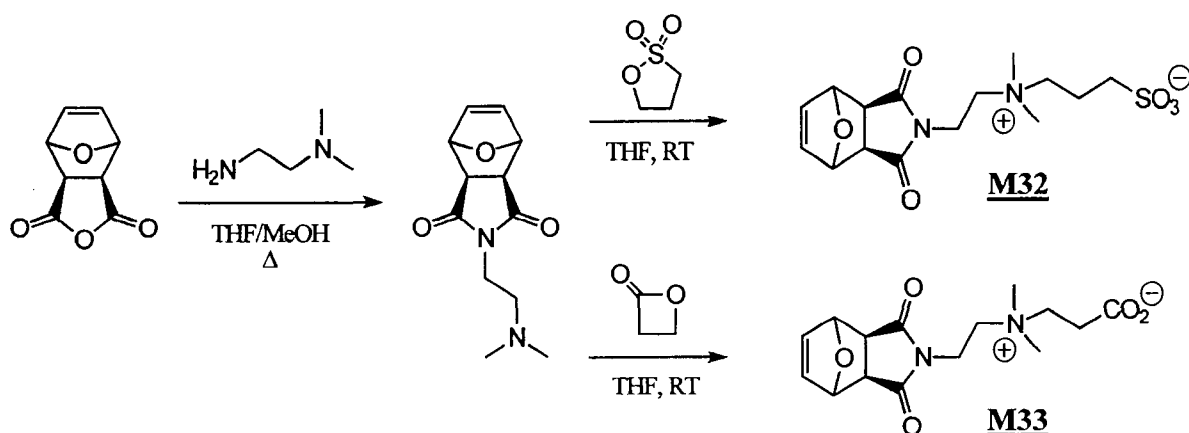
Dynamic Light Scattering (DLS)

DLS experiments were performed on a Malvern Instruments Zetasizer Nano ZS instrument equipped with a 4 mW He-Ne laser operating at $\lambda = 633$ nm, an avalanche photodiode detector with high quantum efficiency, and an ALV/LSE-5003 multiple tau digital correlator electronics system. The data were collected and processed using the Dispersion Technology Software Version 5. Samples were prepared as 0.5 wt % solutions in DI H₂O and 0.1 M NaCl.

Results and Discussion

Both **M32** and **M33** were prepared by a multi-step procedure involving initial reaction of *exo*-3,6-epoxy-1,2,3,6-tetrahydrophthalic anhydride with N,N-dimethylethylenediamine yielding the intermediate tertiary amine functional imide derivative (DMAETDD) which was subsequently modified with 1,3-propanesultone to yield **M32**, or β -propiolactone to yield **M33**, Scheme V-1. Monomers were characterized using a combination of ¹H/¹³C NMR spectroscopy and mass spectrometry. Figure V-2 shows the ¹³C NMR spectra of **M32** recorded in D₂O and **M33** recorded in *d*₆-DMSO with all relevant peak assignments. The structure of **M32** and **M33** was also confirmed by mass spectrometry with *m/z* for **M32** and **M33** determined to be 359.08 (*m/z* theory: 358.12) and 309.17 (*m/z* theory: 308.14) respectively.

In this particular study we have intentionally limited ourselves exclusively to the *exo*-monomer derivatives since *exo*-norbornene substrates are well known to be more readily polymerized than the corresponding *endo*-stereoisomers, especially in the case of polymerizations initiated by first generation Grubbs' catalysts such as **17**.



Scheme V-1. Outline for the preparation of the sulfopropylbetaine **M32** and carboxyethylbetaine **M33**. The intermediate tertiary amine, *exo*-4-(2-dimethylaminoethyl)-10-oxa-4-aza-tricyclo[5.2.1.0^{2,6}]dec-8-ene-3,5-dione (DMAETDD), was prepared from the reaction of *N,N*-dimethylethylenediamine with *exo*-3,6-epoxy-1,2,3,6-tetrahydrophthalic anhydride in a mixture of tetrahydrofuran (THF) and methanol. Subsequent reaction of DMAETDD with 1,3-propanesultone or β -propiolactone in THF yields **M32** and **M33** respectively.

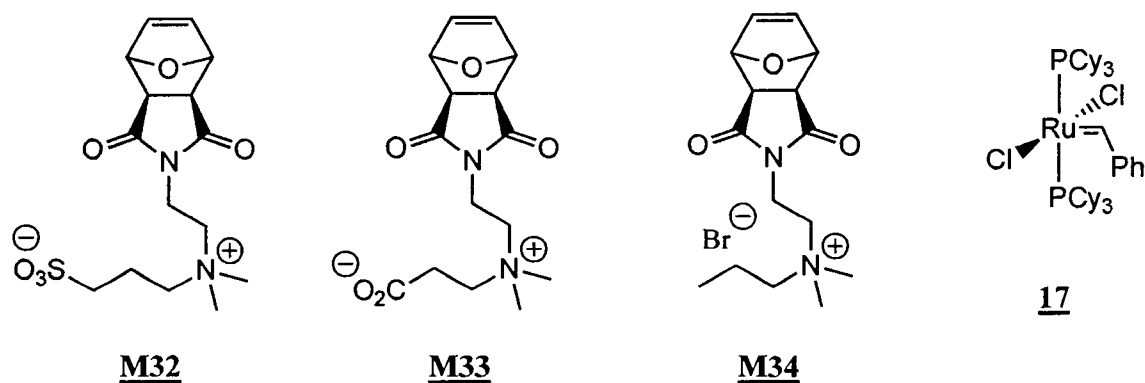


Figure V-1. Chemical structures of the sulfopropylbetaine, **M32**, carboxyethylbetaine, **M33**, and propyl-quaternized cationic, **M34**, *exo*-7-oxanorbornene monomers, and Grubbs' first generation initiator, **17**.

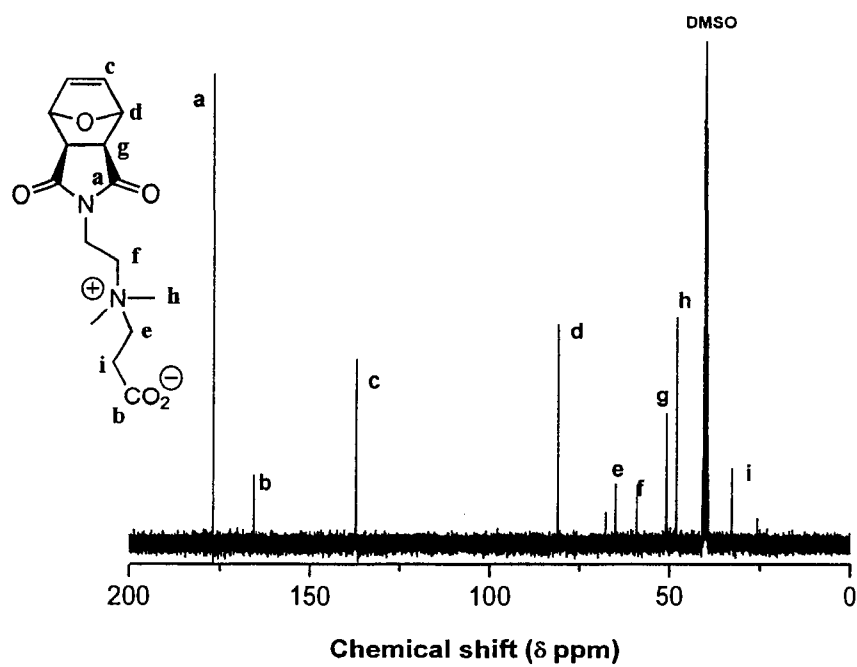
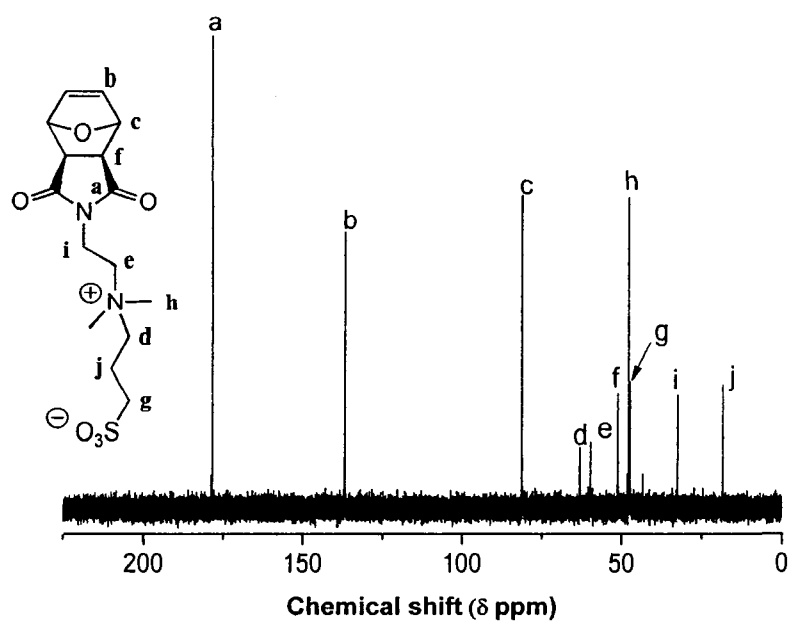


Figure V-2. ¹³C NMR spectra of **M32** recorded in D₂O/NaCl and **M33** recorded in d₆-DMSO.

With the new betaine monomers M32 and M33 in hand, we examined their homo- and copolymerization behavior with 17 in 1:1 v/v TFE/CH₂Cl₂. We will present and discuss the results from the studies with M32 followed by those observed for M33, and conclude with some aqueous solution studies.

Homopolymerizations of M32 were conducted at 7.38 wt% in a 1:1 TFE/CH₂Cl₂ solvent mixture at ambient temperature. TFE was chosen as a cosolvent for several reasons. Firstly, and as discussed in Chapter III, we have demonstrated it to be a suitable cosolvent for the direct homogeneous polymerization of permanently cationic substrates;¹⁹³ secondly, we also demonstrated that 17 is stable towards TFE, at least on the time scale of polymerization, and finally, TFE is known to be a thermodynamically excellent solvent for sulfopropylbetaine monomers and (co)polymers.¹⁹³ Polymerizations were conducted in a nitrogen-filled glove box and monitored by extracting aliquots at various time intervals that were immediately terminated by the addition of EVE. The polymer/monomer was isolated by precipitation into a large excess of THF, and then analyzed by a combination of techniques. Conversions were determined by NMR spectroscopy by monitoring the disappearance of the monomer vinylic resonance and the appearance of the polymer vinylic resonances associated with the unsaturated backbone. For example, Figure V-3 shows the NMR spectra, between $\delta = 8.0$ and 5.5 ppm, of several aliquots extracted from the homopolymerization of M32, and clearly demonstrate the distinct difference in chemical shift between the different vinylic hydrogens. Additionally, the phenyl end-group associated with the original carbene moiety in 17 is visible at ca $\delta \sim 7.25$ -7.50 ppm. The importance/utility of this will be further highlighted below. Clearly a direct ratio of the integrals associated with the monomer and polymer

vinyl species is a quick and convenient method for determining the conversion. The two different resonances associated with the polymeric vinylic hydrogens is a consequence of the stereochemistry associated with the backbone vinylic groups. The formation of polymer containing unsaturation in the backbone leads to the possibility of both cis and trans stereochemistry. A direct ratio of these two signals yields the relative cis/trans ratio, and we find that the resulting homopolymer of **M32** is trans rich with approximately 60-70% trans residues. This is consistent with our previous observations for homopolymers derived from permanently cationic *exo*-7-oxanorbornene substrates **M31** prepared with **17** in TFE/CH₂Cl₂, as well as reports from other research groups.¹⁹³

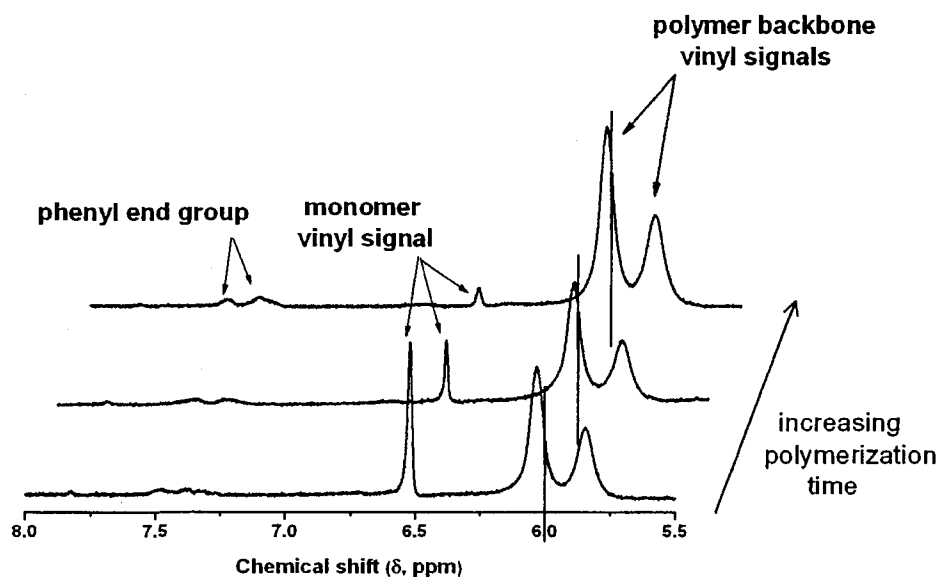


Figure V-3. A series of ¹H NMR spectra from the homopolymerization of **M32** with **17**, recorded in D₂O/NaCl, demonstrating conversion of monomer to polymer as well as the resulting stereochemistry in the polymer backbone. The polymerization was conducted in TFE/CH₂Cl₂ at ambient temperature with **17**.

With the conversion data readily available the pseudo-first order kinetic plots are easily generated. For example, Figure V-4 shows a typical kinetic profile for the homopolymerization of **M32**. Several points are particularly noteworthy. Firstly, even under these relatively dilute conditions, the homopolymerization of **M32** proceeds extremely rapidly with essentially quantitative conversion being reached in 2 min. This is significantly more rapid than the cationic substrates discussed in Chapter III even though the monomer concentration is approximately 3x lower. This is also considerably faster than the homogeneous aqueous systems with cationic substrates reported by Grubbs' and co-workers mediated by water-soluble first generation catalyst derivatives.¹⁶³ Knowing the conversion profile it is straightforward to generate the first order kinetic plot, Figure V-4. The rate expression for a ROMP polymerization is given by $R_p = k_p[\text{Ru}][\text{M}]$, where R_p is the rate of polymerization, k_p is the rate constant of propagation, $[\text{Ru}]$ is the initial initiator concentration, and $[\text{M}]$ is the starting monomer concentration. This formally second order rate expression can be forced to a first order expression since $[\text{Ru}]$ is assumed to be constant, i.e. $R_p = k_{\text{comp}}[\text{M}]$, where $k_{\text{comp}} = k_p[\text{Ru}]$. As such, the first order rate plot, $\ln(1/(1-x))$ vs time, where x is the fractional conversion, should be linear (if the polymerization is first order in monomer and there is no discernable chain length dependence of k_p), and pass through the origin, which is observed to be the case. The slope of the kinetic plot is $= k_p[\text{Ru}]$, and since $[\text{Ru}]$ is known, k_p is readily obtained and for the homopolymerization of **M32** was determined to be $2.87 \text{ Lmol}^{-1}\text{s}^{-1}$.

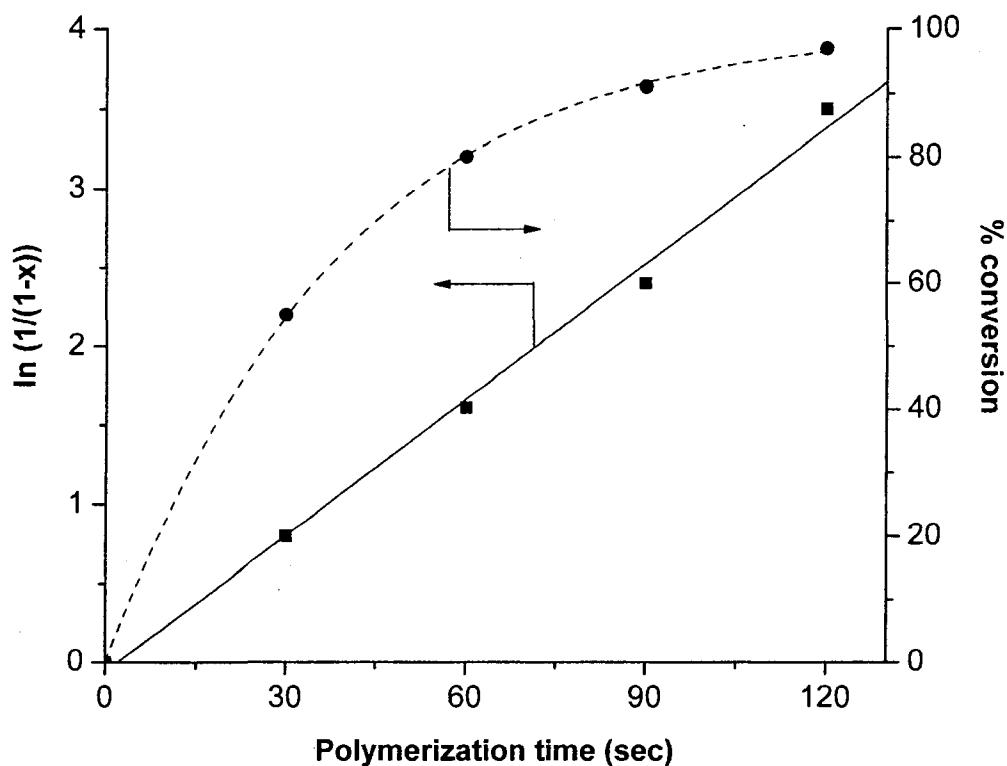


Figure V-4. Conversion vs. time and pseudo-first order rate plot for the homopolymerization of the sulfopropylbetaine **M32** with **17** at 7.38 wt % and ambient temperature.

This value of k_p is an order of magnitude larger than the k_p values we measured for analogous cationic derivatives (Chapter III) and also those reported for an *exo*-7-oxanorbornene derivative polymerized with **17** reported by Holland et al.¹⁹² This difference in k_p may be due to the fact that in our earlier study the cationic substrates all had bromide counterions, although this was not the case in the study by Holland. The nature of the halide ligand is known to have a significant kinetic effect with, for example, $\text{RuBr}_2(\text{PCy}_3)_2\text{CHPh}$ being a faster initiator than **17** but at the expense of lower overall

activity (lower k_p).¹⁴⁷ Indeed, we demonstrated in Chapter IV that monomers with a bromide counterion may serve as a convenient source of bromide and lead to the in situ generation of the mixed, $\text{RuClBr}(\text{PCy}_3)_2\text{CHPh}$, species or the dibromo analog noted above.¹⁹⁴ However, a contributing factor to the generally fast rate of polymerization may also be the nature of the cosolvent mixture, although this does not account for the observed difference between the cationic substrates. Sanford et al. have reported that the dielectric constant (ϵ) of a solvent can have a significant effect on polymerization rate with solvents with higher ϵ leading to faster polymerizations.¹⁴⁷ This was rationalized in terms of enhanced stabilization of the active unsaturated intermediate in more polar solvents. The TFE cosolvent employed in these studies may likewise be imparting a rate enhancing effect given its high ϵ of 27.7. However, it is not entirely clear why the polymerization of **M32** is so rapid.

Regardless of the precise cause of the observed high rate of polymerization, the kinetic data for the homopolymerization of **M32** with **17** is consistent with a controlled polymerization. However, the ability to control the molecular mass is also an important feature associated with such controlled polymerizations. Figure V-5 shows the aqueous size exclusion chromatogram (RI signal) for a homopolymer of **M32** with a theoretical M_n of 9,100. While the trace is unimodal and near symmetric, the chromatogram has an ill-defined baseline, presumably due to its low molecular mass approaching the lower limits of the column set. However, the measured M_n of 7,600 is in close agreement with the theoretical M_n of 9,100. Additionally, the measured polydispersity index (M_w/M_n) is low at 1.19 and is consistent with (co)polymers prepared in a controlled manner.

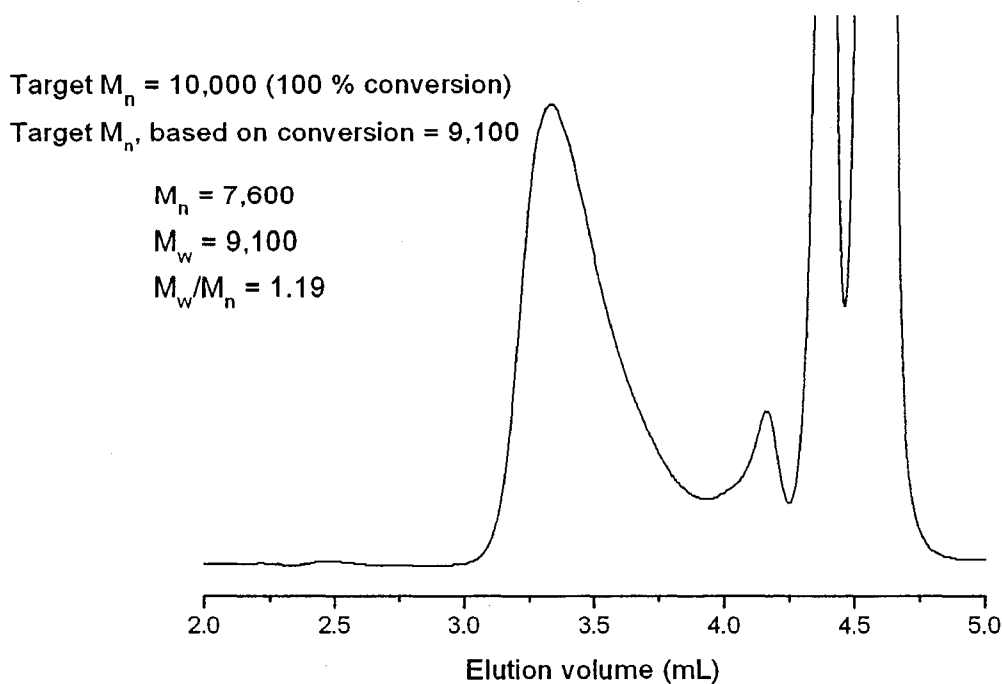


Figure V-5. The ASEC trace (RI signal) for a polyM32 homopolymer with a theoretical M_n of 9,100. Analysis was conducted in 0.25M NaBr at a flow rate of 1.0 mL/min. The system was calibrated with a series of narrow molecular weight distribution poly(ethylene oxide) standards.

While this measured M_n is close to the theoretical value, it must be borne in mind that the ASEC instrument was calibrated with a series of narrow molecular weight distribution poly(ethylene oxide) standards which may be considered to be poor equivalents for the highly functional zwitterionic, betaine (co)polymers. A complimentary method to SEC for determining the *absolute* molecular mass, at least for materials with relatively low molecular masses and appropriate chain-end functionality, is end-group analysis by ^1H NMR spectroscopy. Figure V-6, for example, shows the ^1H NMR spectrum of a polyM32 homopolymer polymerized to ca. 91% conversion. For these lower molecular mass polymers, as noted above, the phenyl end-group derived from the original carbene

moiety in **17** is visible at $\delta \sim 7.4$ - 7.5 ppm, and is labeled **a** in Figure V-6, and serves as a convenient tag for absolute molecular mass determination since every polymer chain should contain one such group at one chain terminus. A direct ratio of this signal with a clear resonance signal associated with the polymer facilitates a determination of the absolute molecular mass. For example, the methylene unit labeled **b** can be employed as such a comparative signal. A direct ratio of **a** and **b** yields a calculated absolute M_n of 11,200. Again this value is close to the theoretical value which given the low sensitivity of NMR and the low intensity of the phenyl end-group is gratifying, and would indicate that initiation by **17** is essentially quantitative.

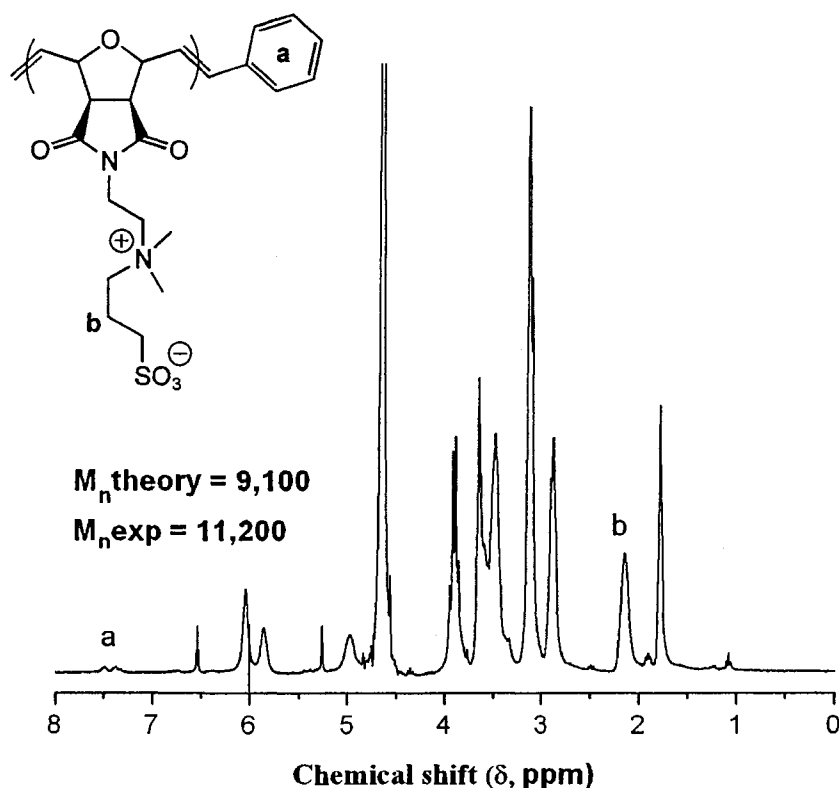


Figure V-6. ^1H NMR spectrum of a poly**M32** homopolymer recorded in $\text{D}_2\text{O}/\text{NaCl}$ with a theoretical M_n of 9,100.

The ability to prepare (co)polymers with pre-determined molecular masses simply by varying the [Ru]:[M] is another important feature associated with a controlled polymerization. As such we conducted three different homopolymerizations of M32 targeting homopolymers with molecular masses of 10K, 20K, and 40K, Table V-1. In all instances the ASEC traces (RI signal, not shown) were symmetric and unimodal and exhibited a clear shift to lower retention volume with increasing targeted molecular mass. However, the measured molecular masses of 7,600, 12,600, and 17,400 did not coincide with the theoretical values, for the reason noted earlier. However, the measured polydispersity indices were low and in the range $M_w/M_n = 1.19-1.21$. Unfortunately, in the case of the polyM32 homopolymers with targeted molecular masses of 20K and 40K, end-group analysis could not be performed since the phenyl end-group was not visible in the ^1H NMR spectra.

The ultimate test for a controlled polymerization is an evaluation of retention of chain-end activity upon the complete conversion of monomer. This is most readily demonstrated via block copolymer synthesis and sequential monomer addition. Figure V-7 shows the ASEC traces (RI signal) obtained from a self-blocking experiment conducted with M32. The trace at higher retention volume (lower molecular mass) represents the homopolymer with a targeted M_n of 10,000 obtained from M32 polymerized to near-quantitative conversion. The trace at lower retention volume (higher molecular mass) represents the “block” copolymer obtained after the addition of a second batch of M32. The “block” copolymer trace is symmetric and unimodal with little, if any, indication of any low molecular mass impurity due to the loss of active chain ends after the quantitative conversion of the first batch of M32. The experimentally

determined polydispersity also falls from $M_w/M_n = 1.25$ for the first batch of **M32** to 1.15 for the “block” copolymer. These observations are entirely consistent with a controlled polymerization and demonstrate the ability, at least in principle, to be able to prepare novel AB diblock copolymers with **M32** as a highly functional comonomer.

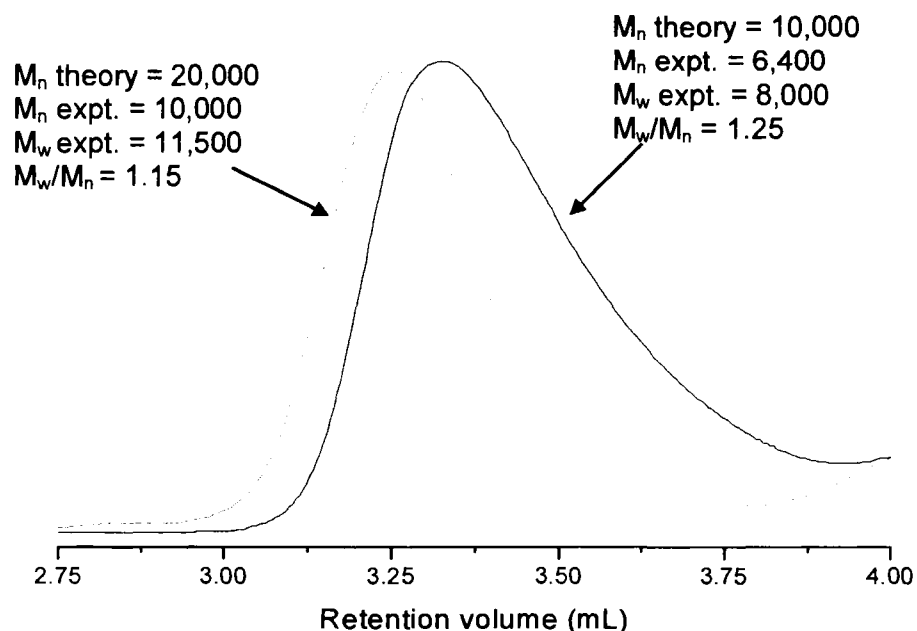


Figure V-7. ASEC traces (RI signal) for the self-blocking experiment with the sulfopropylbetaine **M32**. Analysis was conducted in 0.25M NaBr at a flow rate of 1.0 mL/min. The system was calibrated with a series of narrow molecular weight distribution poly(ethylene oxide) standards.

Having demonstrated the controlled nature of the homopolymerization of **M32** we next evaluated the ROMP of **M33** under the same general conditions. In preliminary experiments we examined the direct polymerization of **M33**. However, we observed little/no conversion presumably due to catalyst deactivation via the competitive

complexation of the carboxylate functional group associated with **M33** to the Ru metal center. To circumvent this problem we first protonated **M33** by treating it with HCl thus converting it to a substrate (**H-M33**) bearing only a formal positive charge while simultaneously introducing a chloride counterion. The polymerization of **H-M33** was then evaluated. Figure V-8 shows the conversion and kinetic profile for the homopolymerization of **H-M33** (target $M_n = 20,000$), at 20 wt% with **M34** at ambient temperature. The linear kinetic profile is consistent with the observations for **M32** and with the polymerization proceeding in a controlled manner. However, the homopolymerization of **H-M33** is significantly slower than for **M32**. Whereas near-quantitative conversion of **M32** was observed within 2 min, it takes 6 min for **H-M33** to reach ca. 95% conversion. This is also evident from the calculated k_p value which was determined to be 0.289 L/mol*s – a significantly lower value than for the homopolymerization of **M32** although it is consistent with the permanently cationic *exo*-7-oxanorbornene substrates **M31** we described in Chapter III.¹⁹³

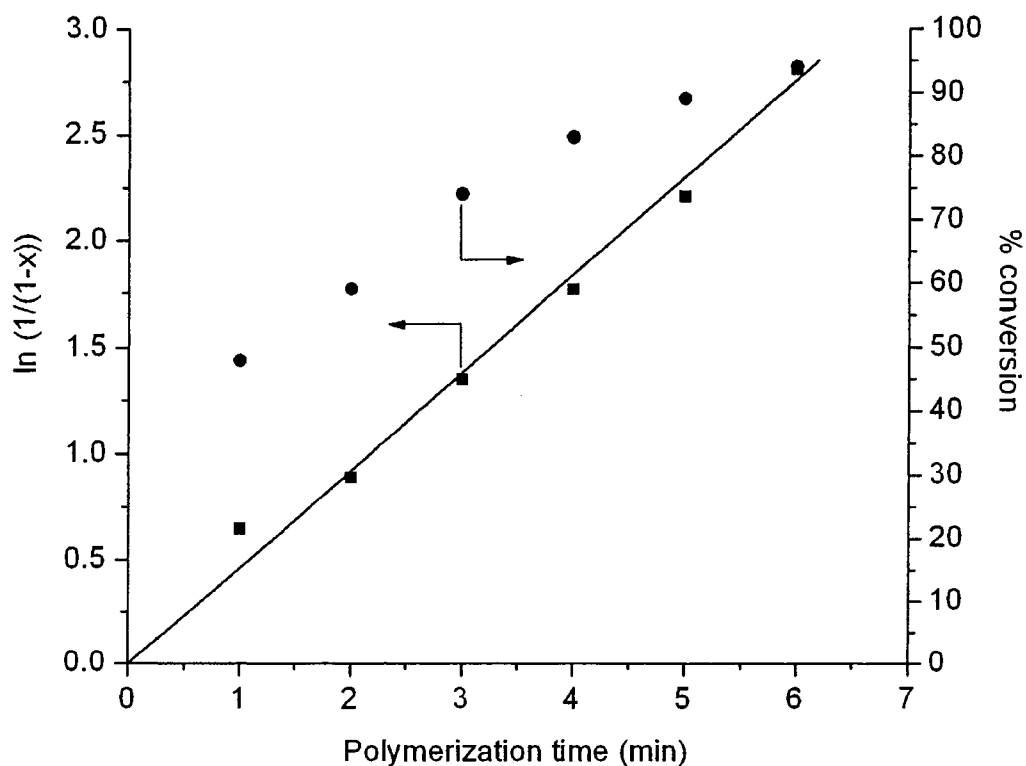


Figure V-8. Conversion and kinetic profile for the homopolymerization of the protonated carboxyethylbetaine **H-M33** with **17** in TFE/CH₂Cl₂ at ambient temperature.

As with **M32**, we next proceeded to demonstrate the ability to control the M_n of the target **H-M33** homopolymers by simply varying [Ru]:[M]. Three **H-M33** homopolymers with M_n 's of 10K, 20K, and 40K were targeted, and the results are summarized in Table V-1.

Table V-1. Summary of the theoretical M_n , measured M_n and M_w/M_n , and the experimentally determined k_p values from the homopolymerizations of the sulfopropylbetaine **M32** and the protonated carboxyethylbetaine **H-M33**.

Monomer	M_n theory ^a	% conversion ^b	M_n ASEC ^c	M_w/M_n ^c	M_n NMR	k_p ^d L/mol*s ^e
M32	10,000	96	7,600	1.19	11,200	2.87
M32	20,000	97	12,600	1.19	-	-
M32	40,000	95	17,400	1.21	-	-
H-M33	10,000	96	3,600	1.25	11,400	0.289
H-M33	20,000	95	7,400	1.21	24,700	-
H-M33	40,000	95	12,600	1.28	32,100	-

a. M_n theory = mass of monomer (g)/moles of initiator

b. As determined by ¹H NMR spectroscopy

c. As determined by ASEC in 0.25 M NaBr. System was calibrated with narrow molecular mass poly(ethylene oxide) standards

d. k_p = rate constant for propagation

e. As determined from the pseudo-first order kinetic plots

Consistent with the results described above for the poly**M32** homopolymers, the M_n as determined by ASEC is significantly different from the theoretical value and is again due to the calibration with poly(ethylene oxide) standards. However, it is apparent that the targeted molecular mass can be tuned by varying the reaction stoichiometry – consistent with the results presented earlier for **M32**. The measured polydispersity indices are, likewise, consistent with a well-controlled polymerization although were found to be slightly higher ($M_w/M_n = 1.21-1.28$) than those determined for the poly**M32** homopolymers.

As with the low molecular mass polyM32 homopolymer we were able to determine the absolute molecular mass by end-group analysis. In contrast, however, to the polyM32 homopolymers we were able to determine the values for all three homopolymers, presumably due to the enhanced dissolution of the polyH-M33 homopolymers in the NMR solvent. As with the polyM32 homopolymer, it is clear from Table V-1 that the absolute molecular masses are more consistent with the targeted values versus those determined by aqueous SEC. For example, in the case of the polyH-M33 homopolymer with a theoretical M_n of 38,000 (based on the degree of conversion), the measured absolute molecular mass by end-group analysis is 32,100.

Having demonstrated the ability to prepare homo- and copolymers of M32 and H-M33 in a controlled manner we next examined the synthesis of an AB diblock copolymer of M32 with the permanently cationic monomer M34, Figure V-1, achieved via sequential monomer addition of M32 followed by M34. Figure V-9 shows the ASEC traces (RI signal) for a polyM32 homopolymer and the corresponding poly(M32-M34) block copolymer. The trace at higher retention volume represents the homopolymer and has a measured M_n of 11,500 (M_n theory = 20,000) and M_w/M_n of 1.23. Based on the kinetics determined earlier, the polymerization of M32 was allowed to run for 2 min prior to the subsequent addition of M34. The trace at lower retention volume represents the M32-M34 AB diblock copolymer. The trace is unimodal although there is some evidence of tailing to lower molecular mass, which may indicate, less than quantitative crossover efficiency. The measured molecular mass is 14,300 and the $M_w/M_n = 1.34$. Given the targeted molecular mass for the block copolymer of 60,000 this value may seem surprisingly low. Aside from the inherent discrepancy associated with the system

calibration with linear non-ionic poly(ethylene oxide) standards, such a low measured M_n might also be rationalized when the behavior of the zwitterionic-cationic block copolymer in the ASEC eluent (0.25 M NaBr) is considered. Such conditions are required to solubilize the polybetaine component, and therefore, under these conditions the polyM32 block is likely somewhat expanded. In contrast, the cationic block will be highly collapsed under these conditions due to the polyelectrolyte effect. As such, the AB diblock copolymer could easily have a hydrodynamic volume not significantly greater than the polyM32 homopolymer and certainly would result in a much lower measured M_n than the true value. However, ASEC clearly demonstrates successful block copolymer formation. The copolymer was intentionally targeted to be rich in M34 residues (30:70 molar ratio of M32:M34) given the planned aqueous solution studies described below. The actual copolymer composition was determined by ^1H NMR spectroscopy and was found to be 31:69 M32:M34 at 94% conversion.

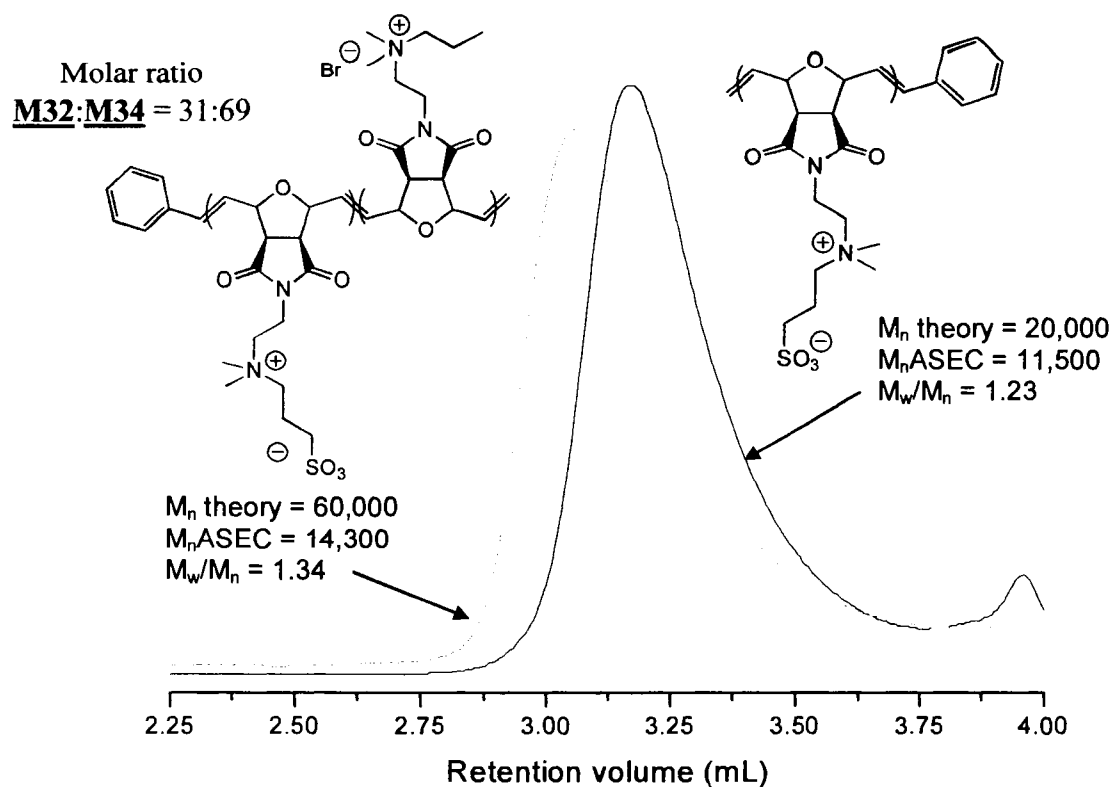


Figure V-9. ASEC traces (RI signal) for the block copolymerization of the sulfopropylbetaine **M32** with the propylquat **M34**. Analysis was conducted in 0.25M NaBr at a flow rate of 1.0 mL/min. The system was calibrated with a series of narrow MMD poly(ethylene oxide) standards.

The aqueous solution properties of the **M32-M34** AB diblock copolymer were anticipated to be complex and to elicit measurable changes in response to the presence/absence of low molecular weight electrolytes. The stimulus responsive behavior of both ionic and zwitterionic (co)polymers towards salts is well documented. Whereas cationic (or anionic) polymers exhibit the well-known polyelectrolyte effect, i.e. chain contraction, upon the addition of low molecular weight salts – a conformational change in response to a stimulus, polymeric betaines exhibit so-called anti-polyelectrolyte behavior. Indeed, the response of polymeric betaines is somewhat more

complex than for polyelectrolytes. Polymeric betaines, as a general rule, are insoluble in pure water, or at best sparingly soluble. This is due to the formation of a 3D ionic network due to the net attractive ionic interactions between the betaine residues which occurs both inter- and intra-molecularly.³⁰ Addition of a critical amount of salt²⁷ – sufficient to screen these inter- and intra-molecular ionic interactions, will result in dissolution. This represents a macroscopic phase response to the applied environmental change, i.e. change in electrolyte concentration. Further addition of low molecular weight salt will result in an additional conformational response by the polymeric betaine as more ionic interactions are screened resulting in chain expansion – opposite to that observed for polyelectrolytes. Such anticipated stimulus-responsive behavior can be conveniently examined using a variety of techniques including NMR spectroscopy and DLS. Figure V-10 shows the experimentally determined hydrodynamic diameter (D_h) size distributions for the M32-M34 AB diblock copolymer in the presence (0.1 M NaCl) and absence of NaCl. In the presence of salt we see that the block copolymer has an average D_h of ca. 10 nm. Under these conditions both blocks are expected to be hydrophilic and the copolymer would be anticipated to exist as single molecularly dissolved chains, or unimers. Indeed, for a block copolymer of the given molecular mass, the measured D_h of ca. 10 nm is entirely consistent with it existing in the unimeric state. In contrast, when the M32-M34 AB diblock copolymer is initially molecularly dissolved in a small volume of TFE, a non-selective solvent, and subsequently diluted with deionized water, a selective solvent for the cationic block, we observe aggregates with an average hydrodynamic diameter of 273 nm. These results are entirely consistent with the predicted hydrophilic (M34)/hydrophobic (M32) nature of the block copolymer under

these solvent conditions and the self-assembly of the block copolymer into multimeric aggregates consisting of a hydrophobic core stabilized by a hydrophilic corona as shown in Scheme V-2.

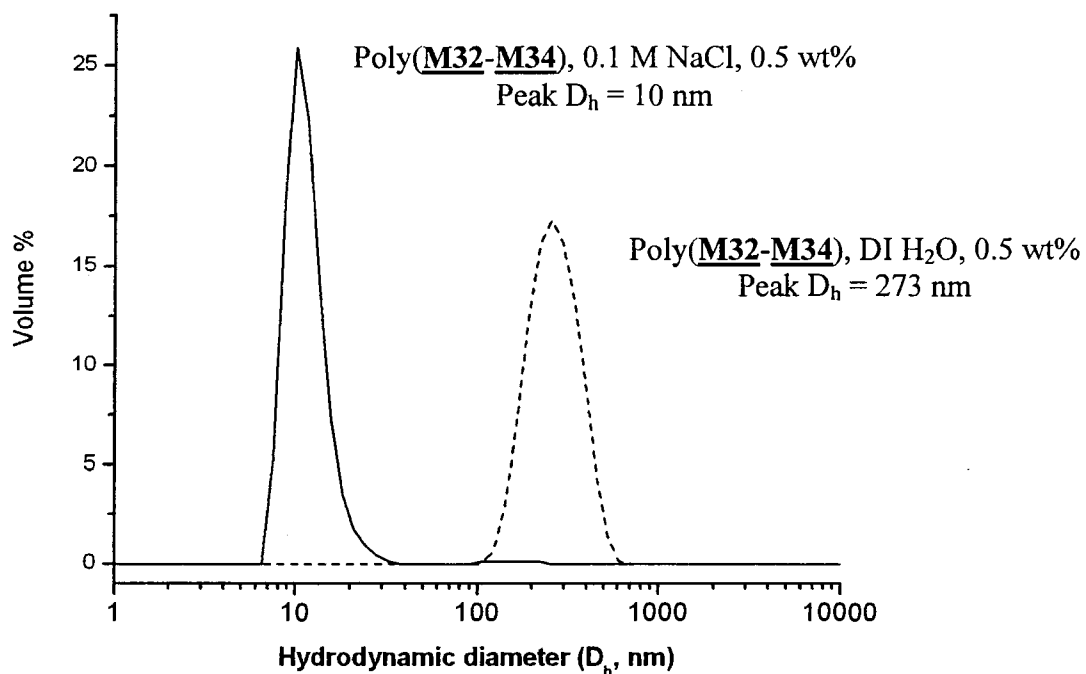
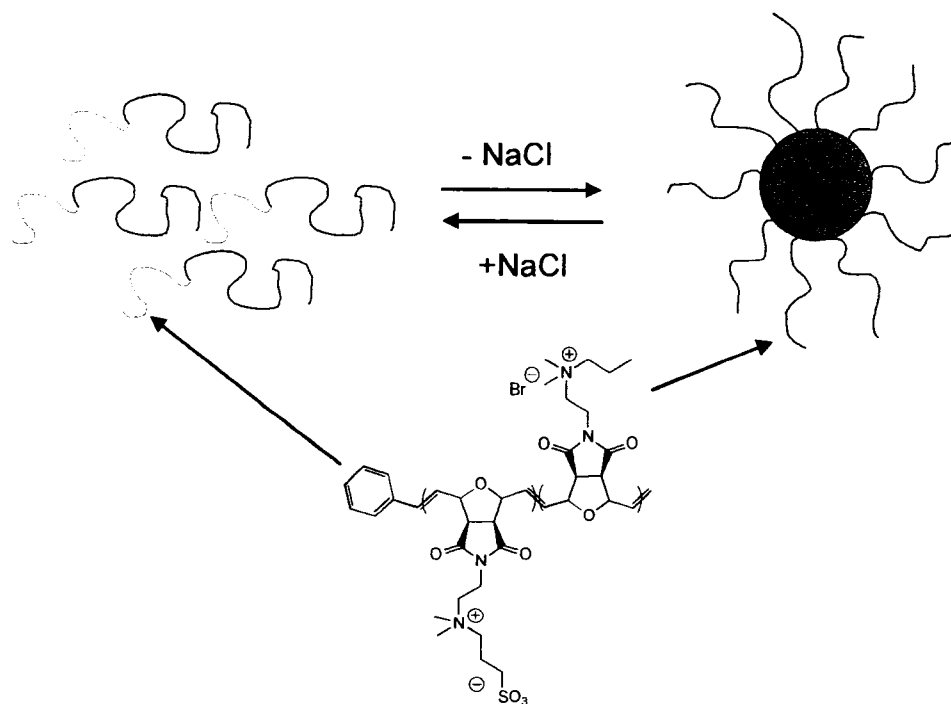


Figure V-10. Hydrodynamic diameter size distributions, as determined by dynamic light scattering, for the M32-M34 AB diblock copolymer in the presence and absence of NaCl. Measurements were made on 0.5 wt% polymer solutions.



Scheme V-2. Cartoon demonstrating the salt-induced assembly/disassembly of the M32-M34 AB diblock copolymer.

Summary/Conclusions

In this chapter we have described the synthesis and controlled ROMP of the first examples of sulfopropylbetaine and carboxyethylbetaine monomers based on the *exo*-7-oxanorbornene structural motif. We have demonstrated that both monomers can be polymerized in a controlled manner, as judged from the kinetic profiles and ASEC analysis, in *organic media* using 17. In the case of the sulfopropylbetaine derivative, homopolymerization proceeded extremely rapidly with essentially quantitative conversion being obtained in 2 min. In contrast, the carboxyethylbetaine monomer needed to be first protonated to facilitate controlled polymerization, presumably to

prevent competitive complexation of the monomer to the Ru metal center. The ability to prepare materials with advanced architectures, i.e block copolymers, was demonstrated by both a self-blocking experiment as well as in the synthesis of an AB diblock copolymer of the sulfopropylbetaine with a permanently cationic comonomer. This represents the first time such betaine monomers have been (co)polymerized directly in a *controlled* fashion by a technique other than a controlled/living free radical process, and also the first time it has been achieved in a solvent other than water and/or salt solution. Finally, in a preliminary experiment we demonstrated the stimulus-responsive behavior of the betaine-cationic block copolymer with the material being able to form polymeric self-assemblies simply by controlling the aqueous solution electrolyte concentration.

CHAPTER VI

CONCLUSIONS AND FUTURE PERSPECTIVES

In this dissertation, utilizing ROMP technology for the synthesis of cationic/betaine WSPs with interesting salt-responsive behavior in aqueous media, we have presented key kinetic and experimental considerations for attaining precise control over (co)polymer composition, molecular weight (MW), end-chain functionality, and narrow molecular weight distribution (MWD).

First, we have established a synthetic protocol that allows for the controlled/'living' polymerization of new, water-soluble cationic and betaine *exo-7*-oxanorbornene derivatives **M31-M33** via ROMP with commercially available Grubb's first generation catalysts $\text{RuCl}_2(\text{PCy}_3)_2\text{CHPh}$ **17** in a novel TFE/ CH_2Cl_2 solvent mixture. It has been demonstrated that the solvent mixture facilitates LROMP of these hydrophilic monomers without the need for catalyst synthesis, post polymerization modification, or protection/deprotection protocols making this synthetic methodology more convenient than previously reported synthetic protocols. The experimental evidence highlights the living characteristics of these polymerizations with regard to controllable MW, narrow MWDs and the ability to prepare advance macromolecular architectures. Other halogenated solvents such as TCE and HFIP were found to be effective in facilitating ROMP of these water-soluble cationic *exo-7*-oxanorbornene derivatives **M31** which may have broader implications as it relates to other metathesis chemistries. As evident by the pseudo first order kinetic and conversion profiles, these polymerizations were found to occur rapidly at room temperature on the time scale between 2 - 12 min for both the cationic and betaine *exo-7*-oxanorbornene derivatives **M28-M34**.

Second, it was demonstrated that the kinetics and MWDs can be influenced by the counterion present in the ROMP of **MON-Bn-Cl** and **MON-Bn-Br** at various molar ratios. This is another important finding, since the ligand environment about the Ru-metal center can have a significant effect on the metathesis activity of a given Grubb's type catalyst. Given this, when using cationic *exo*-7-oxanorbornene derivatives **M31** the polymerization rate can be influenced/controlled by the presence of specific counterions that may enhance LROMP.

Finally, we have demonstrated that this synthetic protocol allows for the synthesis of a cationic-betaine block copolymer exhibiting stimulus-responsive behavior to form polymeric micelles by manipulation of the salt concentration in aqueous media. To the best of our knowledge, this represents the first example of polymeric betaines being prepared under ROMP conditions. Additionally, we believe this to be the first reported example of the synthesis of a salt responsive cationic-betaine block copolymer via LROMP.

Currently, the synthetic methodology developed in this study is being employed to evaluate the LROMP activity of novel benzylidene-functionalized Ru-complexes.¹⁹⁵ In the future this synthetic methodology will be extended to the evaluation of other cationic and zwitterionic cyclic alkene derivatives such as cyclooctene-based monomers. The ultimate goal is the ability to conduct aqueous LROMP of hydrophilic monomers, such as those described in this work, in 'wholly' water. However, this will depend on the development and commercialization of water-soluble catalysts capable of facilitating such aqueous polymerization in a controlled/"living" manner. Until such time, the

synthetic method we have described in this work is a convenient alternative capable of yielding well-defined WSPs via LROMP.

REFERENCES

1. McCormick, C. L.; Lowe, A. B. In *Encyclopedia of Polymer Science*, 3rd Edition, Wiley Publishing: New York, 2004, Vol. 12, pp. 452-521.
2. McCormick, C. L., Ed.; In *Stimuli-Responsive Water Soluble and Amphiphilic Polymers*; Advances in Chemistry Series No. 780; American Chemical Society: Washington, DC, 2001.
3. Qiu, J.; Charleux, B.; Matyjaszewski, K. *Prog. Polym. Sci.* **2001**, *26*, 2083.
4. Stevens, M. P. In *Polymer Chemistry An Introduction* 3rd Ed. Oxford University Press: New York, NY, 1999; pp. 41-42.
5. Kathmann, E. L.; McCormick, C. L. In *Polym. Mater. Encycl.*; Salamone, J. C., Ed.; CRC Press: Boca Raton, FL, 1996; Vol. 7, pp 5462-5476.
6. Lowe, A. B; McCormick, C. L. *Chem. Rev.* **2002**, *102*, 4177.
7. Kern, W. Z. *Phys. Chem.* **1939**, *184*, 197.
8. Fuoss, R. M. *Science* **1948**, *108*, 525.
9. Tanford, C. *Physical Chemistry of Macromolecules*, John Wiley & Sons, Inc., New York, 1961.
10. Lowe, A. B.; McCormick, C. L., Eds., In *Polyelectrolytes and Polyzwitterions: Synthesis, Properties, and Applications*; Lowe, ACS Symposium Series 937, Washington D.C., 2006, p 97.
11. Hashidzume, A.; Morishima, Y; Szczubialka, K. *Amphiphilic Polyelectrolytes* In *Handbook of Polyelectrolytes and Their Applications*; Tripathy, S. K.; Kumar, J.; Nalwa, H. S., Eds., American Scientific Publishers, 2002, Vol 2 Chapter 1 pp. 1-63.
12. Strauss, U. P.; Jackson, E. G. *J. Polym. Sci.* **1951**, *6*, 649.

13. McCormick, C. L.; Bock, J.; Schulz, D. N. In *Encyclopedia of Polymer Science and Engineering*; Kroschwitz, J. I., Ed. Wiley, New York, 1989, Vol 17, p. 730.
14. Schulz, D. N.; Glass, J. E. Eds., *Polymers as Rheology Modifiers*, Advances in Chemistry, Series 462. ACS, Washington, DC, 1991.
15. Bock, J.; Varadaraj, R.; Schulz, D. N.; Maurer, J. J. In *Macromolecular Complexes in Chemistry and Biology*; Dubin, P. L.; Bock, J.; Davies, R. M.; Schulz, D. N.; Thies, C., Eds., Springer-Verlag, Berlin, 1994.
16. Glass, J. E. Ed., *Hyphophilic Polymers: Performance with Environmental Acceptability*; Advances in Chemistry, Series 248, ACS, Washington, DC, 1996.
17. Goddard, E. D.; Gruber, J. V., Ed.; *Principals of Polymer Science and Technology in Cosmetics and Personal Care*, Dekker, New York, 1999.
18. Glass, J. E., Ed., *Associative Polymers in Aqueous Solutions*, ACS Symposium Series 765, ACS, Washington, DC, 2000.
19. Havelka, K. O.; McCormick, C. L., Eds.; *Specialty Monomers and Polymers: Synthesis, Properties, and Applications*, ACS Symposium Series 755, ACS, Washington, DC, 2000.
20. McCormick, C. L.; Armentrout, R. S.; Cannon, G. C.; Martin, G. G.; In *Molecular Interactions and Time-Space Organization in Macromolecular Systems*; Morishima, Y.; Norisuye, T.; Tashiro, K., Eds., Springer-Verlag, Berlin, 1999, p. 125.
21. Harada, A; Katoka, K; *Macromolecules* **1999**, *28*, 5294.
22. Lee, W.-F.; Lee, C.-H. *Polymer* **1997**, *38*, 971.
23. Nakaya, T.; Li, T.-J. *Prog. Poly. Sci.* **1999**, *24*, 143.
24. Kudaibergenov, S.; Werner, J.; Laschewsky, A. *Adv. Polym. Sci.* **2006**, *201*, 157.

25. Ladenheim, H.; Morawetz, H. *J. Polym. Sci.* **1957**, *26*, 251.
26. Hart, R.; Timmerman, D. *J. Polym. Sci.* **1958**, *28*, 638.
27. Monroy, -Soto, V. M.; Galin, J. C. *Polymer* **1984**, *25*, 121.
28. Salamone, J. C.; Volksen, W.; Olsen, A. P.; Israel, S. C. *Polymer* **1978**, *19*, 1157.
29. Itoh, Y.; Abe, K.; Senoh, S. *Makromol. Chem.* **1986**, *187*, 1691.
30. Schulz, D. N.; Peiffer, D. G.; Agarwal, P. K.; Larabee, J.; Kaladas, J. J.; Soni, L.; Handwerker, B.; Garner, R. T. *Polymer* **1986**, *27*, 1734.
31. McCormick, C. L.; Johnson, C. B. *Polymer* **1990**, *31*, 1100.
32. Lee, W.-F., Tsai, C.-C. *Polymer* **1994**, *35*, 2210.
33. Monroy Soto, V. M.; Galin, J. C. *Polymer* **1984**, *25*, 254.
34. Schulz, D. N.; Peiffer, D. G.; Agarwal, P. K.; Larabee, J.; Kaladas, J. J.; Soni, L.; Handwerker, B.; Garner, R. T. **1986**, *27*, 1734.
35. Lowe, A. B.; Billingham, N. C.; Armes, S. P. *Chem. Commun.* **1996**, 1555.
36. Bütün, V.; Bennett, C. E.; Vamvakaki, M.; Lowe, A. B.; Billingham, N. C.; Armes, S. P. *J. Mater. Chem.* **1997**, *7*, 1693.
37. Tuzar, Z.; Pospisil, H.; Plestil, J.; Lowe, A. B.; Baines, F. L.; Billingham, N. C.; Armes, S. P. *Macromolecules* **1997**, *30*, 2509.
38. Lowe, A. B.; Billingham, N. C.; Armes, S. P. *Macromolecules* **1999**, *32*, 2141.
39. Bohrisch, J.; Wendler, U.; Jaeger, W. *Macromol. Rapid Commun* **1997**, *18*, 975.
40. Wendler, U.; Bohrisch, J.; Jaeger, W.; Rother, G.; Dautzenberg, H. *Macromol. Rapid Commun.* **1998**, *19*, 185.
41. Bohrisch, J.; Schimmel, T.; Englehardt, H.; Jaeger, W. *Macromolecules* **2002**, *35*, 4143.

42. Jaeger, W.; Wendler, U.; Lieske, A.; Bohrisch, J. *Langmuir* **1999**, *15*, 4026.
43. Jaeger, W.; Paulke, B.-R.; Zimmerman, A.; Lieske, A.; Wendler, U.; Bohrisch, J. *Polymer Prep.* **1999**, *40*, 980.
44. Jaeger, W.; Wendler, U.; Lieske, A.; Bohrisch, J.; Wandrey, C. *Macromol. Symp.* **2000**, *161*, 87.
45. Lowe, A. B.; McCormick, C. L. *Aust. J. Chem.* **2002**, *55*, 367.
46. Ma, Y.; Tang, Y.; Billingham, N. C.; Armes, S. P.; Lewis, A. L.; Lloyd, A. W.; Salvage, J. P. *Macromolecules* **2003**, *36*, 3475.
47. Lobb, E. J.; Ma, I.; Billingham, N. C.; Armes, S. P.; Lewis, A. L. *J. Am. Chem. Soc.* **2001**, *123*, 7913.
48. Ma, I.; Lobb, E. J.; Billingham, N. C.; Armes, S. P.; Lewis, A. L.; Lloyd, A. W.; Salvage, J. P. *Macromolecules* **2002**, *35*, 9306.
49. McCormick, C. L.; Lowe, A. B. *Acc. Chem. Res.* **2004**, *37*, 312.
50. Lowe, A. B.; McCormick, C. L. *Prog. Polym. Sci.* **2007**, *32*, 283.
51. Donovan, M. S.; Sumerlin, B. S.; Lowe, A. B.; McCormick, C. L. *Macromolecules* **2002**, *35*, 8663.
52. Donovan, M. S.; Lowe, A. B.; Sanford, T. A.; McCormick, C. L. *J. Polym. Sci., Polym. Chem.* **2003**, *41*, 1262.
53. Lowe, A. B.; Vamvakaki, M.; Wassall, M. A.; Wong, L.; Billingham, N.C.; Armes, S.P.; Lloyd, A. W. *J. Biomed. Mater. Res.* **2000**, *52*, 88.
54. Webster, O. *Science* **1991**, *251*, 887.
55. Ziegler, K. *Angew. Chem.* **1936**, *49*, 499.

56. Flory, P. J. *Principles of Polymer Chemistry*. Ithaca, NY; Cornell University Press, 1953.
57. Swarc, M. *Nature* **1956**, *178*, 1168.
58. Penczek, S.; Kubisa, P.; Matyjaszewski, K. *Adv. Polym. Sci.* **1980**, *37*, 1.
59. Penczek, S.; Kubisa, P.; Matyjaszewski, K. *Adv. Polym. Sci.* **1985**, *69*, 1.
60. Penczek, S.; Kubisa, P. In *Encyclopedia of Polymer Science and Technology*; Mark, H. F.; Bikales, N. M.; Overgerger, C. G.; Menges, G; Kroschwitz, J., Eds., 2nd ed. New York, Wiley Interscience, 1989, pp. 390-399, Suppl. 2.
61. Matyjaszewski, K.; Kubisa, P.; Penczek S. *J. Polym. Sci. Polym. Chem. Ed.* **1974**, *12*, 1333.
62. Matyjaszewski, K.; Penczek S. *J. Polym. Sci. Polym. Chem. Symp.* **1977**, *56*, 255.
63. Matyjaszewski, K.; Muller, A. H. E. *ACS Polym. Prepr.* **1997**, *38*, 6.
64. Percec, V.; Tirrell, D. A. *J. Polym. Sci. Part A: Polym. Chem.* **2000**, *38*, 1705.
65. Jenkins, A. D.; Kratchovil, P.; Stepto, R. F. T.; Suter, U. W. - IUPAC Commission on Macromolecular Nomenclature, *Pure Appl. Chem.* **1996**, *68*, 2287.
66. Ivin, K. J.; Mol., J. C. *Olefin Metathesis and Metathesis Polymerization*; Academic: San Diego, 1997.
67. Frenzel, U.; Nuyken, O. *J. Polym. Sci. Part A: Polym. Chem.* **2002**, *40*, 2895.
68. Anderson, A. W.; Merckling, N. G. (Du Pont de Nemours & Co.) U.S. Patent 2,72,1189, 1955. Chem Abstr. **1956**, *50*, 3008.
69. Banks, R. L.; Bailey, G. C. *Ind. Eng. Chem. Prod. Res. Dev.* **1964**, *3*, 170.
70. Calderon, N. *Acc. Chem. Res.* **1972**, *5*, 127.
71. Calderon, N.; Chen, H. Y.; Scott, K. W. *Tetrahedron Lett.* **1967**, *34*, 3327.

72. Calderon, N. *Chem. Eng. News* **1967**, *45*, 51.
73. Trnka, T. M.; Grubbs, R. H. *Acc. Chem. Res.* **2001**, *34*, 18.
74. Bradshaw, C. P. C.; Howman, E. J.; Turner, L. *J. Catal.* **1967**, *7*, 269.
75. Mango, F. D.; Schachtschneider, J. H. *J. Am. Chem. Soc.* **1967**, *89*, 2484.
76. Mango, F. D.; Schachtschneider, J. H. *J. Am. Chem. Soc.* **1971**, *93*, 1123.
77. Lewandos, G. S.; Petit, R. J. *J. Am. Chem. Soc.* **1971**, *93*, 7078.
78. Grubbs, R. H.; Brunck, T. K. *J. Am. Chem. Soc.* **1972**, *94*, 2538.
79. Biefield, C. G.; Eick, H. A.; Grubbs, R. H. *Inorg. Chem.* **1973**, *12*, 2166.
80. Hérisson, J.-L.; Chauvin, Y. *Makromol. Chem.* **1971**, *141*, 161.
81. Grubbs, R. H. In *Comprehensive Organometallic Chemistry*; Wilkinson, G., Ed.; Pergamon: Oxford, 1982; Vol 8.
82. Katz, T. J.; Rothchild, R. *J. Am. Chem. Soc.* **1976**, *98*, 2519.
83. Katz, T. J.; McGinnis, J. *J. Am. Chem. Soc.* **1975**, *97*, 1592.
84. Grubbs, R. H.; Carr, D. D.; Hoppin, C.; Burk, P. L. *J. Am. Chem. Soc.* **1976**, *98*, 3478.
85. Grubbs, R. H.; Burk, P. L.; Carr, D. D. *J. Am. Chem. Soc.* **1975**, *97*, 3264.
86. Bazan, G. C.; Oskam, J. H.; Cho, H.-N.; Park, L. Y.; Schrock, R. R. *J. Am. Chem. Soc.* **1991**, *113*, 6899.
87. Howard, T. R.; Lee, J. B.; Grubbs, R. H. *J. Am. Chem. Soc.* **1980**, *102*, 6876.
88. Kress, J.; Osborn, J. A.; Greene, R. M. E.; Ivin, K. J.; Rooney, J. J. *J. Am. Chem. Soc.* **1987**, *109*, 899.
89. Kress, J.; Osborn, J. A. *Angew. Chem.* **1992**, *104*, 1660.
90. Kress, J.; Osborn, J. A. *Angew. Chem. Int. Ed. Engl.* **1992**, *31*, 1585.

91. Tallarico, J. A.; Bonitatebus, P. J., Jr.; Snapper, M. L. *J. Am. Chem. Soc.* **1997**, *119*, 7157.
92. Bielawski, C. W.; Grubbs, R. H. *Prog. Polym. Sci.* **2007**, *32*, 1.
93. Slugovc, C. *Macromol. Rapid Commun.* **2004**, *25*, 1283.
94. Odian, G. *Principles of Polymerization*, 4th ed. Hoboken: Wiley; 2004.
95. Jacobson, H.; Stockmayer, W. H. *J. Chem. Phys.* **1950**, *18*, 1600.
96. Benedicto, A. D.; Claverie, J. P.; Grubbs, R. H. *Macromolecules* **1995**, *28*, 500.
97. Chen, Z.-R.; Claveria, J. P.; Grubbs, R. H.; Kornfield, J. A. *Macromolecules*, **1995**, *28*, 2147.
98. Grubbs, R. H. *Handbook of Metathesis*, Vol 3, Weinheim: Wiley-VCH; 2003.
99. Ofstead, E. A. *Encyclopedia of Polymer Science and Engineering*, Vol 11, John Wiley, New York, 1988.
100. Buchmeiser, M. R. *Chem. Rev.* **2000**, *100*, 1565.
101. Katz, T. J.; Lee, S. J.; Acton, N. *Tetrahedron Lett.* **1976**, *47*, 4247.
102. Katz, T. J.; Acton, N. *Tetrahedron Lett.* **1976**, *47*, 4251.
103. Grubbs, R. H.; Tumas, W. *Science*, **1989**, *243*, 907.
104. Howard, T. R.; Lee, J. B.; Grubbs, R. H. *J. Am. Chem. Soc.* **1980**, *102*, 6876.
105. Wallace, K. C.; Dewan, J. C.; Schrock, R. R. *Organometallics* **1986**, *5*, 2162.
106. Wallace, K. C.; Liu, A. H.; Dewan, J. C.; Schrock, R. R. *J. Am. Chem. Soc.* **1988**, *110*, 4964.
107. Schaverien, C. J.; Dewan, J. C.; Schrock, R. R. *J. Am. Chem. Soc.* **1986**, *108*, 2771.

108. Schrock, R. R.; DePue, R. T.; Feldman, J.; Schaverien, C. J.; Dewan, J. C.; Lui, A.H. *J. Am. Chem. Soc.* **1988**, *110*, 1423.
109. Schrock, R. R.; Feldman, J. Cannizzo, L. F.; Grubbs, R. H. *Macromolecules* **1987**, *20*, 1169.
110. O'Donoghue, M. B.; Schrock, R. R.; LaPointe, A. M.; Davis, W. M. *Organometallics* **1996**, *15*, 1334.
111. Schrock, R. R.; Yap, K. B.; Yang, D. C.; Sitzmann, H.; Sita, L. R.; Bazan, G. C. *Macromolecules* **1989**, *22*, 3191.
112. Dounis, P.; Feast, W. J. *Polymer* **1996**, *37*, 2547.
113. Trzaska, S. T.; Lee, L.-B.W.; Register, R. A. *Macromolecules* **2000**, *33*, 9215.
114. Wu, Z.; Wheeler, D. R.; Grubbs, R. H. *J. Am. Chem. Soc.* **1992**, *114*, 146.
115. Schrock, R. R.; Murdzek, J. S.; Bazan, G. C.; Robbins, J.; DiMare, M.; O'Regan, M. *J. Am. Chem. Soc.* **1990**, *112*, 3875.
116. Khosravi, E.; Al-Hajaji, A. A. *Polymer* **1998**, *39*, 5619.
117. Khosravi, E.; Feast, W. J.; Al-Hajaji, A. A.; Leejarkpai, T. J. *J. Mol. Catal. A: Chem.* **2000**, *160*, 1.
118. Bazan, G. C.; Khosravi, E.; Schrock, R. R.; Feast, W. J. Gibson, V. C.; O' Regan, M. B. *J. Am. Chem. Soc.* **1990**, *112*, 8378.
119. Schrock, R. R.; Krouse, S. A.; Knoll, K.; Feldman, J.; Murdzek, J. S.; Yang D. C. *J. Mol. Catal.* **1988**, *46*, 243.
120. Dounis, P.; Feast, W. J. *Polymer* **1996**, *37*, 2547.
121. Michelotti, F. W.; Keaveney, W. P. *J. Polym. Sci.* **1965**, *A3*, 895.
122. Rinehart, R. E.; Smith, H. P. *Polym. Lett.* **1965**, *3*, 1049.

123. Porri, L.; Rossi, R.; Diversi, P.; Lucherini, A. *Makromol. Chem.* **1974**, *175*, 3097.
124. Porri, L.; Diversi, P.; Lucherini, A.; Rossi, R.; *Makromol. Chem.* **1975**, *176*, 3121.
125. Novak, B. M.; Grubbs, R. H. *J. Am. Chem. Soc.* **1988**, *110*, 960.
126. Novak, B. M.; Grubbs, R. H. *J. Am. Chem. Soc.* **1988**, *110*, 7542.
127. Hillmyer, M. A.; Lepetit, C.; McGrath, D. V.; Novak, B. M.; Grubbs, R. H. *Macromolecules* **1992**, *25*, 3345.
128. Feast, W. J.; Harrison, D. B. *J. Mol. Catal.* **1991**, *65*, 63.
129. Lu, S. Y.; Quayle, P.; Heatley, F.; Booth, C.; Yeates, S. G.; Padget, J. C. *Macromolecules* **1992**, *25*, 2692.
130. Zenkl, E.; Stelzer, F. *J. Mol. Catal.* **1992**, *76*, 1.
131. France, M. B.; Grubbs, R. H.; McGrath, D. V.; Paciello, R. A. *Macromolecules* **1993**, *26*, 4742.
132. Nguyen, S. T.; Johnson, L. K.; Grubbs, R. H.; Ziller, J. W. *J. Am. Chem. Soc.* **1992**, *114*, 3974.
133. Louie, J.; Grubbs, R. H. *Organometallics* **2002**, *21*, 2153.
134. Wu, Z.; Benedicto, A. D.; Grubbs, R. H. *Macromolecules* **1993**, *26*, 4975.
135. Nguyen, S. T.; Grubbs, R. H.; Ziller, J. W. *J. Am. Chem. Soc.* **1993**, *115*, 9858.
136. Schwab, P.; France, M. B.; Ziller, J. W.; Grubbs, R. H. *Angew. Chem. Int. Ed. Engl.* **1995**, *34*, 2039.
137. Schwab, P.; Grubbs, R. H.; Ziller, J. W. *J. Am. Chem. Soc.* **1996**, *118*, 100.
138. Lynn, D. M.; Kanoaka, S. Grubbs, R. H. *J. Am. Chem. Soc.* **1996**, *118*, 784.
139. Weck, M.; Schwab, P.; Grubbs, R. H. *Macromolecules* **1996**, *29*, 1789.
140. Maughon, B. R.; Grubbs, R. H. *Macromolecules* **1997**, *30*, 3459.

141. Maughon, B. R.; Weck, M.; Mohr, B.; Grubbs, R. H. *Macromolecules* **1997**, *30*, 257.
142. Weck, M.; Mohr, B.; Maughon, B. R.; Grubbs, R.H. *Macromolecules* **1997**, *30*, 6430.
143. Ulman, M.; Grubbs, R. H. *J. Org. Chem.* **1999**, *64*, 7202.
144. Bielawski, C. W.; Louie, J.; Grubbs, R. H. *J. Am. Chem. Soc.* **2000**, *122*, 12872.
145. Dias, E. L.; Nguyen, S. T.; Grubbs, R. H. *J. Am. Chem. Soc.* **1997**, *119*, 3887.
146. Sanford, M. S.; Ulman, M.; Grubbs, R. H. *J. Am. Chem. Soc.* **2001**, *123*, 749.
147. Sanford, M. S.; Love, J. A.; Grubbs, R. H. *J. Am. Chem. Soc.* **2001**, *123*, 6543.
148. Trnka, T. M.; Morgan, J. P.; Sanford, M. S.; Wilhelm, T. E.; Scholl, M.; Choi, T.L.; *J. Am. Chem. Soc.* **2003**, *125*, 2546.
149. Herrmann, W. *Angew. Chem. Int. Ed.* **2002**, *41*, 1290.
150. Scholl, M.; Ding, S.; Lee, C. W.; Grubbs, R. H. *Org. Lett.* **1999**, *1*, 953.
151. Bielawski, C. W.; Grubbs, R. H. *Angew. Chem. Int. Ed.* **2000**, *39*, 2903.
152. Scherman, O. A.; Grubbs, R. H. *Synth. Met.* **2001**, *124*, 431.
153. Sanford, M. S.; Love, J. A.; Grubbs, R. H. *Organometallics* **2001**, *20*, 5314.
154. Love, J. A.; Morgan, J. P. Trnka, T. M.; Grubbs, R. H. *Angew. Chem. Int. Ed.* **2002**, *41*, 4035.
155. Choi, T-L.; Grubbs, R. H. *Angew. Chem. Int. Ed.* **2003**, *43*, 1745.
156. Madan, R.; Srivastava; Anand, R. C.; Varma, I. K. *Prog. Polym. Sci.* **1998**, *23*, 621.
157. Kingsbury, J. S.; Harrity, J. P. A.; Bonitatebus, Jr., P. J.; Hoveyda, A. H. *J. Am. Chem. Soc.* **1999**, *121*, 791.

158. Garber, S. B.; Kingsbury, J. S.; Gray, B. L.; Hoveyda, A. H. *J. Am. Chem. Soc.* **2000**, *122*, 8168.
159. Demel, S.; Riegler, S.; Wewerka, K.; Schoefberger, W.; Slugovc, C.; Stelzer, F. *Inorg. Chim. Acta.* **2003**, *345*, 363.
160. Demel, S.; Schoefberger, W.; Slugovc, C.; Stelzer, F. *J. Mol. Catal. A.* **2003**, *200*, 11.
161. Claverie, J. P.; Soula, R. *Prog. Polym. Sci.* **2003**, *28*, 619.
162. Mohr, B.; Lynn, D. M.; Grubbs, R. H. *Organometallics* **1996**, *15*, 4317.
163. Lynn, D. M.; Mohr, B.; Grubbs, R. H. *J. Am. Chem. Soc.* **1998**, *120*, 1627.
164. Lynn, D. M.; Mohr, B.; Grubbs, R. H.; Henling, L. M.; Day, M. W. *J. Am. Chem. Soc.* **2000**, *122*, 6601.
165. Gallivan, J. P.; Jordan, J. P.; Grubbs, R. H. *Tetrahedron Lett.* **2005**, *46*, 2577.
166. Hong, S. H.; Grubbs, R. H. *J. Am. Chem. Soc.* **2006**, *128*, 3508.
167. Jordan, J. P.; Grubbs, R. H. *Angew. Chem. Int. Ed.* **2007**, *46*, 5152.
168. Mortell, K. H.; Weatherman, R. V.; Kiessling, L. L. *J. Am. Chem. Soc.* **1996**, *118*, 2297.
169. Kanai, M.; Mortell, K. H.; Kiessling, L. L. *J. Am. Chem. Soc.* **1997**, *119*, 9931.
170. Kiessling, L. L.; Strong, L. E. *Top. Organomet. Chem.* **1998**, *1*, 199.
171. Cario, C. W.; Gestwicki, J. E.; Kanai, M.; Kiessling, L. L. *J. Am. Chem. Soc.* **2002**, *124*, 1615.
172. Gibson, V. C.; Marshall, E. L.; North, M.; Robson, D. A.; Williams, P. J. *Chem. Commun.* **1997**, 1095.

173. Davies, R. G.; Gibson, V. C.; Hursthouse, M. B.; Light, M. E.; Marshall, E. L. North, D.; Robson, D. A.; Tompson, I.; White, A. J. P.; Williams, D. J.; Williams, P. J. *J. Chem. Soc. Perkin Trans.* **2001**, *34*, 3365.
174. Maynard, H. D.; Okada, S. Y.; Grubbs, R. H. *Macromolecules* **2000**, *33*, 6239.
175. Maynard, H. D.; Okada, S. Y.; Grubbs, R. H. *J. Am. Chem. Soc.* **2001**, *123*, 1275.
176. Watson, K. J.; Anderson, D. R.; Nguyen, S. T. *Macromolecules* **2001**, *34*, 3507.
177. Bell, B.; Hamilton, J. G.; Law, E. E.; Rooney, J. J. *Macromol. Rapid Commun.* **1994**, *15*, 543.
178. Hamilton, J. G.; Law, E. E.; Rooney, J. J. *J. Mol. Catal. A: Chem.* **1997**, *115*, 1.
179. McArdle, C. M.; Hamilton, J. G.; Law, E. E.; Rooney, J. J. *Macromol. Rapid Commun.* **1995**, *16*, 703.
180. Amir-Ebrahimi, V.; Byrne, D.; Hamilton, J. G.; Rooney, J. J. *Macromol. Chem. Phys.* **1995**, *196*, 327.
181. Feast, W. J.; Hesselink, J. L.; Khosravi, E.; Rannard, S. P. *Polymer Bulletin* **2002**, *49*, 135.
182. Ilker, M. F.; Schule, H.; Coughlin, E. B. *Macromolecules* **2004**, *37*, 694.
183. Ahmed, S. R.; Bullock, S. E.; Cresce, A. V.; Kofinas, P. *Polymer* **2003**, *44*, 4943.
184. Liaw, D. J.; Huang, C. C.; Wu, P. L. *Macromol. Chem. Phys.* **2002**, *203*, 2177.
185. Liaw, D. J.; Chen, T.-P.; Huang, C. C. *J. Polym. Sci. Part A: Polym. Chem.* **2005**, *43*, 4233.
186. Zheng, L.; Chen, F.; Xie, M.; Han, H.; Dai, Q.; Zhang, Y.; Song, C. *React. Funct. Polym.* **2007**, *67*, 19.

187. Breitenkamp, R. B.; Ou, Z.; Breitenkamp, K.; Muthukumar, M.; Emrick, T.
Macromolecules, 2007 **ASAP** online.
188. Lapinte, V.; Brosse, J.-C.; Fontaine, L. *Macromol. Chem. Phys.* **2004**, *205*, 824.
189. Rule, J. D.; Moore, J. S. *Macromolecules* **2002**, *35*, 7878.
190. Huglin, M. B.; Radwan, M. A. *Makromol. Chem.* **1991**, *192*, 2433.
191. Amir-Ebrahimi, V.; Corry, D. A.; Hamilton, J. G.; Thompson, J. M.; Rooney, J. J.;
Macromolecules **2000**, *33*, 717.
192. Holland, M. G.; Griffith, V. A.; France, M. B.; Desjardins, S. G. *J. Polym. Sci.*
Polym. Chem. **2003**, *41*, 2125.
193. Rankin, D. A.; P'Pool, S. J.; Schanz, H.-J.; Lowe, A. B. *J Polym. Sci. Polym.*
Chem. **2007**, *45*, 2113.
194. Rankin, D. A.; Schanz, H.-J.; Lowe, A. B. *Macromol. Chem. Phys.* **2007**, *208*,
2389.
195. Roberts, A. N.; Cochran, A. C.; Rankin, D. A.; Lowe, A. B.; Schanz, H.-J.
Organometallics **2007**, *26*, 6515.